Supporting Information for

Spontaneous N_2-diboranylation of $[W(N_2)_2(dppe)_2]$ with $B_2Br_4(SMe_2)_2$

Lisa C. Haufe, Merle Arrowsmith, Maximilian Dietz, Annalena Gärtner, Rüdiger Bertermann and Holger Braunschweig*

Institute for Inorganic Chemistry and Institute for Sustainable Chemistry & Catalysis with Boron, Julius-Maximilians-Universität Würzburg, Am Hubland, 97074 Würzburg, Germany

Table of Contents

Methods and materials

All manipulations were performed under dry nitrogen atmosphere using Schlenk techniques or in a glovebox filled with argon. Deuterated solvents were dried over molecular sieves and degassed by three freeze-pump-thaw cycles prior to use. All other solvents were distilled and degassed from appropriate drying agents. The deuterated as well as non-deuterated solvents were stored under argon over activated 4 Å molecular sieves. NMR spectra were acquired either on a Bruker Avance Neo I 500, Bruker Avance Neo I 600 or a Bruker Avance 400 NMR spectrometer. Chemical shifts (δ) are reported in parts per million (ppm) and internally referenced to residual solvent peaks. Heteronuclei NMR spectra are referenced to external standards (^{11}B: $BF_3 \cdot OEt_2$; ^{31}P: 85% H_3PO_4). NMR multiplicities are given as: s (singlet), d (doublet), t (triplet), sept (septet), m (multiplet). The solid-state ^{11}B RSHE/MAS (RSHE = rotor synchronized Hahn-Echo) NMR spectra of **1-CAAC** was recorded using a Bruker Avance Neo 400 spectrometer operating at 128.4 MHz, using a 4 mm (o. d.) ZrO_2 rotor. Chemical shifts were calibrated for all nuclei externally by adjusting the field manually, so that the low-field ^{13}C NMR shift of adamantane appears at 38.48 ppm to comply with IUPAC recommendations for reference. The solid-state ^{11}B magic-angle spinning (MAS) spectra was acquired by a rotor-synchronized Hahn-Echo (RSHE) at a spinning speed of 14.8 kHz. The ^{11}B second-order quadrupolar powder pattern of **1-CAAC** (Figure S22) was simulated with the software package SOLA[1] within Topspin™ by Bruker. IR spectra were recorded on a Bruker FT-IR spectrometer ALPHA II inside a glovebox. UV-vis spectra were measured on a METTLER TOLEDO UV-vis-Excellence UV5 spectrophotometer at room temperature. Elemental analyses were performed on an Elementar vario MICRO cube elemental analyzer.

As similar compounds have been shown to be very sensitive towards moisture in previous work,[2] reactions were performed in silanised glassware or Kartell™ polyethylene sample tubes. sealable NMR tubes were silanised by adding approximately 0.2 mL of hexamethyldisilazane (HMDS) and heated to reflux for 1 min using a heat gun, prior to removal of the residual HMDS *in vacuo* while heating with a heat gun for 1 min.

Unless stated otherwise, solvents and reagents were purchased from Sigma-Aldrich or Alfa Aesar. $W(N_2)_2(dppe)_2$,[3] CAAC (1-(2,6-di*iso*propylphenyl)-3,3,5,5-tetramethylpyrrolidin-2-

ylidene),[4] I*i*Pr (1,3-di*iso*propylimidazol-2-ylidene),[5] PMe_3,[6] PCy_3[7] and CNMes* (2,4,6-tris(*tert*-butyl)phenylisocyanide)[8] were synthesised using literature procedures.

Synthetic procedures

[BrW(dppe)$_2$NNB(Br)BBr$_2$SMe$_2$], 1-SMe$_2$

[W(N$_2$)$_2$(dppe)$_2$] (15 mg, 15 µmol) was suspended in benzene (0.3 mL) in a sealable NMR tube. B$_2$Br$_4$(SMe$_2$)$_2$ (6.7 mg, 15 µmol, 1.0 equiv.) was added, followed by benzene (0.3 mL). The orange suspension turned to a dark red-brown solution with accompanying gas evolution. The conversion to **1-SMe$_2$** was almost quantitative (ca. 96%) as determined by ^{31}P{^{1}H} NMR spectroscopy. Orange single crystals of **1-SMe$_2$** suitable for X-ray crystallography were obtained from a benzene/pentane mixture. *Note: Compound **1-SMe$_2$** was used and characterised in situ as partial decomposition was observed after evaporation of the solvent under ambient glovebox conditions. This is probably due to the partial loss of the coordinating SMe$_2$ group during evaporation.* ^{1}H NMR (500.1 MHz, C$_6$D$_6$): δ(ppm) = 7.79 (m, 8H, *o*-Ph-C*H*), 7.37 (t, $^3J_{HH}$ = 7.6 Hz, 8H, *m*-Ph-C*H*), 7.16–7.10 (m, 12H, *o/p*-Ph-C*H*, *overlap with C$_6$D$_6$*), 6.93 (t, $^3J_{HH}$ = 7.5 Hz, 4H, *p*-Ph-C*H*), 6.84 (t, $^3J_{HH}$ = 7.6 Hz, 8H, *m*-Ph-C*H*), 2.82–2.63 (m, 8H, PC*H*$_2$), 1.71 (br s, 12H, BS(C*H*$_3$)$_2$ + *free S(CH$_3$)$_2$*). ^{13}C{^{1}H} NMR (125.8 MHz, C$_6$D$_6$): δ(ppm) = 138.3–137.8 (m, *i*-Ph-*C$_q$*), 137.4–136.9 (m, *i*-Ph-*C$_q$*), 134.9–134.6 (m, *o*-Ph-*C*H), 134.3–134.1 (m, *o*-Ph-*C*H), 129.9 (s, *p*-Ph-*C*H), 129.1–128.9 (m, *m*-Ph-*C*H), 128.9 (s, *p*-Ph-*C*H), 127.6–127.4 (m, *m*-Ph-*C*H), 32.9–32.4 (m, CH$_2$, P*C*H$_2$), 20.7 (s, CH$_3$, S(*C*H$_3$)$_2$), 17.8 (s CH$_3$, S(*C*H$_3$)$_2$). ^{11}B{^{1}H} NMR (160.5 MHz, C$_6$D$_6$): *not detected*. ^{31}P{^{1}H} NMR (202.5 MHz, C$_6$D$_6$): δ(ppm) = 33.2 (s + satellites, $^1J_{WP}$ = 288 Hz). FT-IR (C$_6$H$_6$): $\tilde{\nu}$(NN) = 1535 cm^{-1}. UV-vis (C$_6$H$_6$): λ_{max} = 305 nm.

[BrW(dppe)$_2$NNB(Br)BBr$_2$(PMe$_3$)], 1-PMe$_3$

[W(N$_2$)$_2$(dppe)$_2$] (40.0 mg, 38.6 µmol) was suspended in benzene (0.3 mL) in a sealable NMR tube. B$_2$Br$_4$(SMe$_2$)$_2$ (18.0 mg, 38.6 µmol, 1.00 equiv.) was added, followed by benzene (0.3 mL). The orange suspension turned to a dark red-brown solution with accompanying gas evolution. After 5 min, PMe$_3$ (50.0 µL, 492 µmol, 12.7 equiv.) was added and the solution remained dark red-brown. After 10 min, excess PMe$_3$ was removed by injecting N$_2$ gas into the NMR tube. Pentane (1.0 mL) was added to initiate precipitation of an orange solid. The orange suspension was filtered and the resulting solid washed with benzene (1 × 0.1 mL) followed by pentane (3 × 1.5 mL). The resulting solid was dried under ambient glovebox conditions overnight to afford **1-PMe$_3$** (48.2 mg, 33.8 µmol, 88%) as an orange solid. Orange single crystals suitable for X-ray crystallography were obtained from a benzene solution. ^{1}H NMR

(500.1 MHz, C_6D_6): δ (ppm) = 7.84 (m, 8H, *o*-Ph-C*H*), 7.41 (t, $^3J_{HH}$ = 7.7 Hz, 8H, *m*-Ph-C*H*), 7.19–7.13 (m, 12H, *o/p*-Ph-C*H*, overlap with C_6D_6), 6.94 (t, $^3J_{HH}$ = 7.4 Hz, 4H, *p*-Ph-C*H*), 6.86 (t, $^3J_{HH}$ = 7.5 Hz, 8H, *m*-Ph-C*H*), 2.83–2.66 (m, 8H, PCH_2), 1.06 (d, $^2J_{PH}$ = 11.8 Hz, 9H, P(CH_3)$_3$). $^{13}C\{^1H\}$ NMR (125.8 MHz, C_6D_6): δ (ppm) = 138.7–138.3 (m, *i*-Ph-C_q), 137.5–137.1 (m, *i*-Ph-C_q), 134.8 (m, *o*-Ph-*C*H), 134.2 (m, *o*-Ph-*C*H), 129.8 (s, *p*-Ph-*C*H), 129.1 (m, *m*-Ph-*C*H), 128.9 (s, *p*-Ph-*C*H), 127.5 (m, *m*-Ph-*C*H), 32.9–32.5 (m, P*C*H_2), 8.0 (d, $^1J_{CP}$ = 44.5 Hz, P(*C*H_3)$_3$). ^{11}B NMR (128.5 MHz, C_6D_6): δ (ppm) = –7.0 (br s, fwmh ≈ 190 Hz, *B*PMe_3). *Note: The ^{11}B NMR resonance can only be observed at the high in-situ concentrations of the reaction mixture.* $^{31}P\{^1H\}$ NMR (202.5 MHz, C_6D_6): δ (ppm) = 33.3 (s, $^1J_{WP}$ = 289 Hz, dppe), –13.1 (br s, fwmh ≈ 50 Hz, PMe_3). FT-IR (solid-state): $\tilde{\nu}$(NN) = 1528 cm^{-1}. UV-vis (C_6H_6): λ_{max} = 318 nm. Elemental analysis [%] calculated for $C_{55}H_{57}B_2Br_4N_2P_5W$ (1426.02 g mol^{-1}): C 46.33, H 4.03, N 1.96; found: C 46.22, H 4.38, N 1.95.

[BrW(dppe)$_2$NNB(Br)BBr$_2$(PCy$_3$)], 1-PCy$_3$

[W(N_2)$_2$(dppe)$_2$] (40.0 mg, 38.6 µmol) was suspended in benzene (1.5 mL) in a polyethylene vial. $B_2Br_4(SMe_2)_2$ (18.0 mg, 38.6 µmol, 1.00 equiv.) was added with stirring, followed by benzene (0.5 mL). The orange suspension turned to a dark red-brown solution with accompanying gas evolution. The solution was stirred for 5 min, after which PCy_3 (10.8 mg, 38.6 µmol, 1.00 equiv.) was added, followed by benzene (0.5 mL). The dark red-brown solution was stirred for 2 h, then treated with pentane (8.0 mL) to induce precipitation. The light orange-brown suspension was filtered and the resulting solid washed with pentane (3 × 2.0 mL). The resulting solid was dried under ambient glovebox conditions overnight to afford **1-PCy$_3$** as a beige yellow solid (37.2 mg, 22.8 µmol, 60%). Vapor diffusion of pentane into the benzene solution instead of precipitation increased the isolated yield to 82% (51.7 mg, 31.7 µmol). Yellow single crystals suitable for X-ray crystallography were obtained from a benzene/pentane mixture. ^1H NMR (500.1 MHz, C_6D_6): δ (ppm) = 8.04 (m, 8H, *o*-Ph-C*H*), 7.44 (t, $^3J_{HH}$ = 7.6 Hz, 8H, *m*-Ph-C*H*), 7.15 (t, overlap with C_6D_6, 4H, *p*-Ph-C*H*), 6.97–6.91 (m, 12H, *o/p*-Ph-C*H*), 6.85 (t, $^3J_{HH}$ = 7.4 Hz, 8H, *m*-Ph-C*H*), 2.91–2.66 (m, 11H, PCH_2 (dppe) + Cy-PC*H*), 2.37–2.27 (m, 6H, Cy-CH_2), 1.71–1.60 (m, 12H, Cy-CH_2), 1.58–1.51 (m, 3H, Cy-CH_2), 1.23–1.14 (m, 6H, Cy-CH_2, overlap with residual pentane), 1.14–1.04 (m, 3H, Cy-CH_2). $^{13}C\{^1H\}$ NMR (125.8 MHz, C_6D_6): δ (ppm) = 140.0–139.5 (m, *i*-Ph-C_q), 137.5–136.9 (m, *i*-Ph-C_q), 135.6–135.3 (m, *o*-Ph-*C*H), 134.4–134.1 (m, *o*-Ph-*C*H), 129.7 (s, *p*-Ph-*C*H), 129.2–129.0 (m, *m*-Ph-*C*H), 128.6 (s, *p*-Ph-*C*H, overlap with residual C_6H_6), 127.3–127.2 (m, *m*-Ph-*C*H), 34.2–33.8 (m, P*C*H_2),

32.9 (d, $^{1}J_{PC}$ = 30 Hz, Cy-P*C*H), 29.1 (d, J_{PC} = 3.6 Hz, Cy-*C*H$_2$), 27.8 (d, J_{PC} = 10 Hz, Cy-*C*H$_2$), 26.3 (s, Cy-*C*H$_2$). ^{11}B NMR (160.5 MHz, C_6D_6): *not detected.* ^{31}P{^{1}H} NMR (202.5 MHz, C_6D_6): δ (ppm) = 37.6 (s + satellites, $^{1}J_{WP}$ = 289 Hz, dppe), –5.0 (br s, fwmh ≈ 35 Hz, *P*Cy$_3$). FT-IR (solid-state): $\tilde{\nu}$(NN) = 1528 cm^{-1}. UV-vis (C_6H_6): λ_{max} = 306 nm. Elemental analysis [%] calculated for $C_{70}H_{81}B_2Br_4N_2P_5W$ (1630.38 g mol^{-1}): C 51.57, H 5.01, N 1.72; found: C 51.85, H 4.95, N 1.75.

[BrW(dppe)$_2$NNB(Br)BBr$_2$(CNMes*)], 1-CNMes*

[W(N$_2$)$_2$(dppe)$_2$] (40.0 mg, 38.6 µmol) was suspended in benzene (0.3 mL) in a sealable NMR tube. $B_2Br_4(SMe_2)_2$ (18.0 mg, 38.6 µmol, 1.00 equiv.) was added, followed by benzene (0.3 mL). The orange suspension turned to a dark red-brown solution with accompanying gas evolution. After 10 min, 2,4,6-tris(*tert*-butyl)phenyl isocyanide (11.5 mg, 42.4 µmol, 1.10 equiv.) was added as a solid and the solution stayed dark red-brown. Overnight, dark brown crystals precipitated from the solution. The supernatant was decanted and the crystals were washed with benzene (3 × 0.5 mL), followed by pentane (3 × 1.0 mL). The resulting solid was dried under ambient glovebox conditions overnight to afford **1-CNMes*** as dark brown crystals (56.6 mg, 34.9 µmol, 90%). Orange single crystals suitable for X-ray crystallography were obtained from a benzene solution. ^{1}H NMR (600.2 MHz, CD_2Cl_2): δ (ppm) = 7.61–7.56 (m, 8H, *o*-Ph-C*H*), 7.45 (s, 2H, *m*-Mes*-C*H*), 7.33–7.25 (m, 12H, *m/p-Ph-CH*), 7.18 (t, $^{3}J_{HH}$ = 7.3 Hz, 4H, *p*-Ph-C*H*), 7.01 (t, $^{3}J_{HH}$ = 7.8 Hz, 8 H, *m*-Ph-C*H*), 6.89 (br s, 8H, *o*-Ph-C*H*), 2.97–2.87 (m, 4H, PC*H*$_2$), 2.78–2.67 (m, 4H, PC*H*$_2$), 1.50 (s, 18H, *o*-Mes*-C(C*H*$_3$)$_3$), 1.33 (s, 9H, *p*-Mes*-C(C*H*$_3$)$_3$). ^{13}C{^{1}H} NMR (150.9 MHz, CD_2Cl_2): δ (ppm) = 155.4 (s, *p*-Mes*-*C*$_q$), 149.6 (s, *o*-Ph-*C*$_q$), 139.0–138.7 (m, *i*-Ph-*C*$_q$), 136.6–136.3 (m, *i*-Ph-*C*$_q$), 134.6 (m, *o*-Ph-*C*H), 134.1 (m, *o*-Ph-*C*H), 129.8 (s, *p*-Ph-*C*H), 129.2 (s, *p*-Ph-*C*H), 128.9 (m, *m*-Ph-*C*H), 128.2 (m, B*C*$_q$N), 127.5 (m, *m*-Ph-*C*H), 123.0 (s, *m*-Mes*-*CH*), 118.7 (*i*-Mes*-*C*$_q$, identified by HMBC), 36.3 (s, *o*-Mes*-*C*(CH$_3$)$_3$), 36.0 (s, *p*-Mes*-*C*(CH$_3$)$_3$), 33.3–32.9 (m, P*C*H$_2$), 31.2 (s, CH$_3$, *p*-Mes*-C(*C*H$_3$)$_3$), 30.6 (s, CH$_3$, *o*-Mes*-C(*C*H$_3$)$_3$). ^{11}B NMR (192.6 MHz, CD_2Cl_2): *not detected*. ^{31}P{^{1}H} NMR (243.0 MHz, CD_2Cl_2): δ (ppm) = 34.2 (s, $^{1}J_{WP}$ = 288 Hz). FT-IR (solid-state): $\tilde{\nu}$(C≡N) = 2259 cm^{-1}, $\tilde{\nu}$(NN) = 1545 cm^{-1}. UV-vis (CH_2Cl_2): λ_{max} = 268 nm. Elemental analysis [%] calculated for $C_{71}H_{77}B_2Br_4N_3P_4W\cdot(C_6H_6)_2$ (1777.62 g mol^{-1}): C 56.08, H 5.05, N 2.36; found: C 55.94, H 5.23, N 2.35.

[BrW(dppe)$_2$NNB(Br)BBr$_2$(CAAC)], 1-CAAC

[W(N$_2$)$_2$(dppe)$_2$] (200 mg, 193 µmol) was placed in a polyethylene vial and was suspended in benzene (2.0 mL). B$_2$Br$_4$(SMe$_2$)$_2$ (89.9 mg, 193 µmol, 1.00 equiv.) was added as a solid with stirring and subsequent addition of benzene (1.5 mL). The orange suspension turned to a dark red-brown solution with accompanying gas evolution. The solution was stirred for 15 min, after which CAAC (82.6 mg, 289 µmol, 1.50 equiv.) was added, followed by benzene (0.5 mL). The dark red-brown solution was stirred for 3.5 h, then treated with pentane (5.0 mL) to induce precipitation. The yellow-orange suspension was filtered and the resulting solid washed with benzene (2 × 0.2 mL) and pentane (3 × 4 mL). The resulting solid was dried under ambient glovebox conditions overnight to afford **1-CAAC** as a yellow-orange solid (275 mg, 168 µmol, 87%). ^{1}H NMR (500.1 MHz, C$_6$D$_6$): δ(ppm) = 8.12–8.04 (m, 4H, Ph-C*H*), 8.04–7.96 (m, 4H, Ph-C*H*), 7.51–7.43 (m, 4H, Ph-C*H*), 7.43–7.35 (m, 4H, Ph-C*H*), 7.15–7.06 (m, 7H, overlap with C$_6$D$_6$, Ph-C*H* + *m*/*p*-Dip-C*H*), 6.98–6.80 (m, 20H, Ph-C*H*), 3.36–3.25 (m, 1H, C*H*(CH$_3$)$_2$), 3.15–3.03 (m, 1H, C*H*(CH$_3$)$_2$), 2.96–2.65 (m, 8H, PC*H*$_2$), 2.03 (s, 3H, C(C*H*$_3$)$_2$), 1.95 (d, $^3J_{HH}$ = 5.5 Hz, 3H, CH(C*H*$_3$)$_2$), 1.74 (s, 3H, C(C*H*$_3$)$_2$), 1.63 (d, $^2J_{HH}$ = 12.2 Hz, 1H, C*H*$_2$), 1.44 (d, $^3J_{HH}$ = 5.1 Hz, 3H, CH(C*H*$_3$)$_2$), 1.38 (d, $^2J_{HH}$ = 12.0 Hz, 1H, C*H*$_2$), 1.20 (d, $^3J_{HH}$ = 5.2 Hz, 3H, CH(C*H*$_3$)$_2$), 1.15 (d, $^3J_{HH}$ = 5.6 Hz, 3H, CH(C*H*$_3$)$_2$), 0.92 (s, 3H, NC(C*H*$_3$)$_2$, overlap with residual pentane), 0.86 (s, 3H, NC(C*H*$_3$)$_2$, overlap with residual pentane). ^{13}C{^{1}H} NMR (125.8 MHz, C$_6$D$_6$): δ(ppm) = 221.7 (*C*$_{Carbene}$-*C*$_q$, identified by HMBC), 146.9 (*o*-Dip-*C*$_q$), 146.8 (*o*-Dip-*C*$_q$), 140.3–139.8 (m, 2 × *i*-Ph-*C*$_q$), 138.1–137.6 (m, *i*-Ph-*C*$_q$), 136.5–136.0 (m, *i*-Ph-*C*$_q$), 135.8–135.6 (m, Ph-*C*H), 135.2–134.9 (m, Ph-*C*H), 134.6–134.3 (m, Ph-*C*H), 134.3–134.1 (m, Ph-*C*H), 134.0 (s, *i*-Dip- C$_q$), 129.7 (s, Ph-*C*H), 129.7–129.6 (m, Ph-*C*H), 129.3–129.0 (m, Ph-*C*H), 128.7–128.6 (m, Ph-*C*H), 128.5–128.4 (m, Ph-*C*H, identified by DEPT), 128.4 (*p*-Dip-*C*H, identified by DEPT), 127.4–127.0 (m, Ph-*C*H), 125.8 (s, *m*-Dip-C*H*), 124.9 (s, *m*-Dip-C*H*), 79.1 (s, C$_q$, N*C*(CH$_3$)$_2$), 54.8 (s, C$_q$, *C*(CH$_3$)$_2$), 51.5 (s, *C*H$_2$), 35.2 (s, C(*C*H$_3$)$_2$), 35.1–34.6 (m, P*C*H$_2$), 34.4–33.9 (m, P*C*H$_2$), 30.4 (s, C(*C*H$_3$)$_2$), 30.1 (*C*H(CH$_3$)$_2$ + NC(*C*H$_3$)$_2$), 28.9 (s, *C*H(CH$_3$)$_2$), 28.6 (s, CH(*C*H$_3$)$_2$), 27.9 (s, CH(*C*H$_3$)$_2$), 27.4 (s, NC(*C*H$_3$)$_2$), 25.4 (s, *C*H(CH$_3$)$_2$), 25.2 (s, *C*H(CH$_3$)$_2$). ^{11}B NMR (160.5 MHz, C$_6$D$_6$): *not detected*. ^{11}B NMR (RSHE/MAS, 14.8 kHz): δ_{iso} = 23.7 (C_Q = 3200 MHz, η_Q = 0.50, N-*B*-B), δ_{iso} = – 6.2 (C_Q = 2400 MHz, η_Q = 0.46) ppm. ^{31}P{^{1}H} NMR (202.5 MHz, C$_6$D$_6$): δ(ppm) = 38.9 (s), 38.4 (s). FT-IR (solid-state): $\tilde{\nu}$(NN) = 1536 cm^{-1}. UV-vis (C$_6$H$_6$): λ_{max} = 306 nm. Elemental analysis [%] calculated for C$_{72}$H$_{79}$B$_2$Br$_4$N$_3$P$_4$W (1635.42 g/mol): C 52.88, H 4.87, N 2.57; found: C 53.04, H 4.90, N 2.53.

[BrW(dppe)$_2$NNB(Br)BBr$_2$(I*i*Pr)], 1-I*i*Pr

[W(N$_2$)$_2$(dppe)$_2$] (40 mg, 39 µmol) was suspended in benzene (0.4 mL) in a sealable NMR tube. B$_2$Br$_4$(SMe$_2$)$_2$ (18 mg, 39 µmol, 1.0 equiv.) was added, followed by benzene (0.2 mL). After the addition, the orange suspension turned to a dark red-brown solution with accompanying gas evolution. After 5 min, I*i*Pr (7.0 mg, 46 µmol, 1.2 equiv.) was added and the solution turned dark green brown. After three days on a nutating mixer, small amounts of solid by-products were removed by filtration and the resulting dark red solution was treated with pentane (1.5 mL) to induce precipitation. The light brown suspension was filtered and the residue was washed with pentane (3 × 1.0 mL). The resulting solid was dried under ambient glovebox conditions overnight to afford **1-I*i*Pr** as a light brown solid (48 mg, 32 µmol, 82%). ^{1}H NMR (500.1 MHz, C$_6$D$_6$): δ(ppm) = 8.12 (br s, 8H, *o*-Ph-C*H*), 7.47 (t, $^3J_{HH}$ = 7.6 Hz, 8H, *m*-Ph-C*H*), 7.12 (t, $^3J_{HH}$ = 7.5 Hz, 4H, *p*-Ph-C*H*, overlap with C$_6$D$_6$), 6.97–6.82 (m, 20H, *o/m/p*-Ph-C*H*), 6.14 (s, 2H, I*i*Pr-C*H*), 5.95 (sept, $^3J_{HH}$ = 6.3 Hz, 2H, I*i*Pr-C*H*(CH$_3$)$_2$), 2.93–2.81 (m, 4H, PC*H*$_2$, overlap with the second PC*H*$_2$ resonance), 2.81–2.70 (m, 4H, PC*H*$_2$, overlap with the second PCH$_2$ resonance), 1.10 (d, $^3J_{HH}$ = 6.6 Hz, 12H, I*i*Pr-CH(C*H*$_3$)$_2$). ^{13}C{^{1}H} NMR (125.8 MHz, C$_6$D$_6$): δ(ppm) = 156.7 (B*C*$_{carbene}$, identified by HMBC), 140.4–139.9 (m, *i*-Ph-*C*$_q$), 137.2–136.5 (m, *i*-Ph-*C*$_q$), 135.7–135.5 (m, *o*-Ph-*C*H), 134.4–134.2 (m, *o*-Ph-*C*H), 129.8 (s, *p*-Ph-*C*H), 129.2–129.0 (m, *m*-Ph-*C*H), 128.6 (s, *p*-Ph-*C*H, overlap with residual C$_6$H$_6$), 127.3–127.2 (m, *m*-Ph-*C*H), 117 (s, I*i*Pr-*C*H), 50.4 (s, I*i*Pr-*C*H(CH$_3$)$_2$), 34.7–34.2 (m, P*C*H$_2$), 23.2 (s, I*i*Pr-CH(*C*H$_3$)$_2$). ^{11}B{^{1}H} NMR (160.5 MHz, C$_6$D$_6$): *not detected.* ^{31}P{^{1}H} NMR (202.5 MHz, C$_6$D$_6$): δ(ppm) = 39.1 (s, $^1J_{WP}$ = 289 Hz). FT-IR (solid-state): $\tilde{\nu}$(NN) = 1550 cm^{-1}. UV-vis (C$_6$H$_6$): λ_{max} = 311 nm. Elemental analysis [%] calculated for C$_{61}$H$_{64}$B$_2$Br$_4$N$_4$P$_4$W·C$_6$H$_6$ (1580.30 g mol^{-1}): C 50.92, H 4.46, N 3.55; found: C 50.67, H 4.71, N 3.61.

[BrW(dppe)$_2$NNB(DMAP)BBr$_3$], 3-DMAP

[W(N$_2$)$_2$(dppe)$_2$] (50 mg, 48 µmol) was suspended in benzene (1.5 mL) in a polyethylene vial. B$_2$Br$_4$(SMe$_2$)$_2$ (23 mg, 48 µmol, 1.0 equiv.) was added under stirring, followed by benzene (0.5 mL). The orange suspension turned to a dark red-brown solution with accompanying gas evolution. After 10 min, DMAP (5.3 mg, 43 µmol, 0.9 equiv.) was added and a dark green suspension was formed. After 45 min, the green suspension was filtered and the resulting solid was washed with benzene (3 × 2.5 mL), THF (2 × 2.0 mL) and pentane (3 × 3.0 mL). The resulting solid was dried under ambient glovebox conditions to afford **3-DMAP** as a light green solid (35 mg, 24 µmol, 56%). Dark green single crystals were obtained by slow diffusion of

hexane into a saturated dichloromethane solution. ^{1}H NMR (600.1 MHz, C_6D_6): δ (ppm) = 7.37 (d, ^{3}J = 7.5 Hz, 2H, *o*-C*H* DMAP), 7.36–6.87 (m, 40H, *o/m/p*-Ph-C*H*), 5.14 (d, ^{3}J = 7.7 Hz, 2H, *m*-C*H* DMAP), 3.36–2.91 (br, 8H, PCH_2), 2.80 (s, 6H, N(CH_3)$_2$ DMAP). ^{13}C{^{1}H} NMR (150.9 MHz, C_6D_6): δ (ppm) = 154.9 (s, C_q, *C*N(CH$_3$) DMAP), 142.6 (s, *o*-*C*H DMAP), 134.4–133.7 (*i*-Ph-C_q), 133.7–133.1 (*i*-Ph-C_q), 129.8 (m, Ph-*C*H), 129.7 (m, Ph-*C*H), 128.7 (m, Ph-*C*H), 128.7 (m, Ph-*C*H), 127.9 (m, Ph-*C*H), 127.8 (m, Ph-*C*H), 103.4 (s, *m*-*C*H DMAP), 39.7 (s, CH$_3$, N(*C*H$_3$)$_2$ DMAP), 31.6–30.8 (m, P*C*H$_2$). ^{11}B NMR (192.6 MHz, C_6D_6): *not detected.* ^{31}P{^{1}H} NMR (243.0 MHz, C_6D_6, 223.15 K): δ (ppm) = 33.5 ($^{2}J_{PP}$ = 135 Hz), 24.1 ($^{2}J_{PP}$ = 135 Hz). FT-IR (solid-state): $\tilde{\nu}$(NN) = 1564 cm^{-1}. UV-vis (CH_2Cl_2): λ^{1}_{max} = 264 nm, λ^{2}_{max} = 290 nm, λ^{3}_{max} = 325 nm, λ^{4}_{max} = 404 nm. Elemental analysis [%] calculated for $C_{59}H_{58}B_2Br_4N_4P_4W$ (1472.11 g mol^{-1}): C 48.14, H 3.97, N 3.81; found: C 48.12, H 4.03, N 3.90.

[BrW(dppe)$_2$NNB(Br)B(Br)NNWBr(dppe)$_2$], 2

[W(N$_2$)$_2$(dppe)$_2$] (40 mg, 39 µmol, 2.0 equiv.) was suspended in benzene (0.4 mL) in a sealable NMR tube. $B_2Br_4(SMe_2)_2$ (9.0 mg, 19 µmol, 1.0 equiv.) was added, followed by benzene (0.2 mL). The orange suspension turned to a dark red brown solution with accompanying gas evolution. Afterwards, the mixture was heated to 60 °C for two hours, resulting in the formation of dark green crystals. The supernatant pale orange solution was decanted and the crystals were washed with benzene (6 × 1.5 mL) followed by pentane (5 × 1 mL). The resulting solid was dried under ambient glovebox conditions overnight to afford **2** as dark green crystals (37 mg, 16 µmol, 84%). Single crystals suitable for X-ray crystallography were obtained from a benzene solution. *Note: compound **2** is very poorly soluble in common organic solvents, hence the NMR samples were very weakly concentrated.* ^{1}H NMR (500.1 MHz, C_6D_5Br): δ (ppm) = 7.76–7.70 (m, 16H, *o*-Ph-C*H*), 7.30–7.25 (m, 24H, *m/p*-Ph-C*H*, overlap with C_6D_5Br), 7.09–7.03 (m, 24H, *m/p*-Ph-C*H*, overlap with C_6D_5Br), 6.94–6.89 (m, 16H, *o*-Ph-C*H*, overlap with C_6D_5Br), 2.88–2.68 (m, 16H, PCH_2). ^{13}C{^{1}H} NMR (125.8 MHz, C_6D_5Br): δ (ppm) = 138.3 (*i*-Ph-C_q, identified by HMBC), 136.6 (*i*-Ph-C_q, identified by HMBC), 134.6–134.3 (m, *o*-Ph-*C*H), 133.8–133.6 (m, *o*-Ph-*C*H), 129.7 (*p*-Ph-*C*H, identified by HSQC), 128.5 (s, *p*-Ph-*C*H), 128.5–128.3 (m, *m*-Ph-*C*H), 127.2–127.0 (m, *m*-Ph-*C*H), 33.3 (P*C*H$_2$, *identified by HSQC*). ^{11}B NMR (160.5 MHz, C_6D_5Br): *not detected*. ^{31}P{^{1}H} NMR (162.0 MHz, C_6D_5Br): δ (ppm) = 34.9 (s + satellites, $^{1}J_{WP}$ = 286 Hz, dppe). FT-IR (solid-state): $\tilde{\nu}$(NN) = 1529 cm^{-1}. UV-vis (C_6H_5Br): λ^{1}_{max} = 425 nm, λ^{2}_{max} = 437 nm. Elemental analysis [%] calculated for $C_{104}H_{96}B_2Br_4N_4P_8W_2$ (2358.65 g mol^{-1}): C 52.96, H 4.10, N 2.38; found: C 53.34, H 4.28, N 2.39.

Attempted reduction reactions with complex 2

*Note: Compound **2** shows no resonance in the ^{31}P NMR spectrum in benzene due to high insolubility.*

Reaction of **2** with KC_8 and $[Pt(nbe)_3]$: **2** (20 mg, 8.5 µmol, 1.0 equiv.), KC_8 (2.9 mg, 22 µmol, 2.5 equiv.) and $[Pt(nbe)_3]$ (8.5 mg, 18 µmol, 2.1 equiv.) were suspended in benzene (0.6 mL) in a sealable NMR tube. The dark green suspension turned dark brown. After four days at room temperature, the ^{31}P NMR spectrum showed an unselective reaction with several resonances in the range of 31 to 48 ppm.

Reaction of **2** with KC_8 and $[Ni(cod)_2]$: **2** (20 mg, 8.5 µmol, 1.0 equiv.), KC_8 (2.9 mg, 22 µmol, 2.5 equiv.) and $[Ni(cod)_2]$ (4.9 mg, 18 µmol, 2.1 equiv.) were suspended in benzene (0.6 mL) in a sealable NMR tube. The dark green suspension showed no resonance in the ^{31}P NMR spectrum. After four days at room temperature, the dark brown suspension showed an unselective reaction in the ^{31}P NMR spectrum with several resonances in the range of 31 to 48 ppm very similar to the reaction with $[Pt(nbe)_3]$.

Reaction of **2** with KC_8 and diphenylacetylene: **2** (15 mg, 6.4 µmol, 1.0 equiv.), KC_8 (2.1 mg, 16 µmol, 2.5 equiv.) and diphenylacetylene (4.6 mg, 26 µmol, 4.0 equiv.) were suspended in benzene (0.6 mL) in a sealable NMR tube. The dark green suspension turned dark brown. After one day at room temperature, the ^{31}P NMR spectrum showed an unselective reaction with several resonances in the range of –26 to 68 ppm.

Reaction of **2** with KC_8 and 4-dimethylaminopyridine: **2** (10 mg, 4.2 µmol, 1.0 equiv.), KC_8 (1.4 mg, 11 µmol, 2.5 equiv.) and 4-dimethylaminopyridine (1.1 mg, 9.0 µmol, 2.1 equiv.) were suspended in benzene (0.6 mL) in a sealable NMR tube. The dark green suspension turned dark red-brown. After one day at room temperature, the ^{31}P NMR spectrum showed an unselective reaction with several resonances in the range of 34 to 64 ppm.

Reaction of **2** with KC_8 and 1-(2,6-di*iso*propylphenyl)-3,3,5,5-tetramethylpyrrolidin-2-ylidene: **2** (10 mg, 4.2 µmol, 1.0 equiv.), KC_8 (1.4 mg, 11 µmol, 2.5 equiv.) and 1-(2,6-di*iso*propylphenyl)-3,3,5,5-tetramethylpyrrolidin-2-ylidene (2.5 mg, 8.8 µmol, 2.1 equiv.) were suspended in benzene (0.6 mL) in a sealable NMR tube. The dark green suspension turned dark brown. After one day at room temperature, the ^{31}P NMR showed an unselective reaction with several resonances in the range of 32 to 47 ppm.

Reaction of **2** with KC_8 and PMe_3: **2** (10 mg, 4.2 µmol, 1.0 equiv.), KC_8 (1.4 mg, 11 µmol, 2.5 equiv.) were placed in a sealable NMR tube. The tube was cooled to –78 °C and benzene (0.6 mL) was added. PMe_3 (0.05 mL, 490 µmol, 116 equiv.) was added to the frozen reaction

mixture. After the addition, the reaction mixture was warmed to room temperature. The ^{31}P NMR spectrum of the yellow-brown suspension showed an unselective reaction with several resonances in the range of –65 to 130 ppm.

NMR spectra

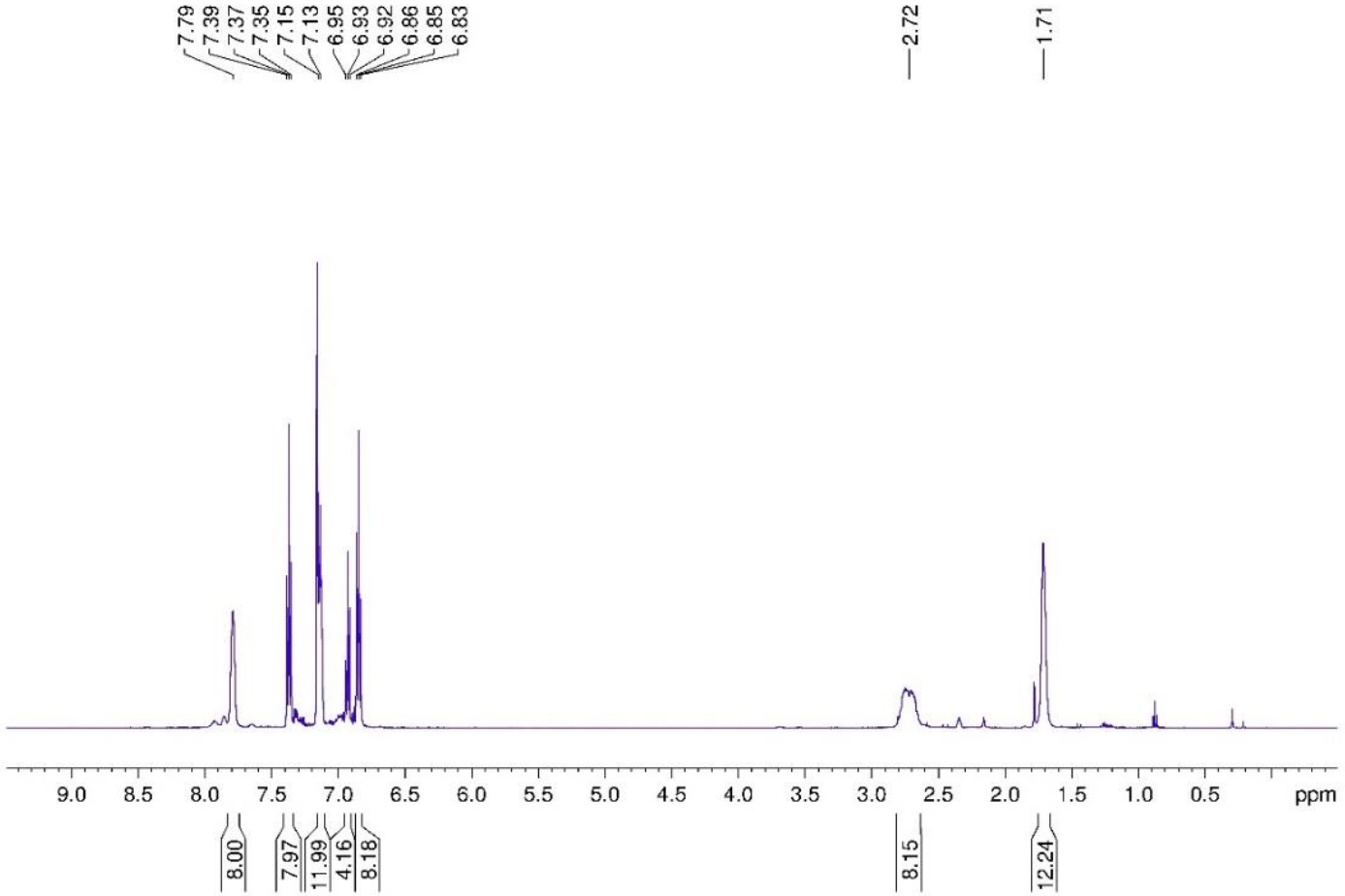

Figure S1. ^{1}H NMR spectrum of **1-SMe$_2$** in C_6D_6. The additional resonances at 0.87 and 1.25 ppm correspond to residual pentane and the resonance at 0.29 ppm to silicon grease. The small additional resonance at 1.78 ppm corresponds to the starting material $B_2Br_4(SMe_2)_2$.

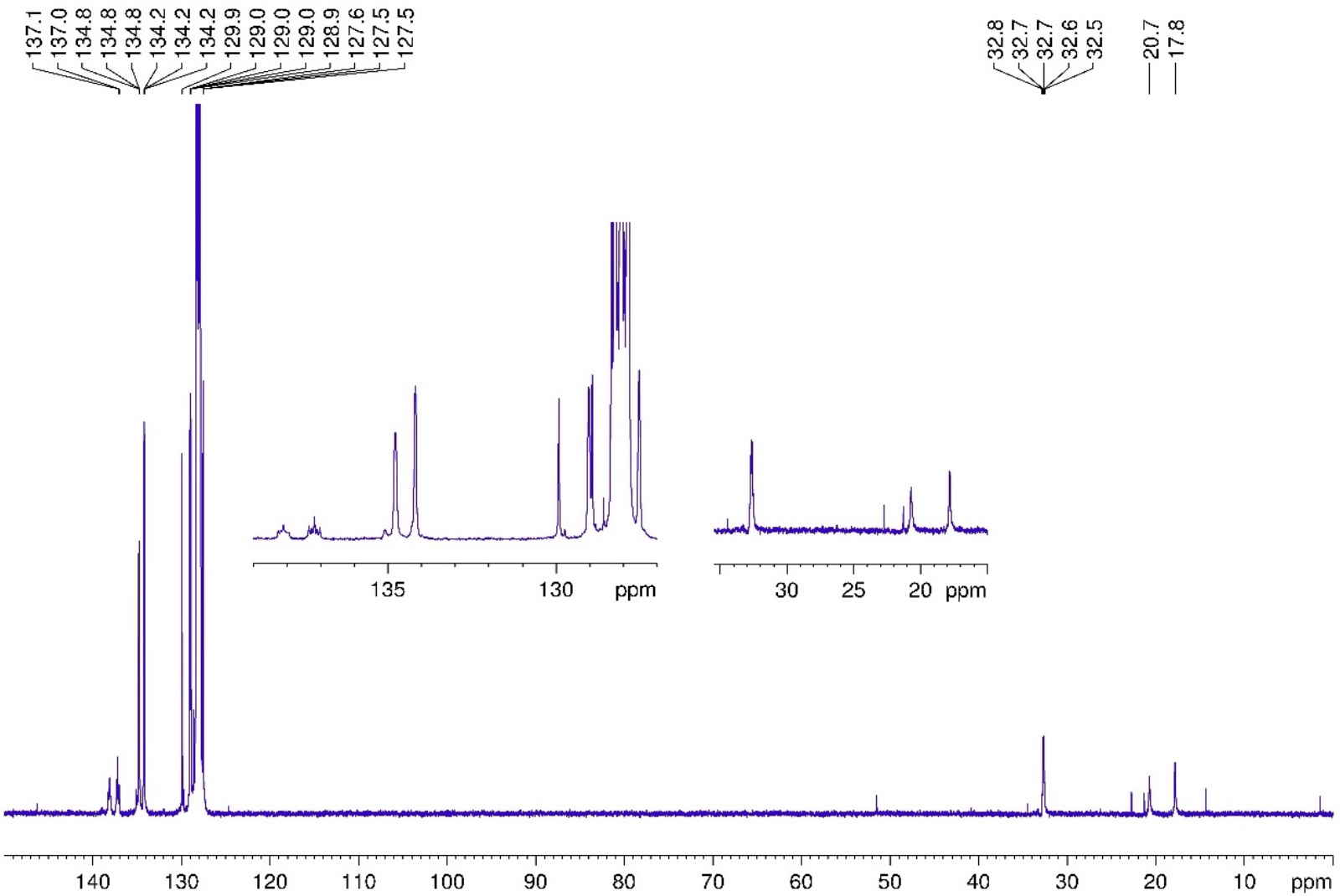

Figure S2. *In situ* $^{13}C\{^{1}H\}$ NMR spectrum of **1-SMe$_2$** in C_6D_6. The additional resonances at 14.3, 22.7 and 34.3 ppm correspond to residual pentane and the resonance at 1.4 ppm to silicon grease.

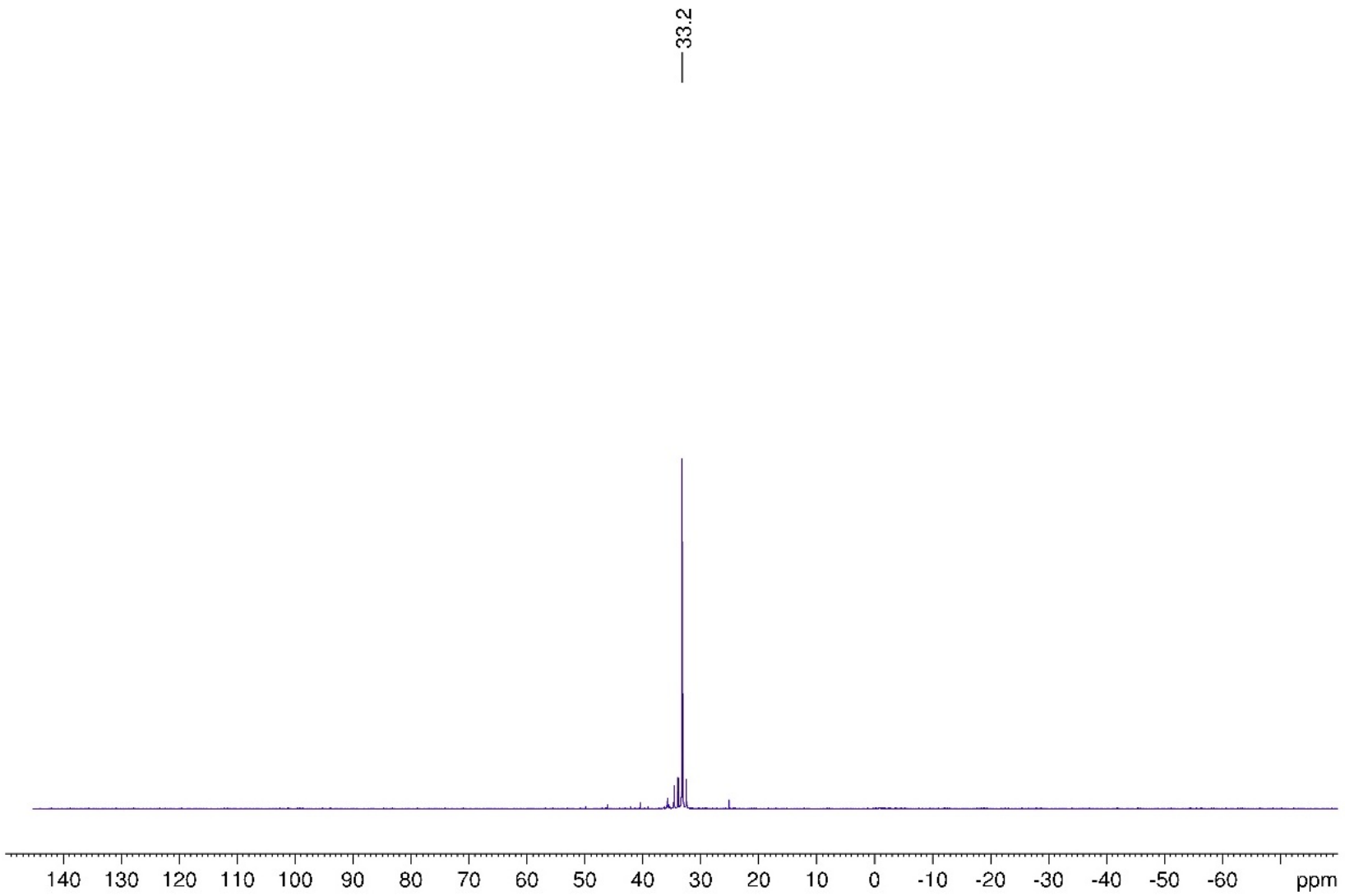

Figure S3. *In situ* $^{31}P\{^{1}H\}$ NMR spectrum of **1-SMe$_2$** in C_6D_6.

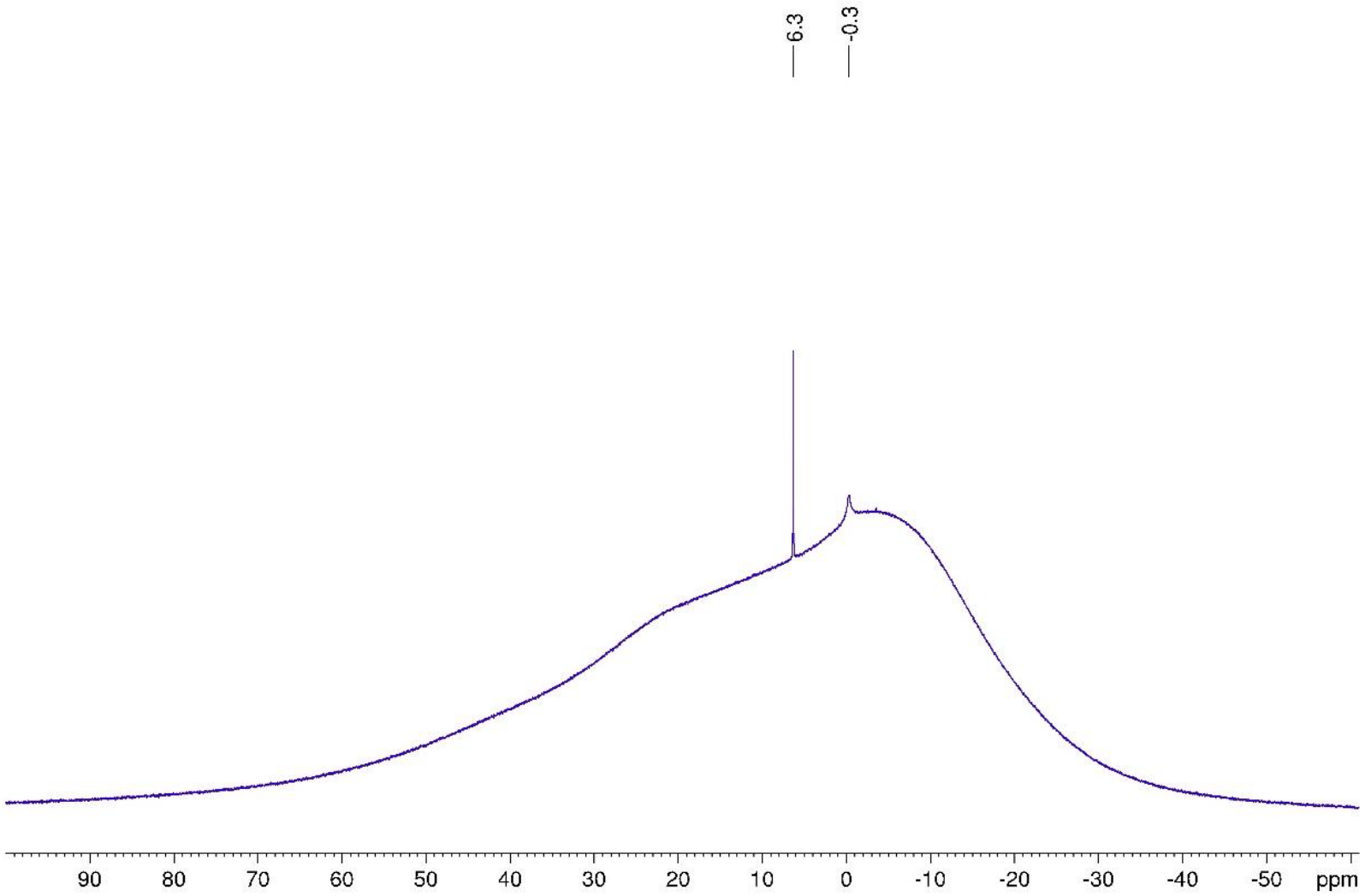

Figure S4. *In situ* $^{11}B\{^{1}H\}$ NMR spectrum of **1-SMe$_2$** in C_6D_6. The resonances at –0.3 ppm correspond to the starting material $B_2Br_4(SMe_2)_2$ and the resonance at 6.3 ppm to a unidentified impurity from $B_2Br_4(SMe_2)_2$.

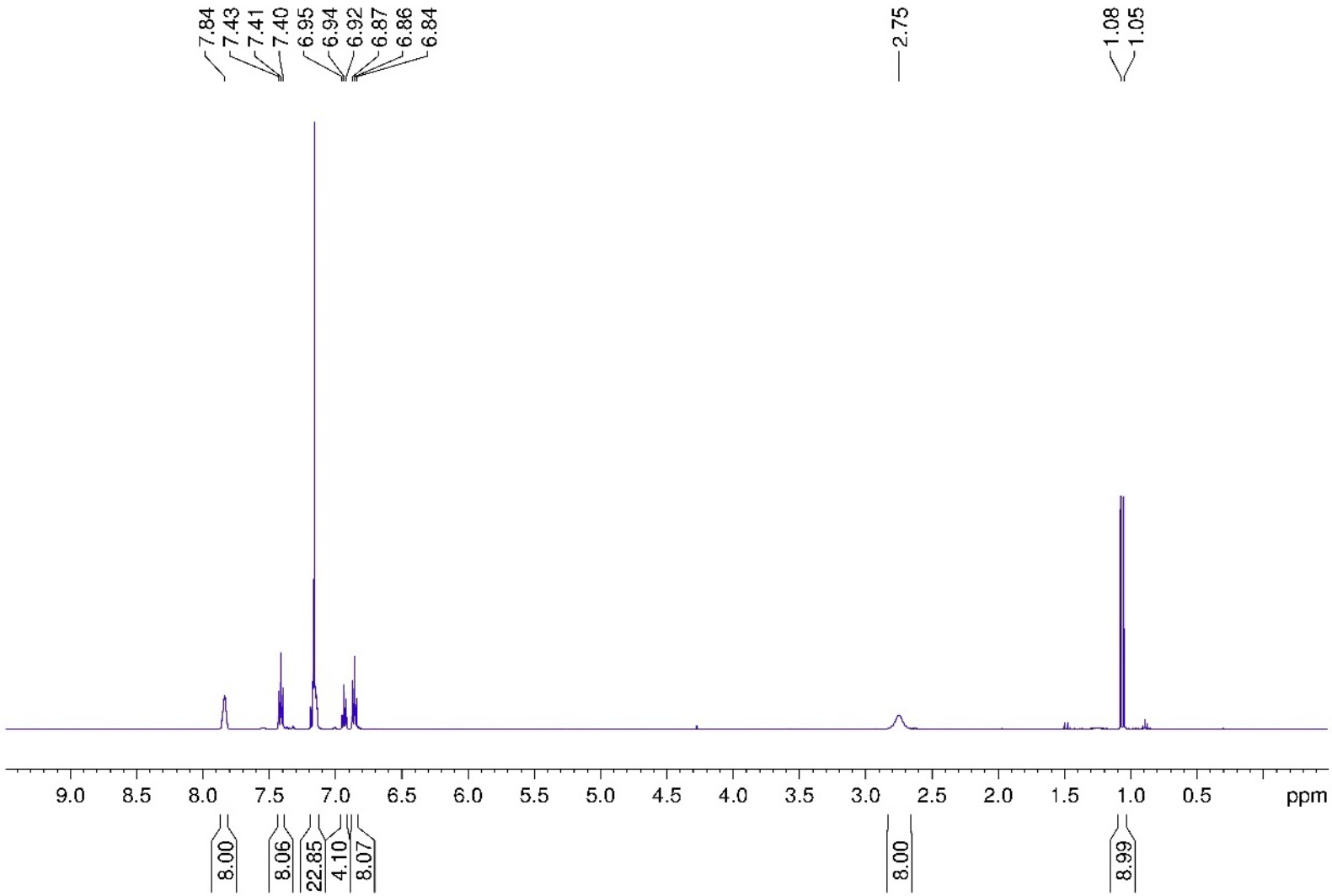

Figure S5. ^{1}H NMR spectrum of **1-PMe$_3$** in C_6D_6. The additional resonances at 0.89 and 1.24 ppm correspond to residual hexane.

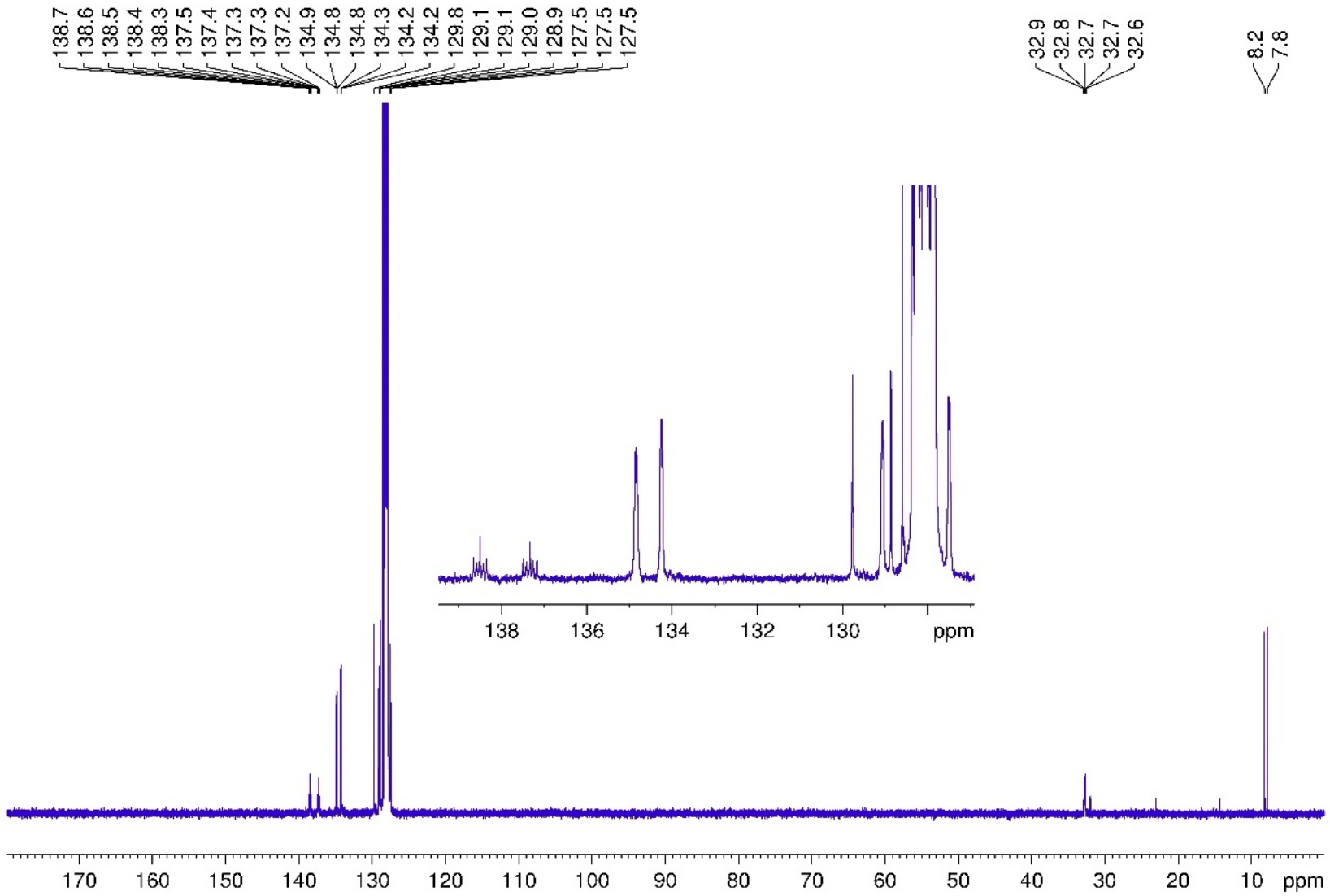

Figure S6. $^{13}C\{^{1}H\}$ NMR spectrum of **1-PMe$_3$** in C_6D_6. The additional resonances at 14.4, 23.0 and 32.0 ppm correspond to residual hexane.

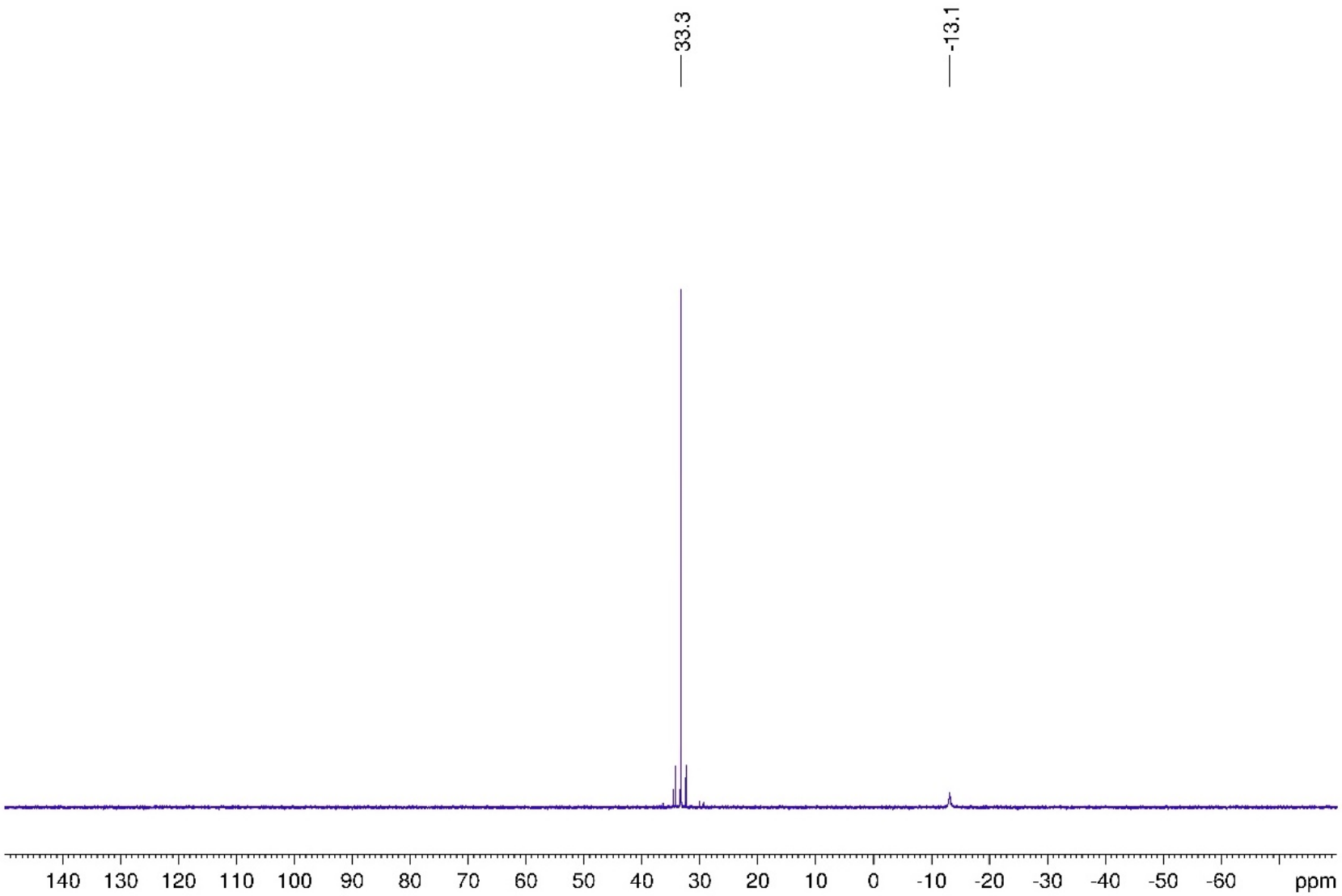

Figure S7. $^{31}P\{^{1}H\}$ NMR spectrum of **1-PMe$_3$** in C_6D_6.

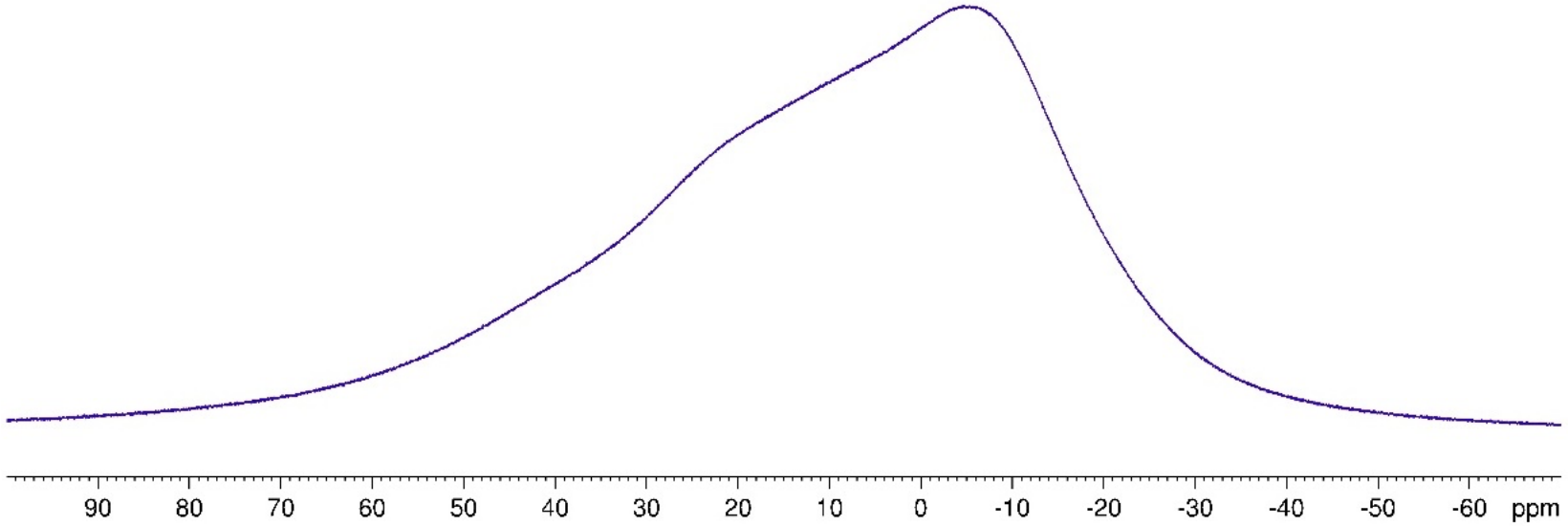

Figure S8. ^{11}B NMR spectrum of **1-PMe$_3$** in C_6D_6.

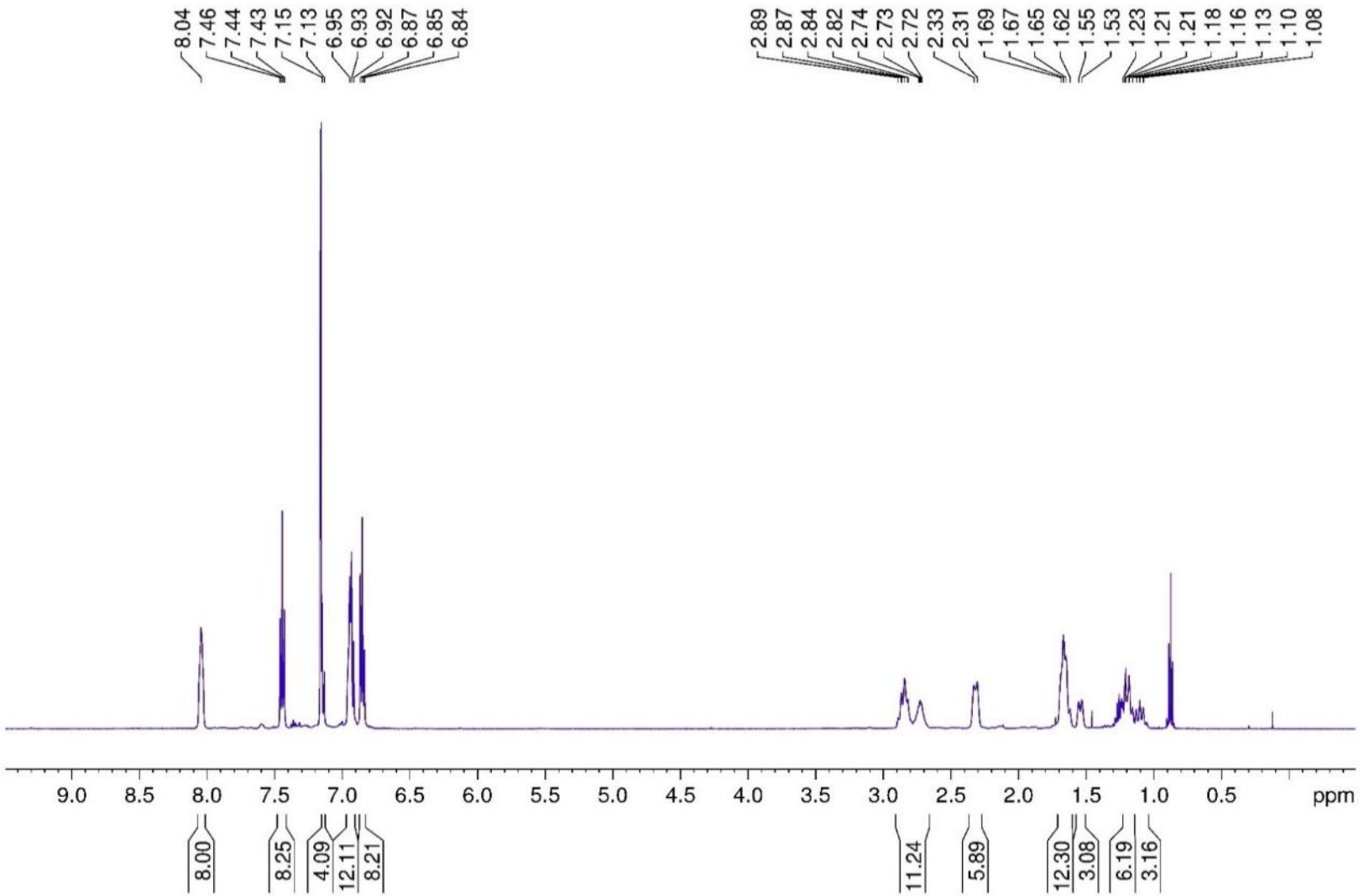

Figure S9. ^{1}H NMR spectrum of **1-PCy$_3$** in C_6D_6. The additional multiplets at 0.87 and 1.26 ppm correspond to residual pentane and hexane.

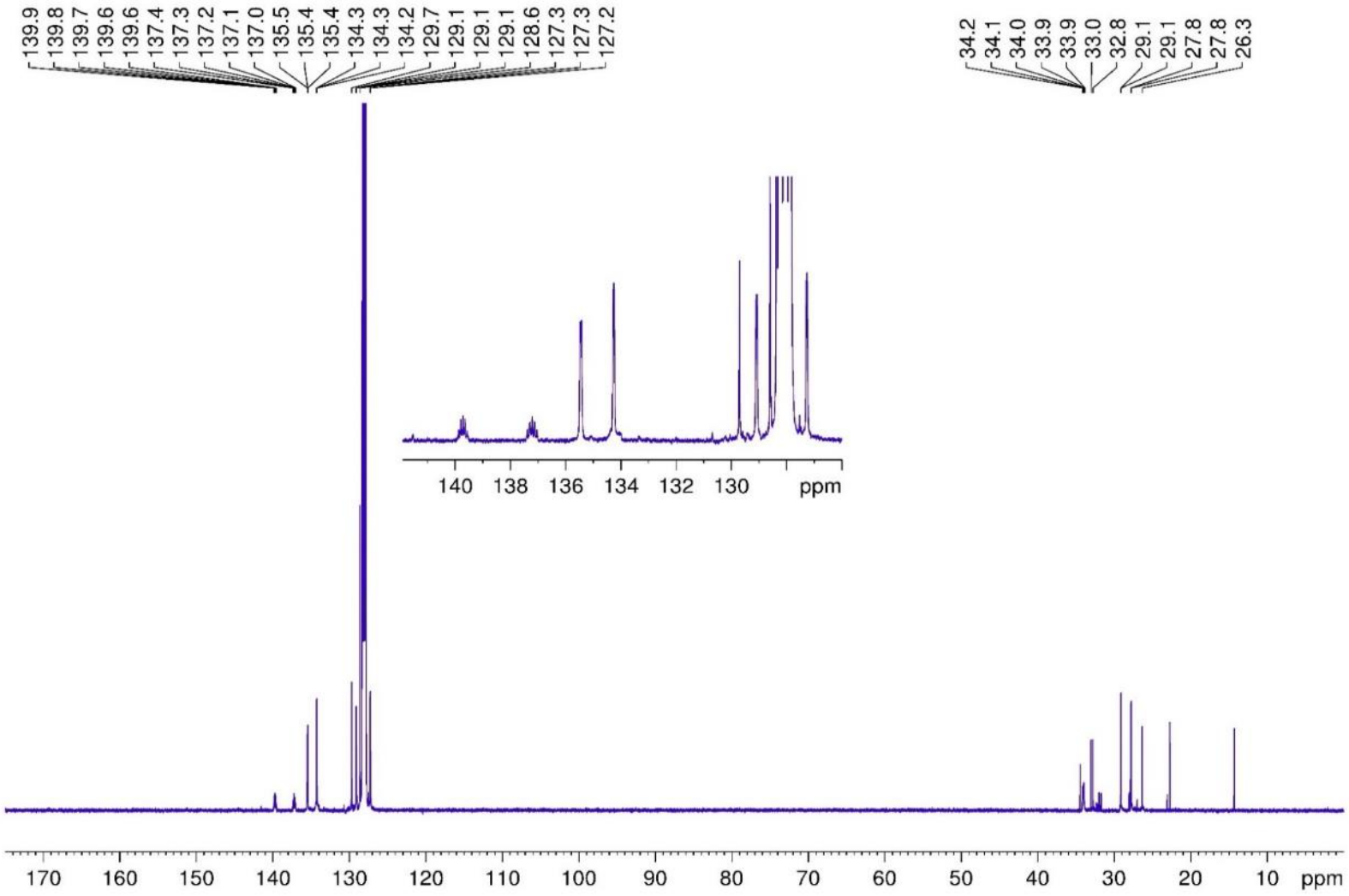

Figure S10. $^{13}C\{^{1}H\}$ NMR spectrum of **1-PCy$_3$** in C_6D_6. The additional resonances at 14.3, 22.7 and 34.5 ppm correspond to residual pentane and additional resonances at 14.3, 23.0 and 32.0 ppm to residual hexane.

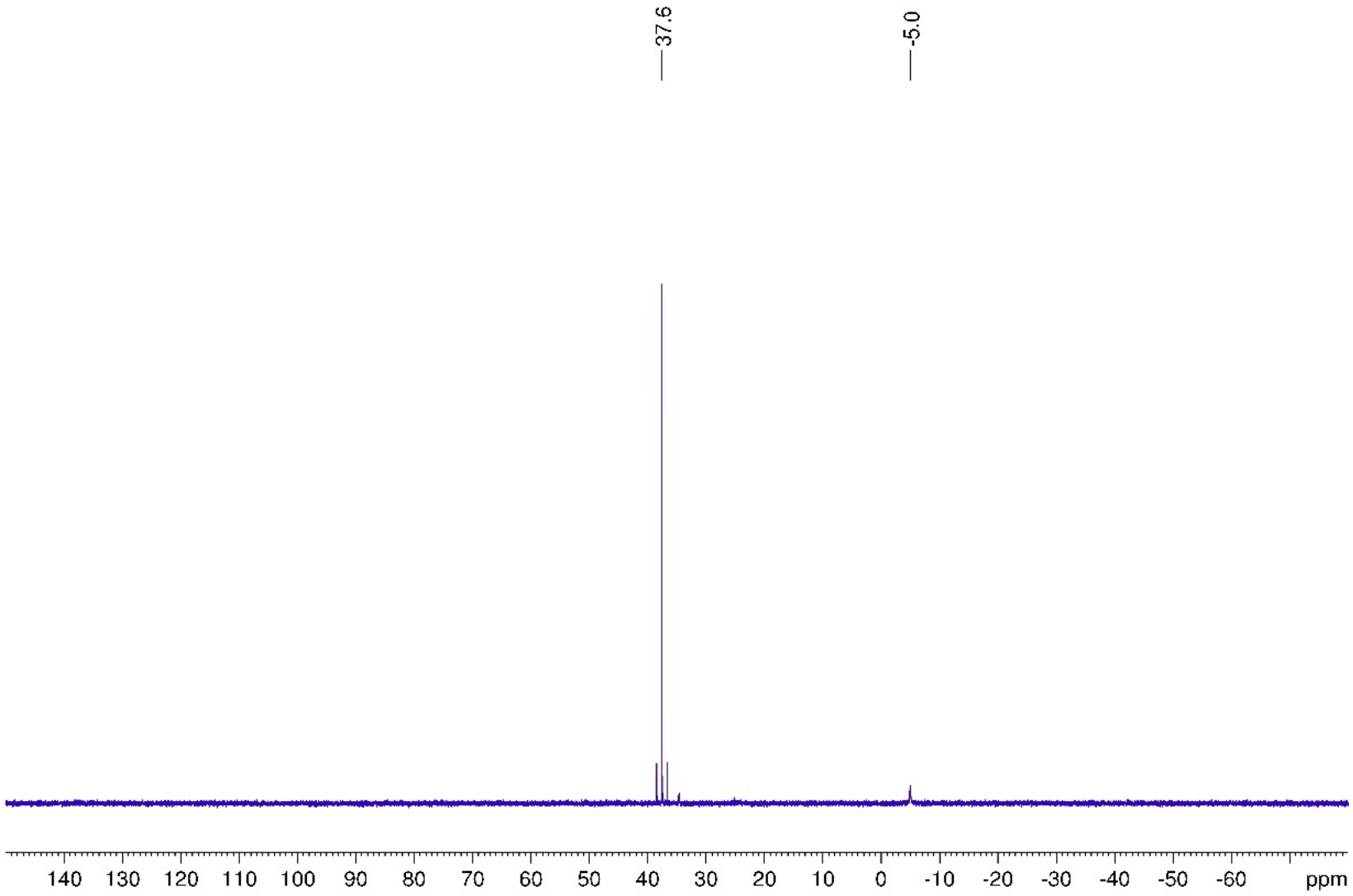

Figure S11. $^{31}P\{^{1}H\}$ NMR spectrum of **1-PCy$_3$** in C_6D_6.

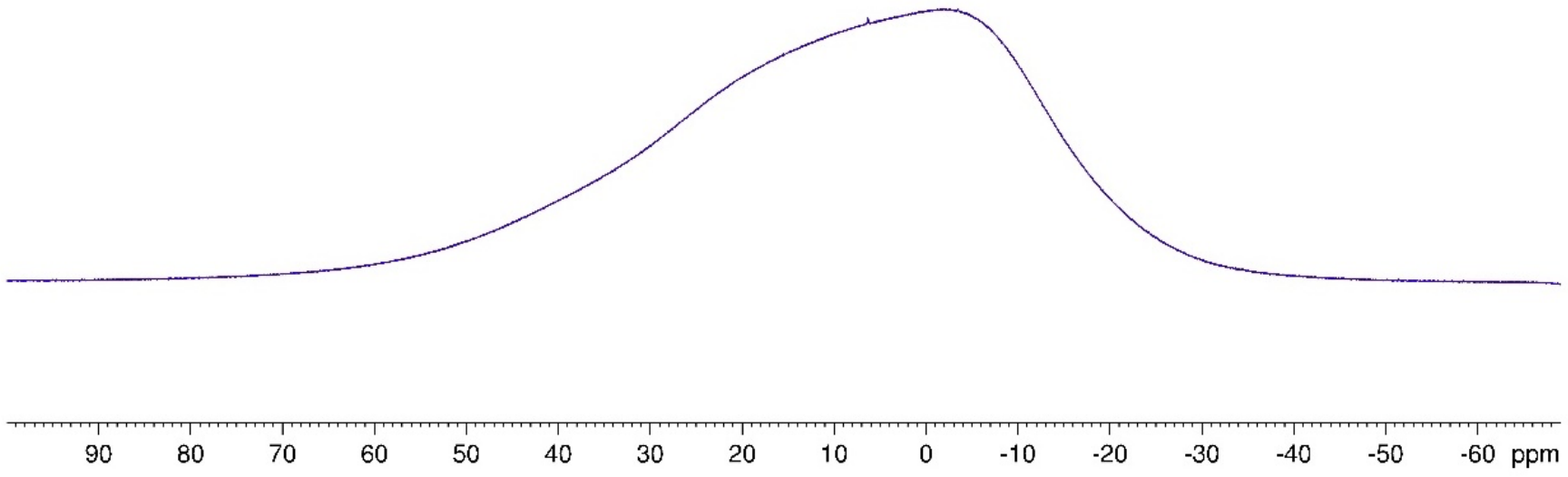

Figure S12. ^{11}B NMR spectrum of **1-PCy$_3$** in C_6D_6.

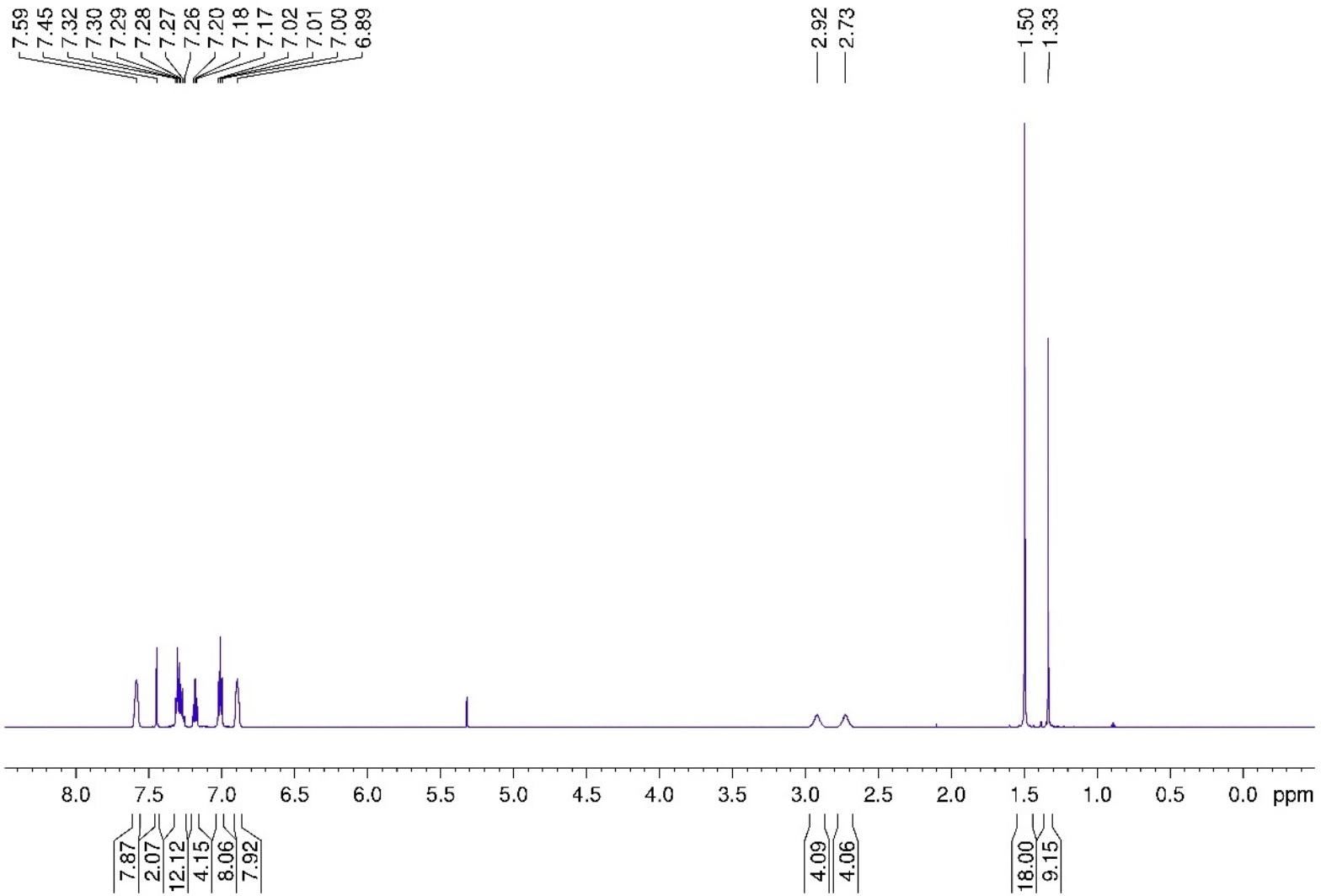

Figure S13. ^{1}H NMR spectrum of **1-CNMes*** in CD_2Cl_2. The additional resonances at 0.89 and 1.30 ppm correspond to residual pentane.

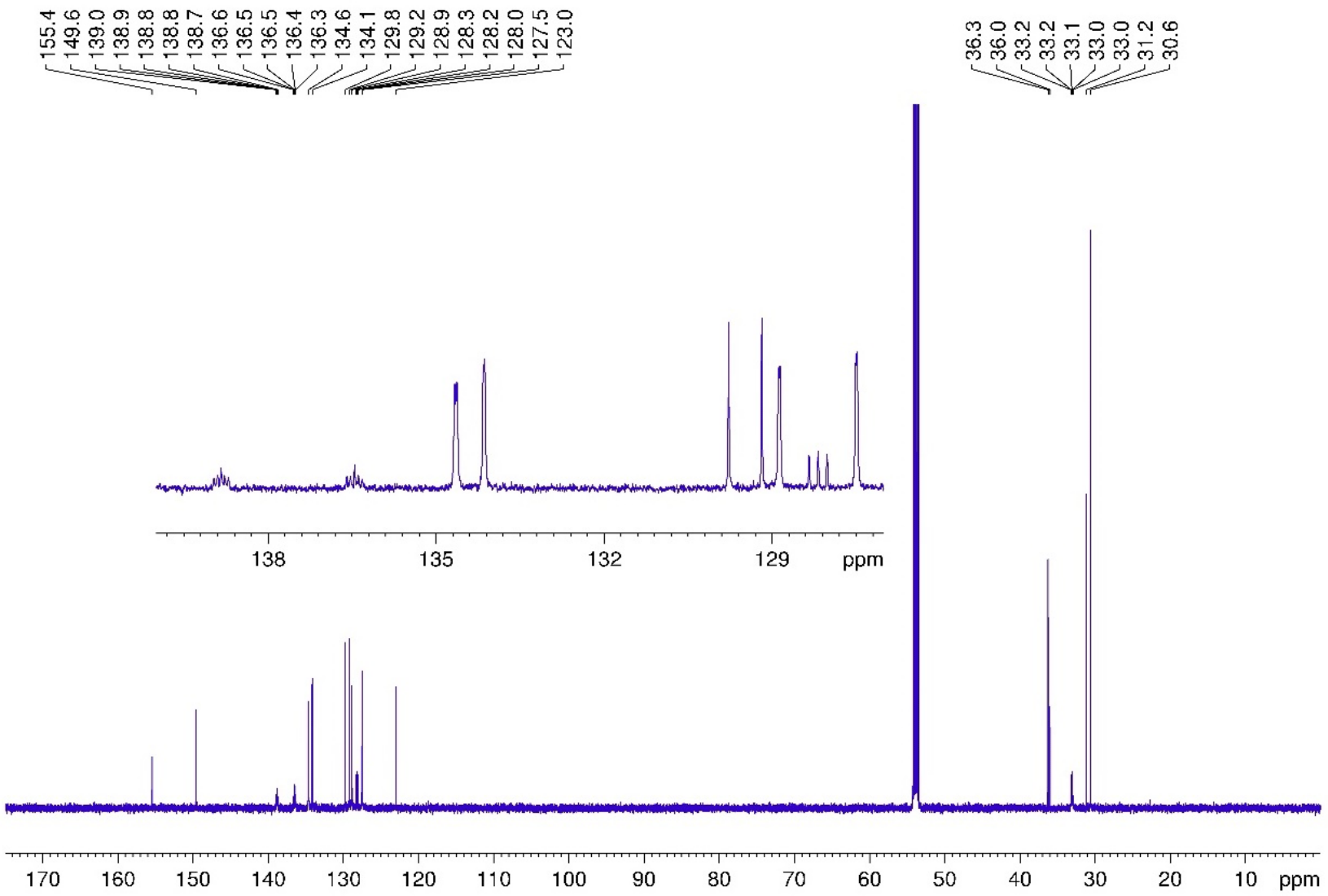

Figure S14. $^{13}C\{^{1}H\}$ NMR spectrum of **1-CNMes*** in CD_2Cl_2.

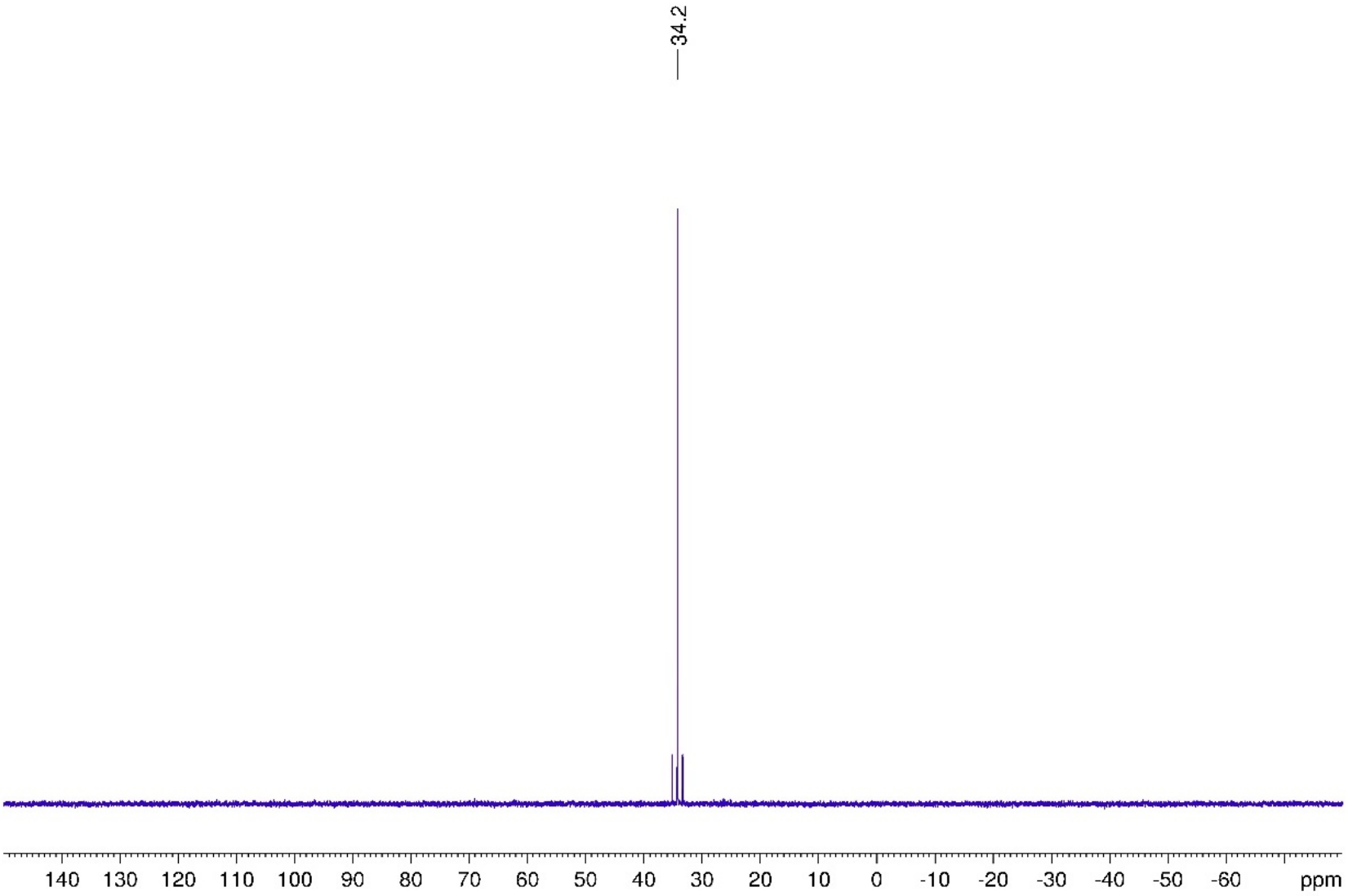

Figure S15. $^{31}P\{^{1}H\}$ NMR spectrum of **1-CNMes*** in CD_2Cl_2.

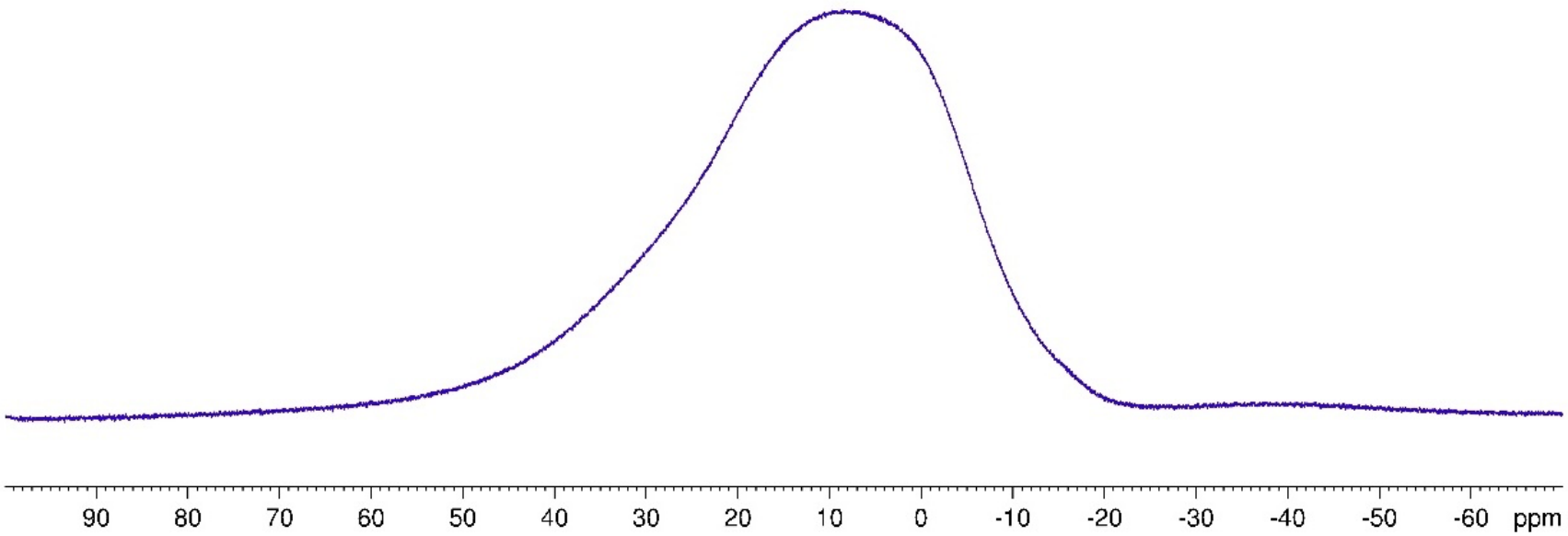

Figure S16. $^{11}B\{^{1}H\}$ NMR spectrum of **1-CNMes*** in CD_2Cl_2

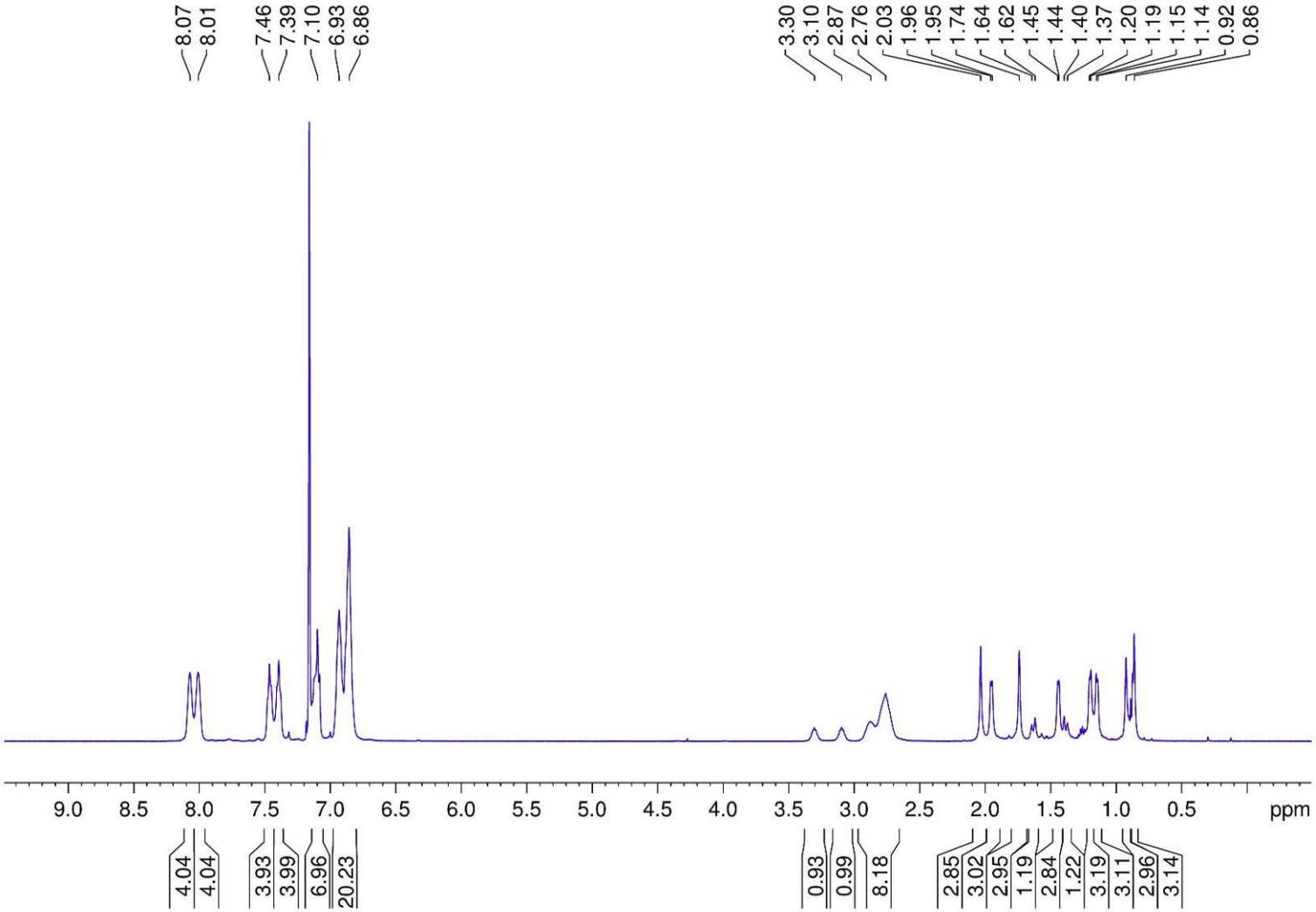

Figure S17. ^{1}H NMR spectrum of **1-CAAC** in C_6D_6. The additional resonances at 0.87 and 1.26 ppm correspond to residual pentane.

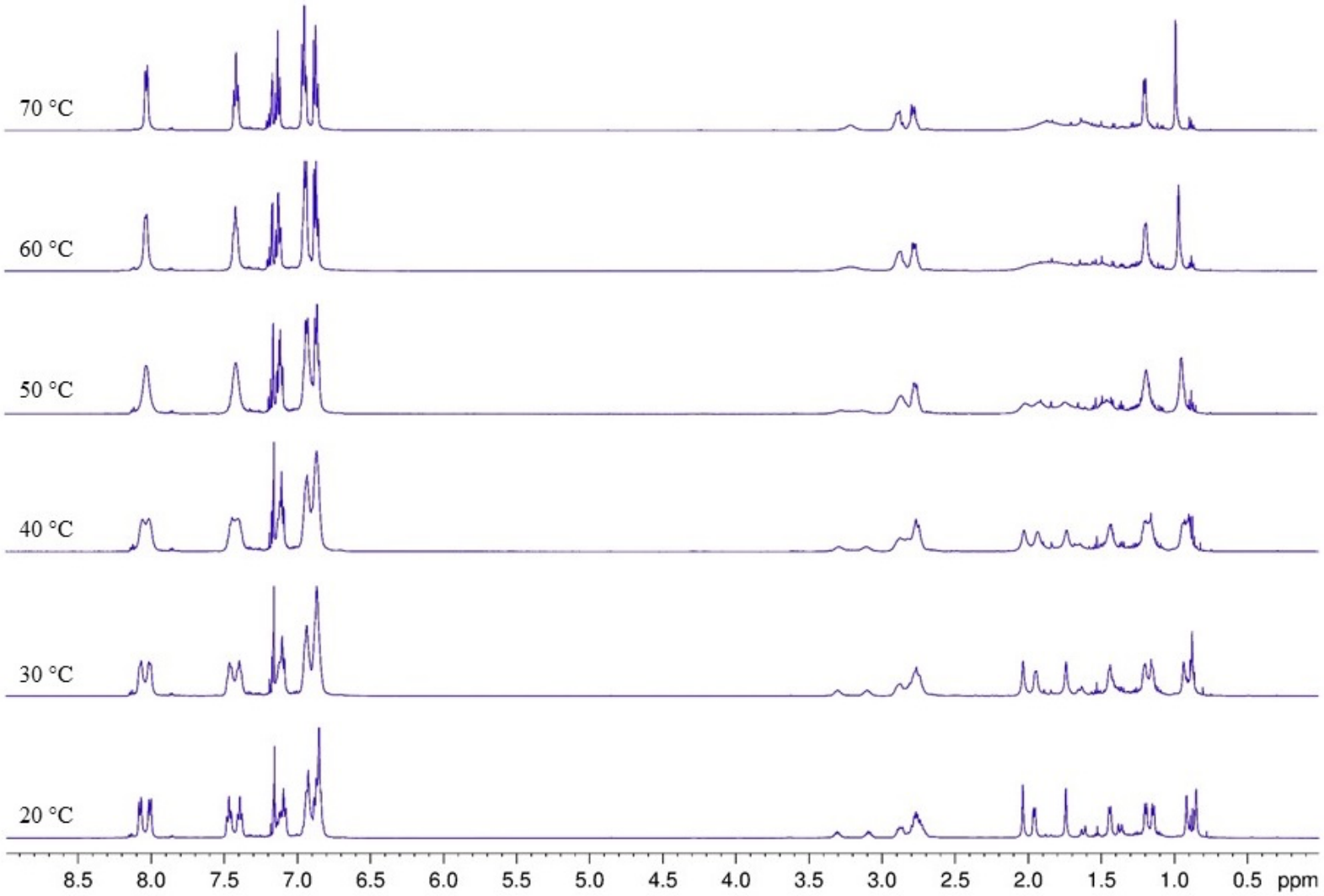

Figure S18. Stack-plot of $^{1}H\{^{31}P\}$ NMR spectra at variable temperature of **1-CAAC** in C_6D_6. The additional resonances at 0.87 and 1.26 ppm correspond to residual pentane.

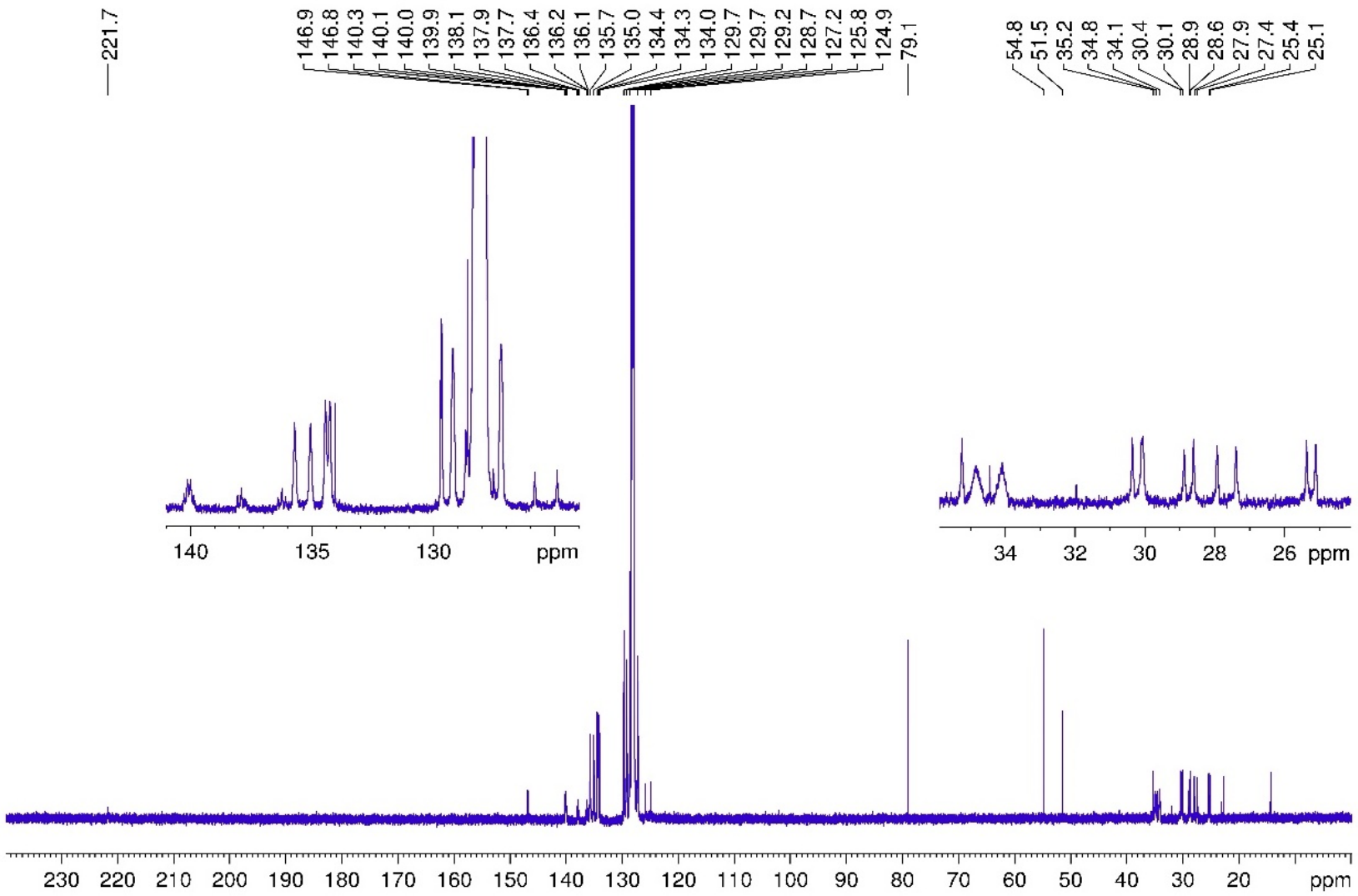

Figure S19. $^{13}C\{^{1}H\}$ NMR spectrum of **1-CAAC** in C_6D_6. The additional resonances at 14.3, 22.7 and 34.5 ppm correspond to residual pentane.

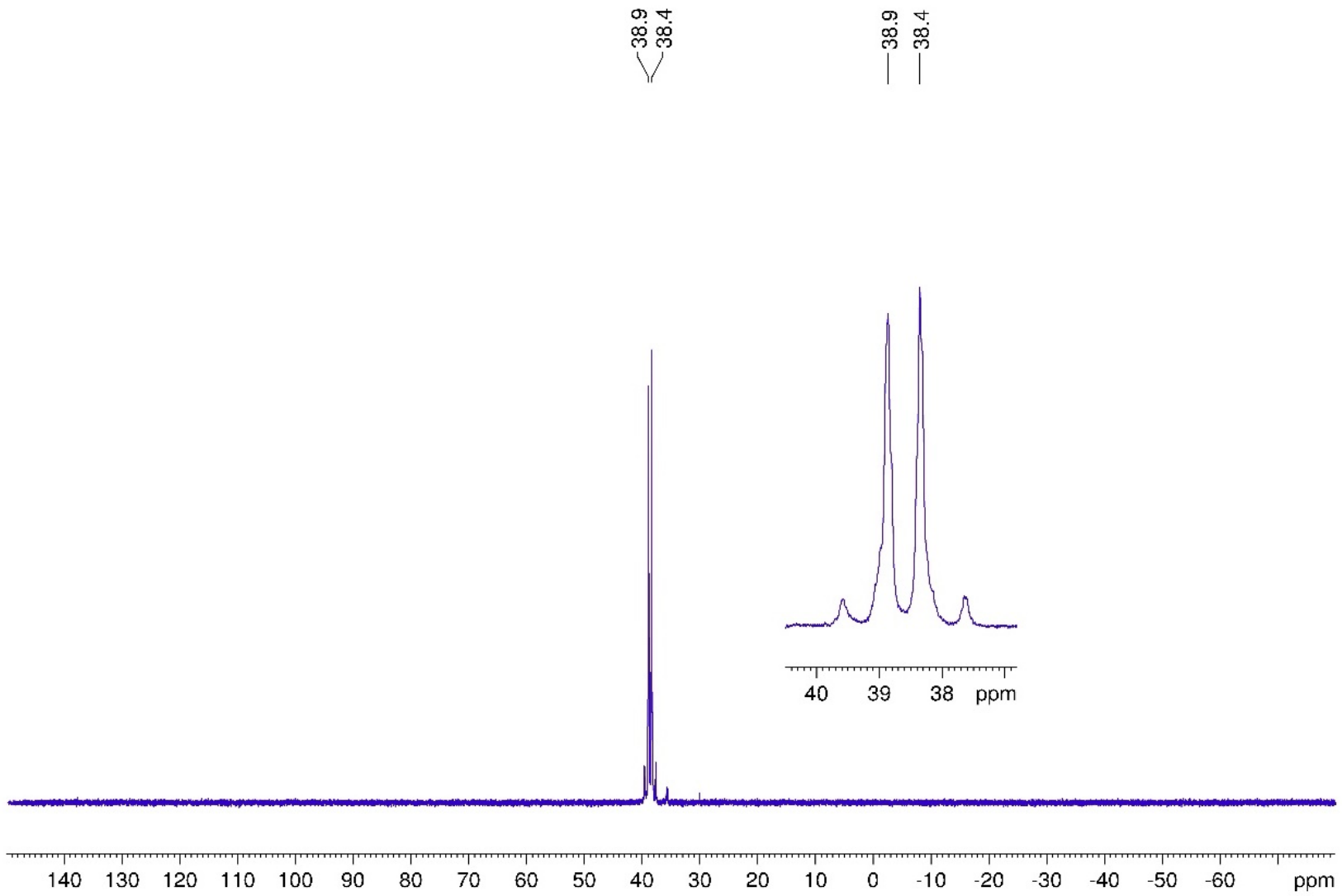

Figure S20. $^{31}P\{^{1}H\}$ NMR spectrum of **1-CAAC** in C_6D_6.

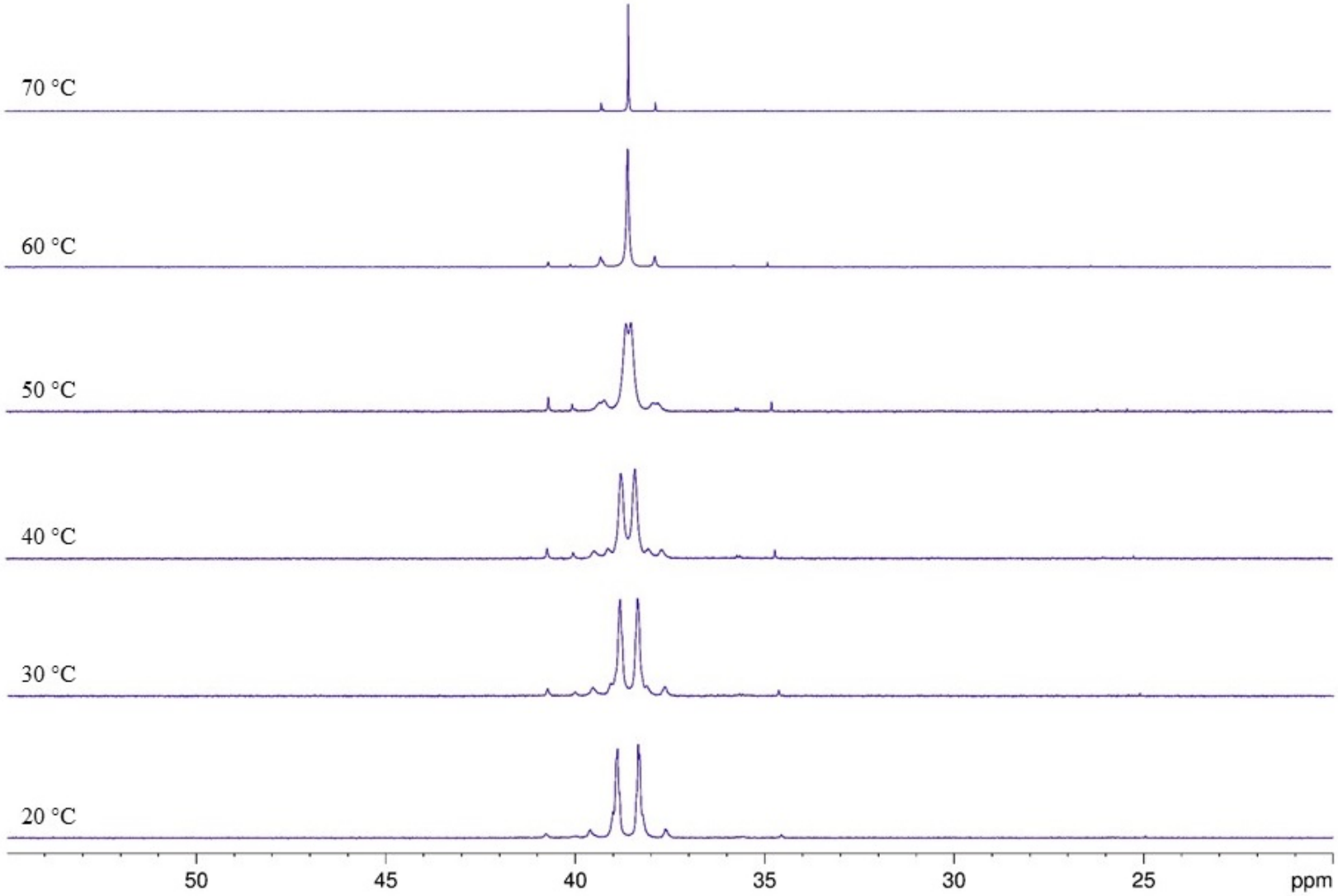

Figure S21. Stack-plot of $^{31}P\{^{1}H\}$ NMR spectra at variable temperature of **1-CAAC** in C_6D_6.

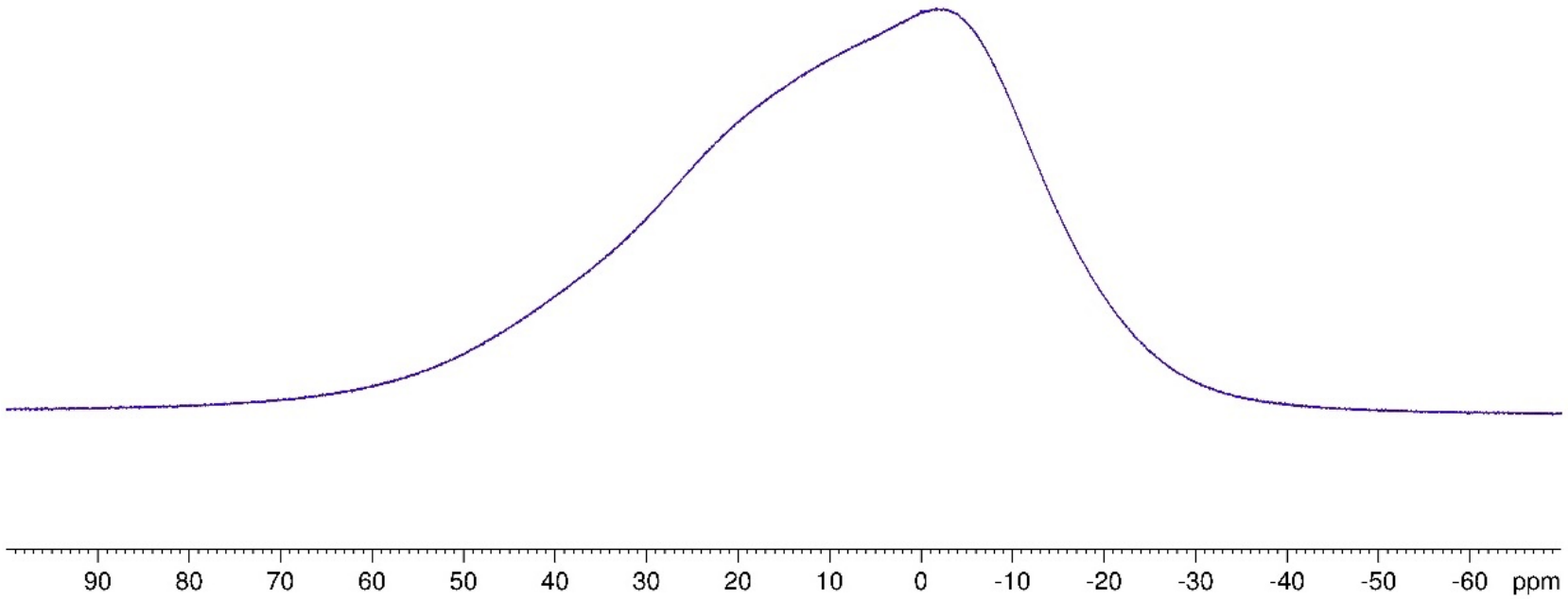

Figure S22. ^{11}B NMR spectrum of **1-CAAC** in C_6D_6.

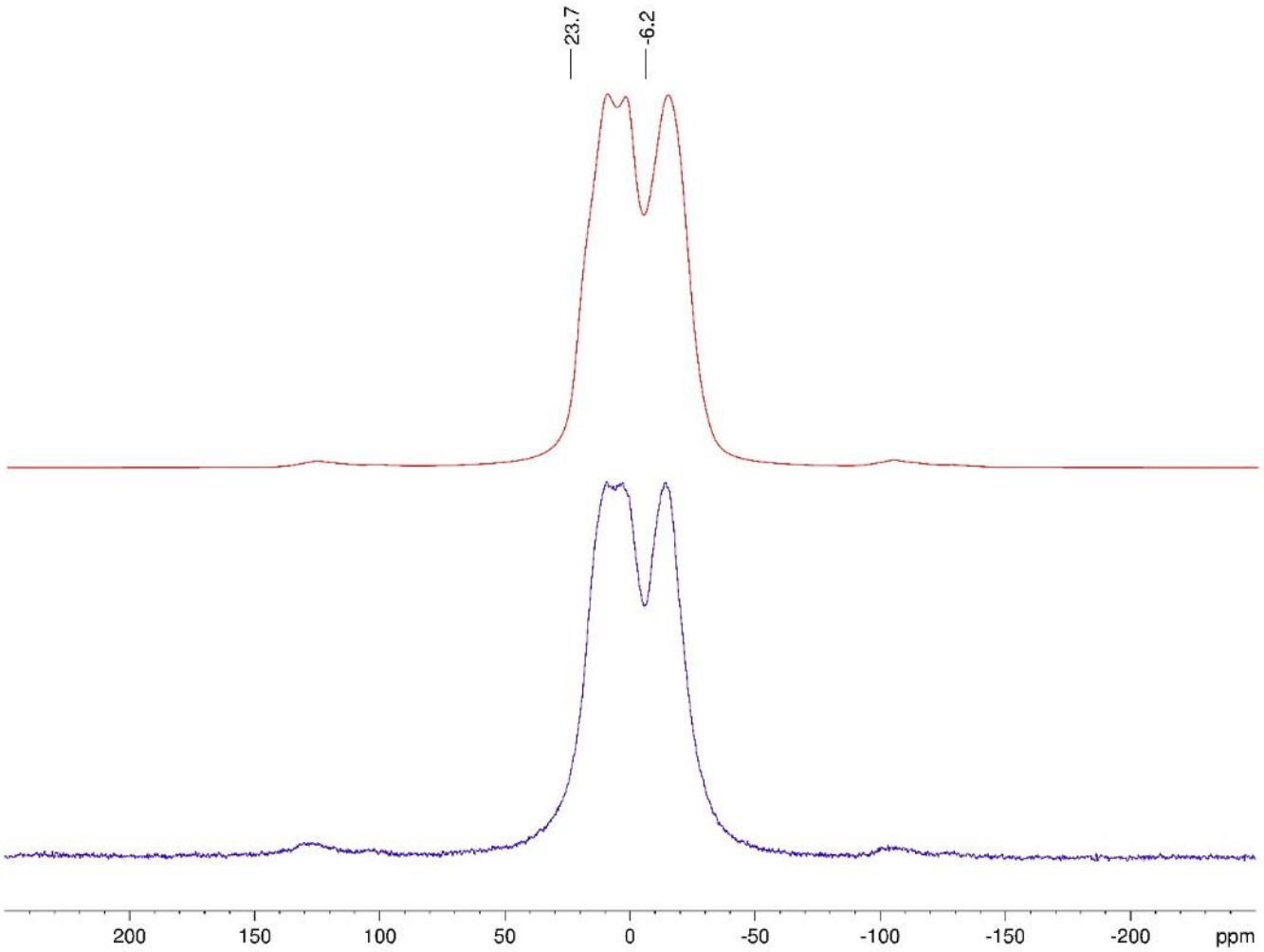

Figure S23. Solid-state ^{11}B RSHE/MAS NMR spectrum of **1-CAAC** at 14.8 kHz (top: Simulation). (N-*B*-B): Isotropic chemical shift δ_{iso} = 23.7 ppm, quadrupolar coupling constant C_Q = 3200 MHz, quadrupolar asymmetry parameter η_Q = 0.50; (N-B-*B*): Isotropic chemical shift δ_{iso} = –6.2 ppm, quadrupolar coupling constant C_Q = 2400 MHz, quadrupolar asymmetry parameter η_Q = 0.46.

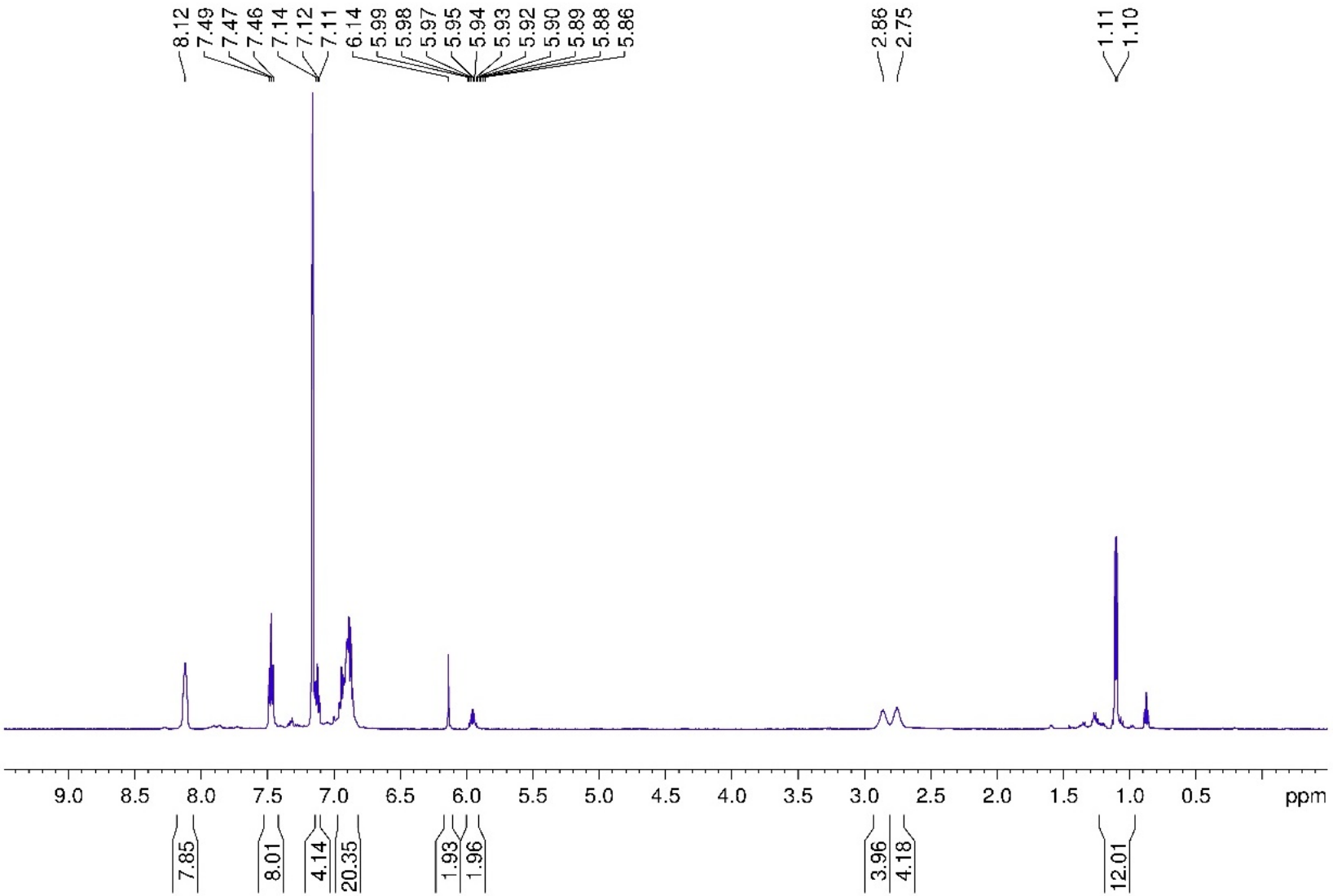

Figure S24. ^{1}H NMR spectrum of **1-I*i*Pr** in C_6D_6. The additional resonances at 0.87 and 1.26 ppm correspond to residual pentane.

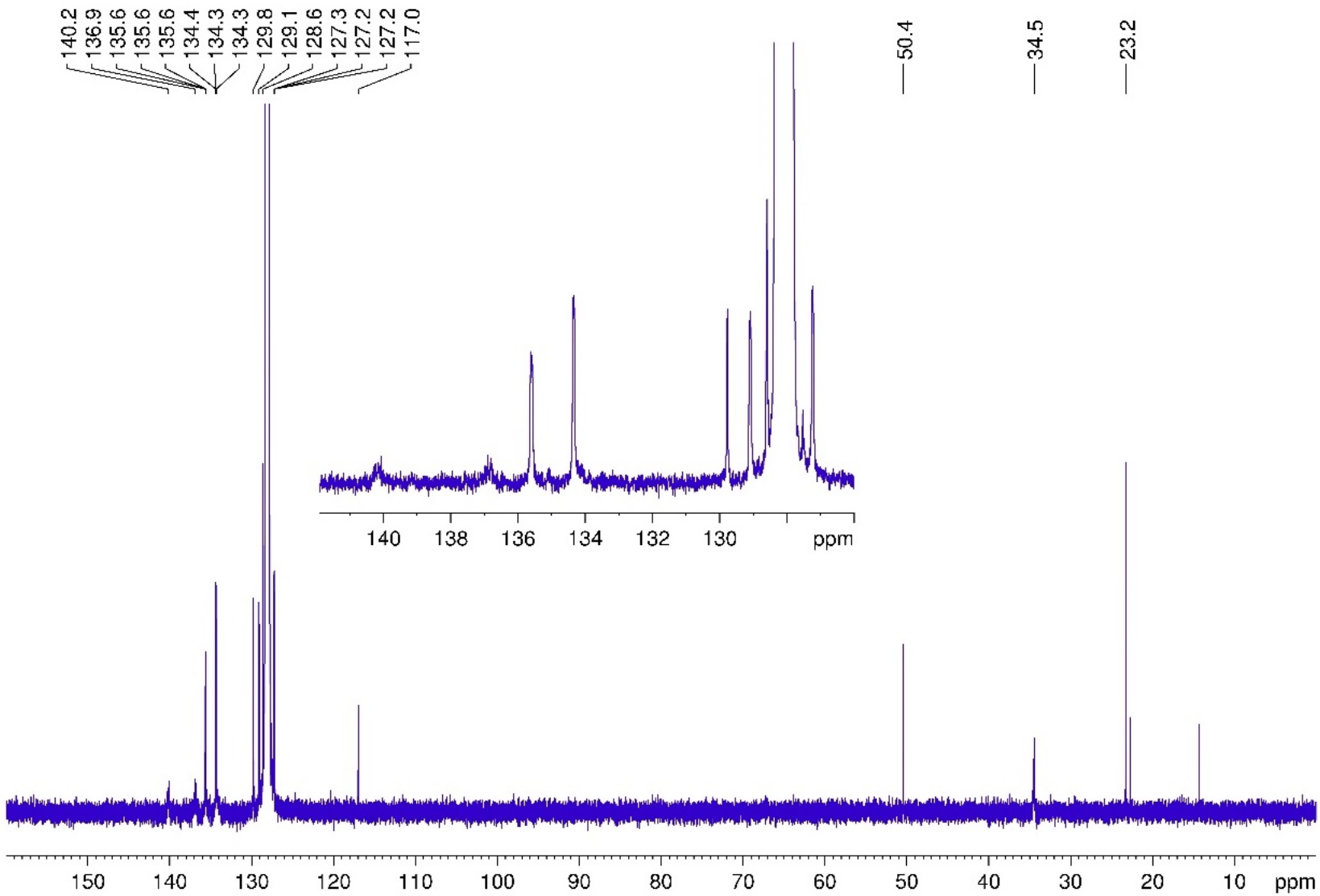

Figure S25. $^{13}C\{^{1}H\}$ NMR spectrum of **1-I*i*Pr** in C_6D_6. The additional resonances at 14.3, 22.7 and 34.4 ppm correspond to residual pentane.

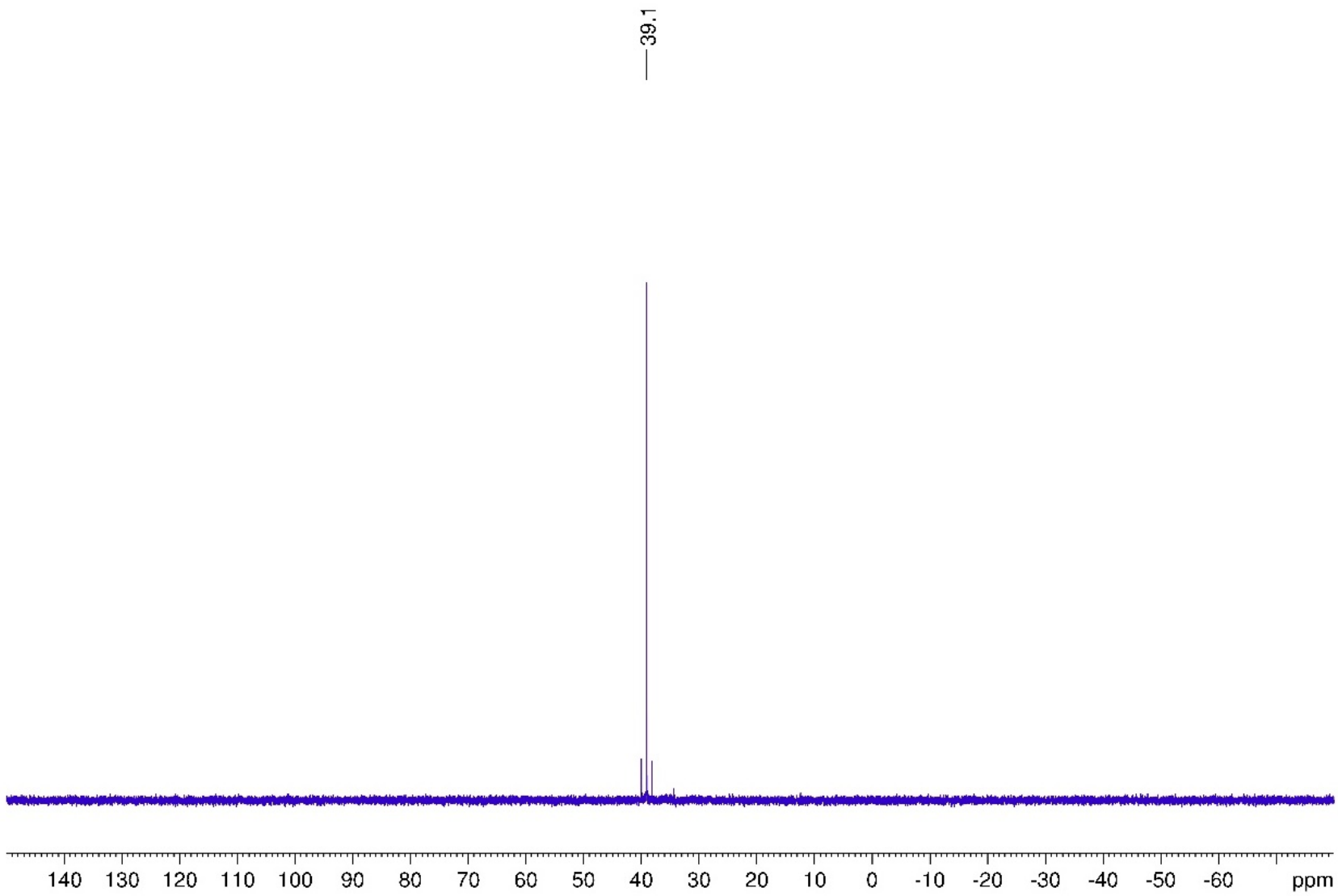

Figure S26. $^{31}P\{^{1}H\}$ NMR spectrum of **1-I*i*Pr** in C_6D_6.

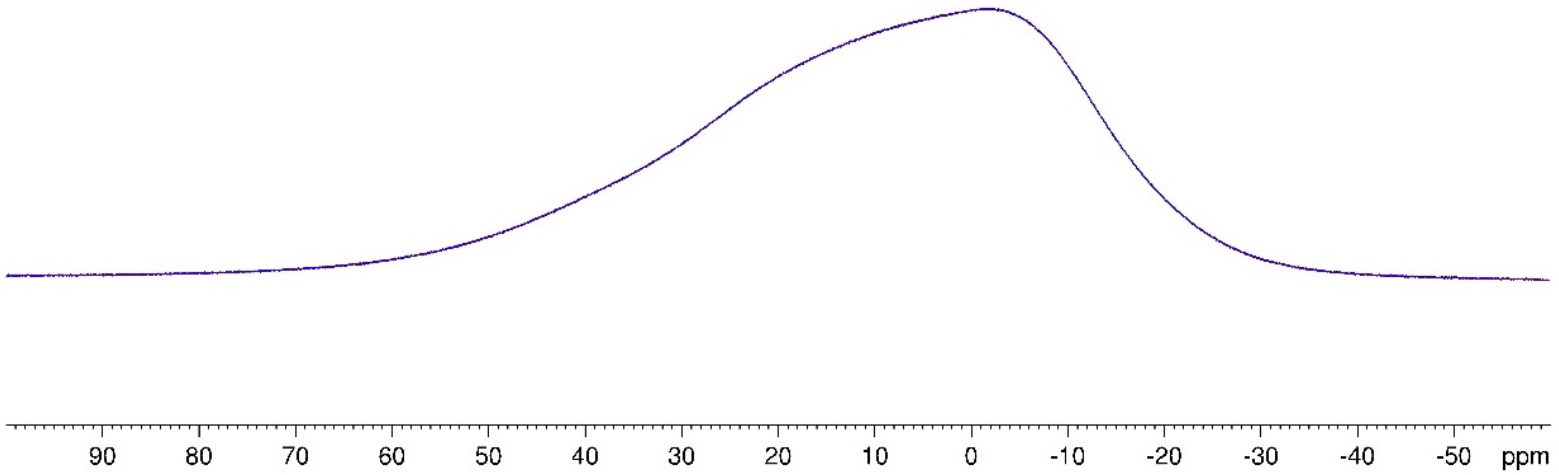

Figure S27. $^{11}B\{^{1}H\}$ NMR spectrum of **1-I*i*Pr** in C_6D_6.

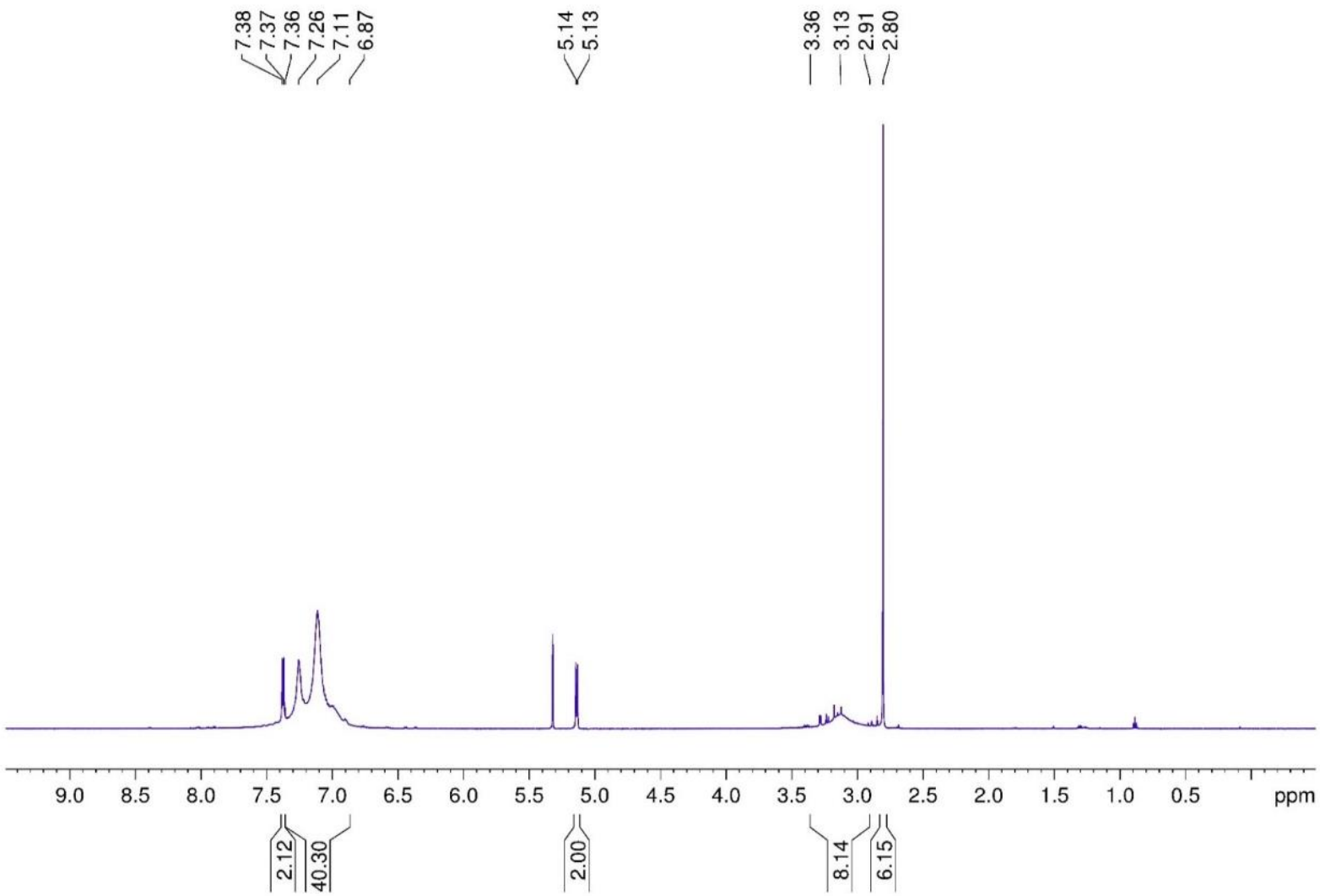

Figure S28. ^{1}H NMR spectrum of **3-DMAP** in CD_2Cl_2. The additional resonances at 0.89 and 1.30 ppm correspond to residual pentane.

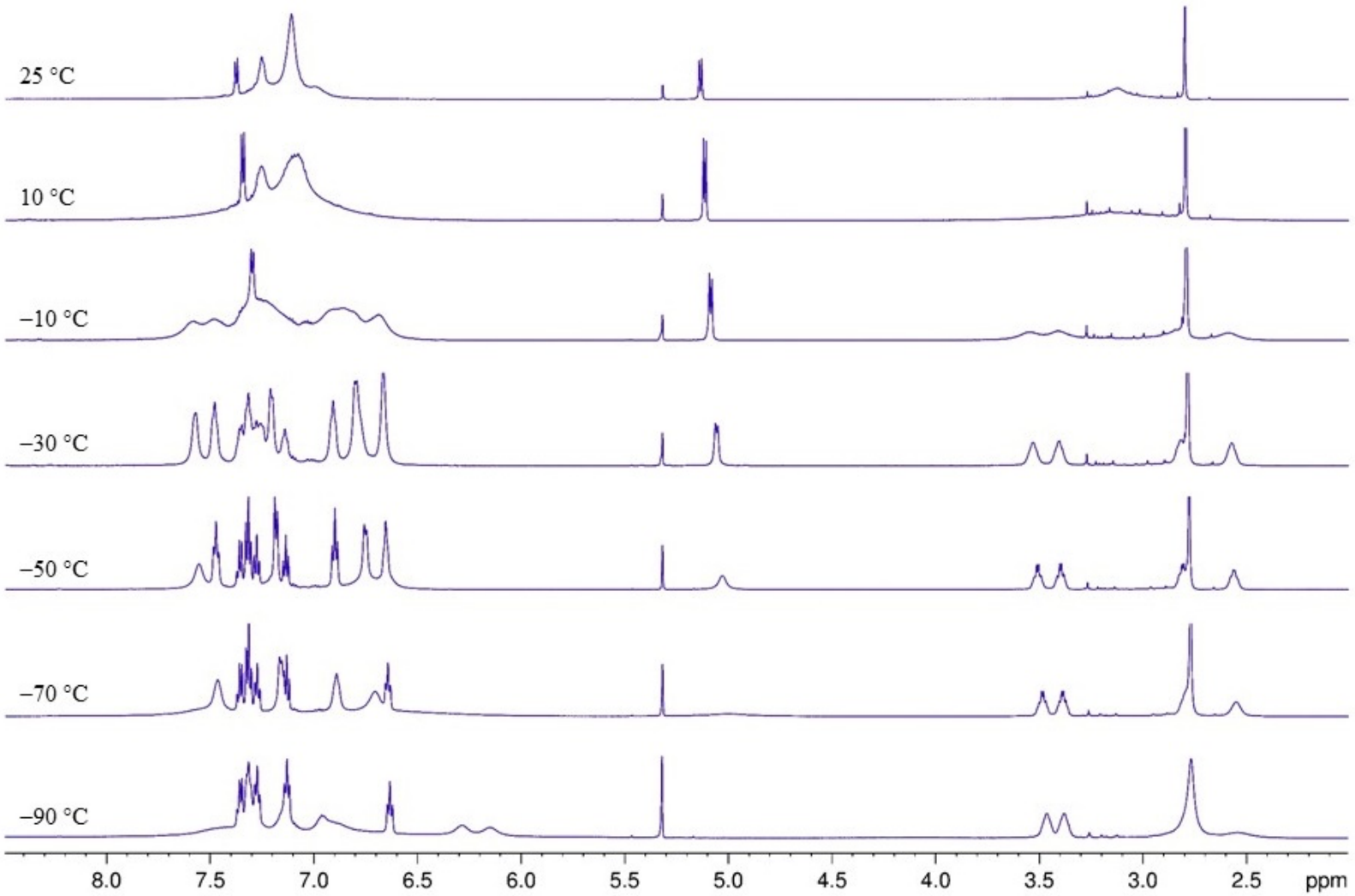

Figure S29. Stack-plot of $^{1}H\{^{31}P\}$ NMR spectra at variable temperature of **3-DMAP** in CD_2Cl_2.

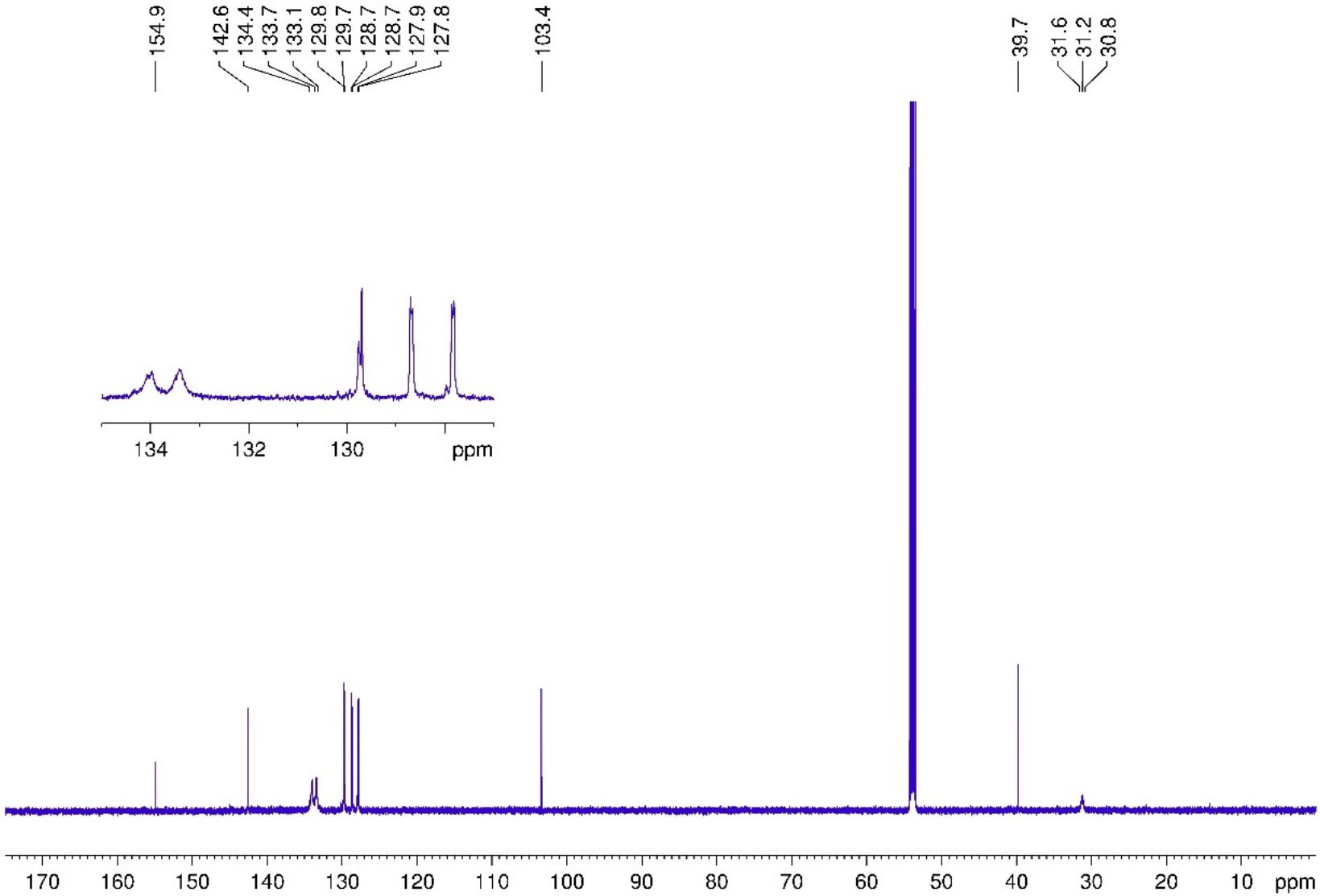

Figure S30. $^{13}C\{^{1}H\}$ NMR spectrum of **3-DMAP** in CD_2Cl_2.

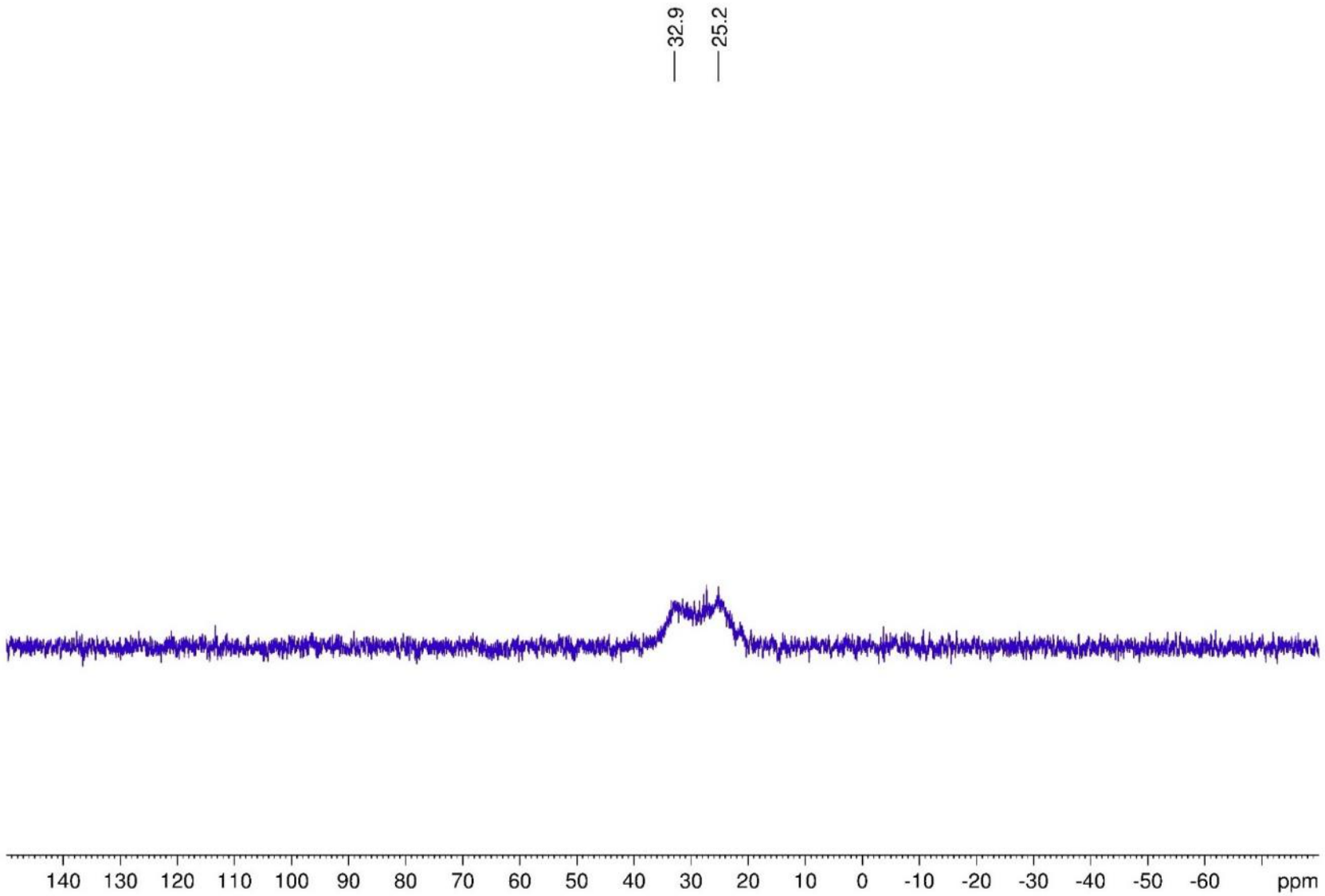

Figure S31. $^{31}P\{^{1}H\}$ NMR spectrum of **3-DMAP** in CD_2Cl_2.

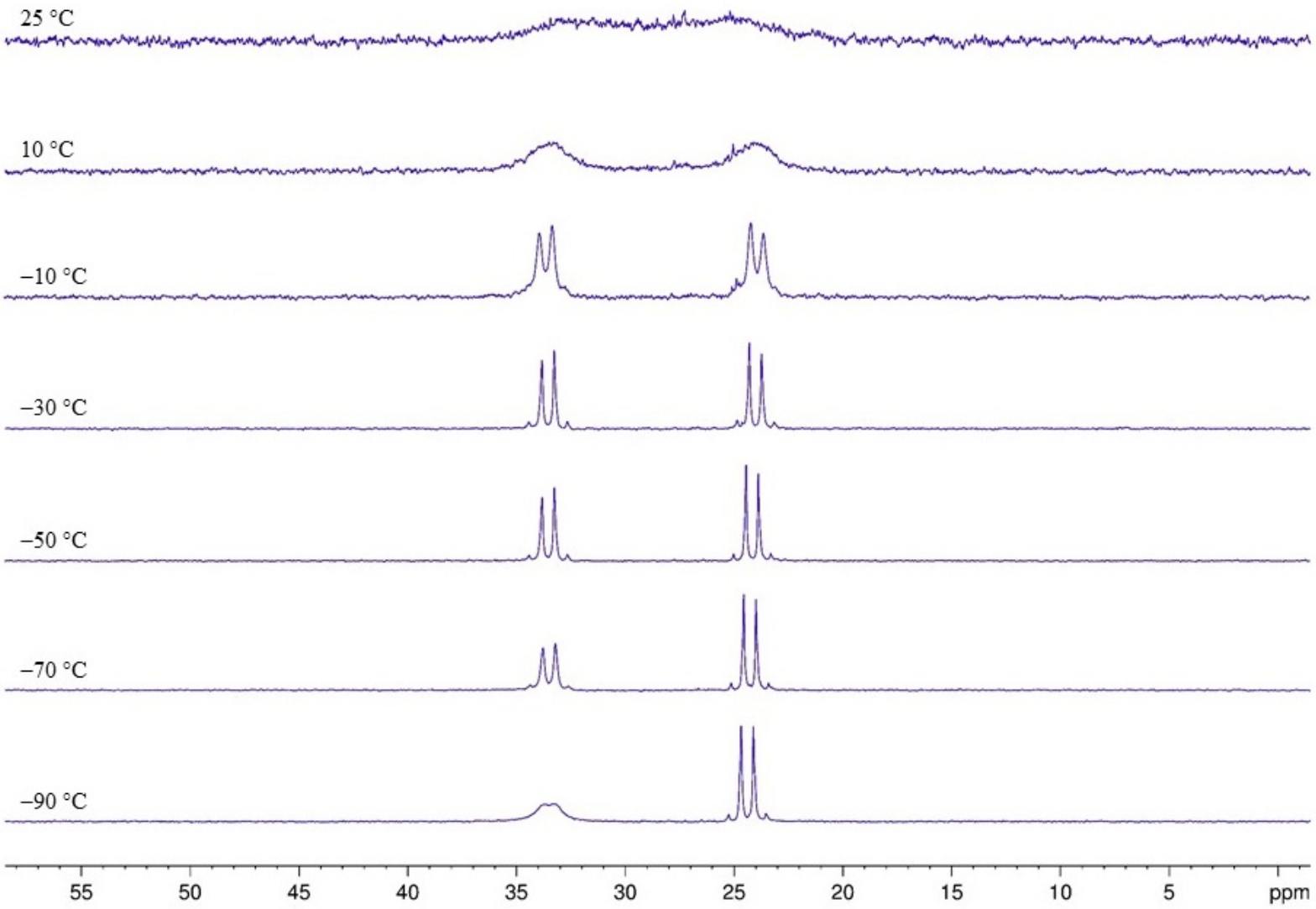

Figure S32. Stack-plot of $^{31}P\{^{1}H\}$ NMR spectra at variable temperature of **3-DMAP** in CD_2Cl_2.

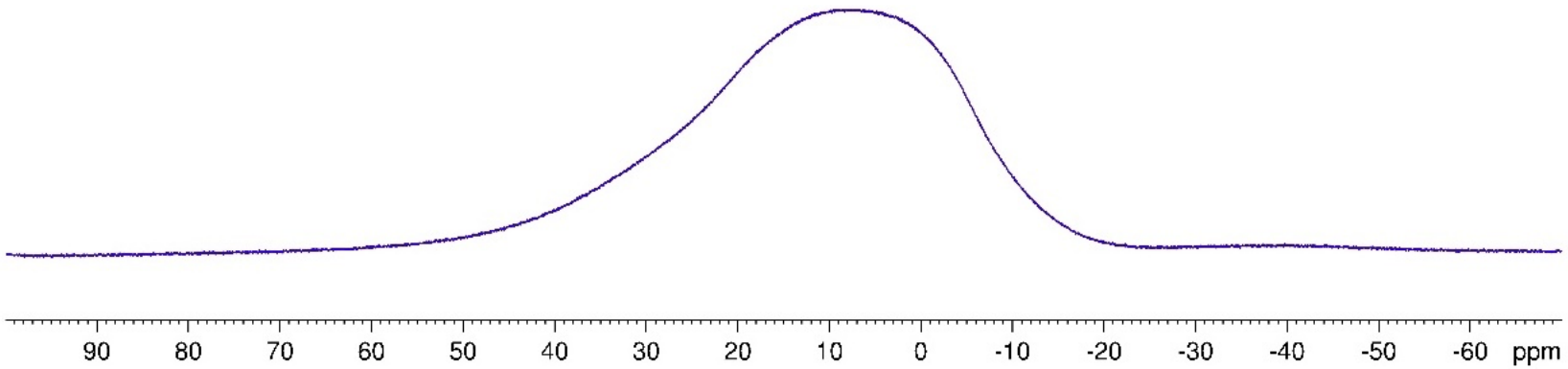

Figure S33. ^{11}B NMR spectrum of **3-DMAP** in CD_2Cl_2.

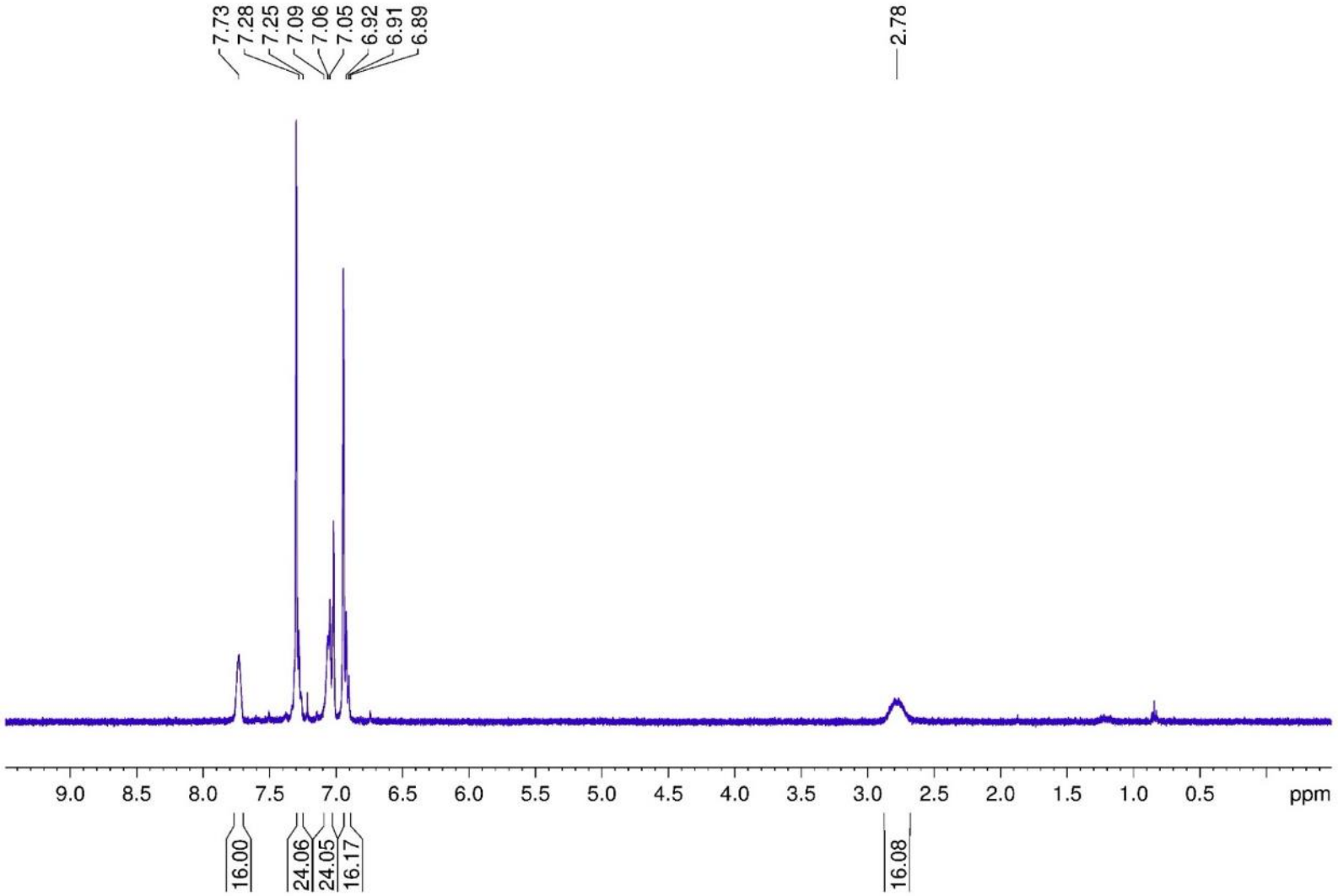

Figure S34. ^{1}H NMR spectrum of **2** in C_6D_5Br. The additional resonances at 0.85 and 1.22 ppm correspond to residual pentane and the additional resonance at 7.22 ppm to residual benzene.

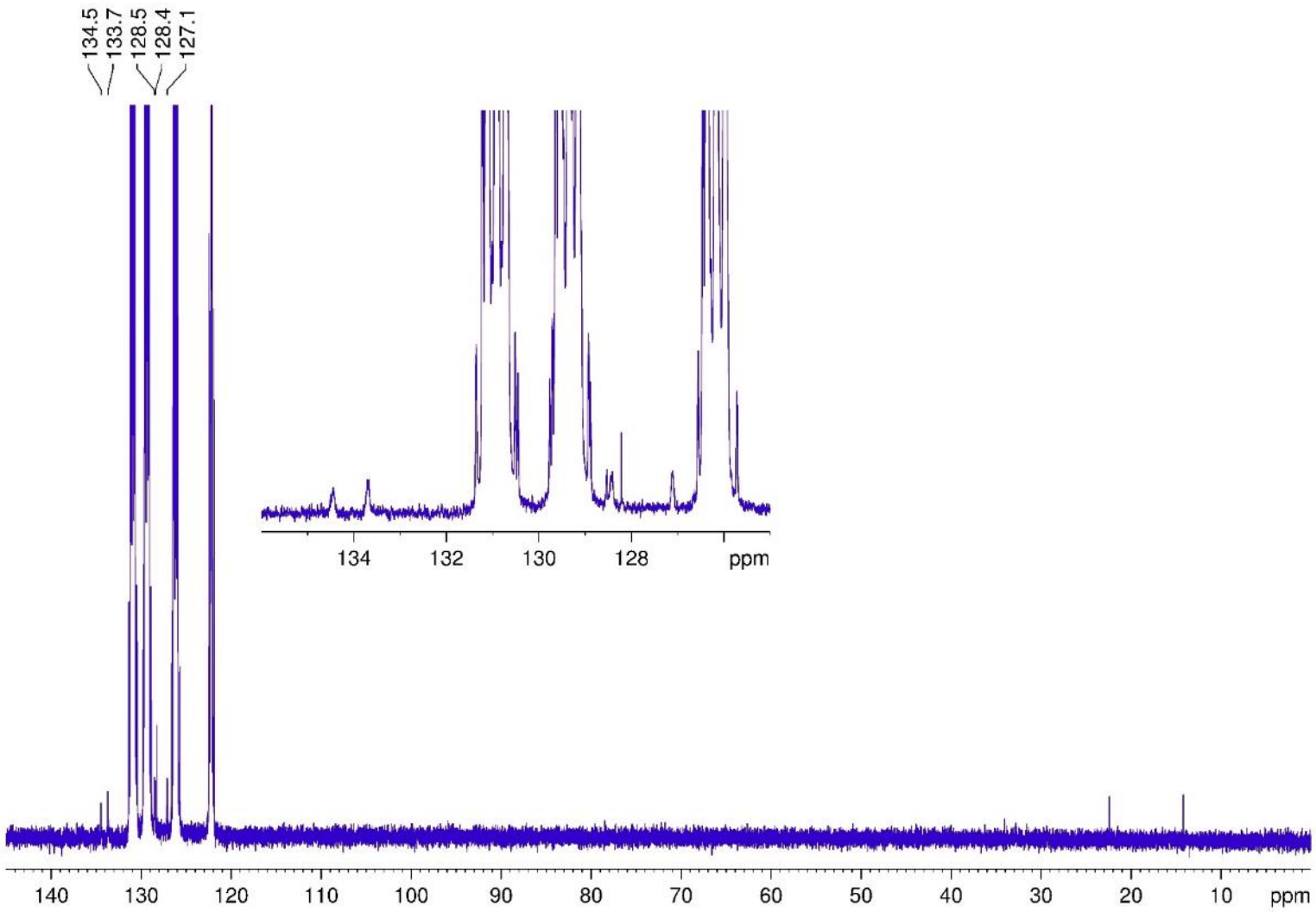

Figure S35. $^{13}C\{^{1}H\}$ NMR spectrum of **2** in C_6D_5Br. The additional resonances at 14.2, 22.4 and 34.0 ppm correspond to residual pentane and the resonance at 128.2 ppm to residual benzene.

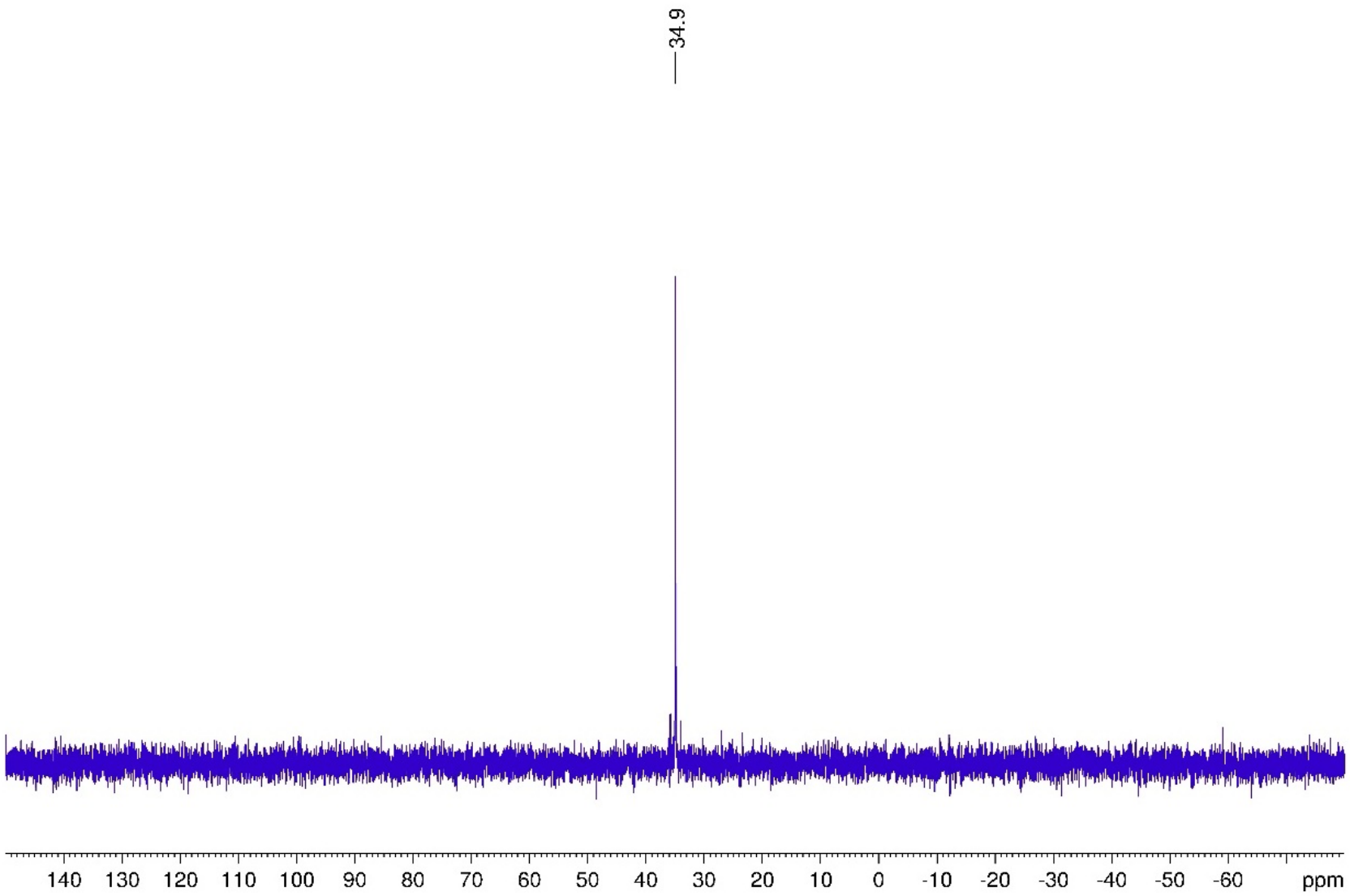

Figure S36. $^{31}P\{^{1}H\}$ NMR spectrum of **2** in C_6D_5Br.

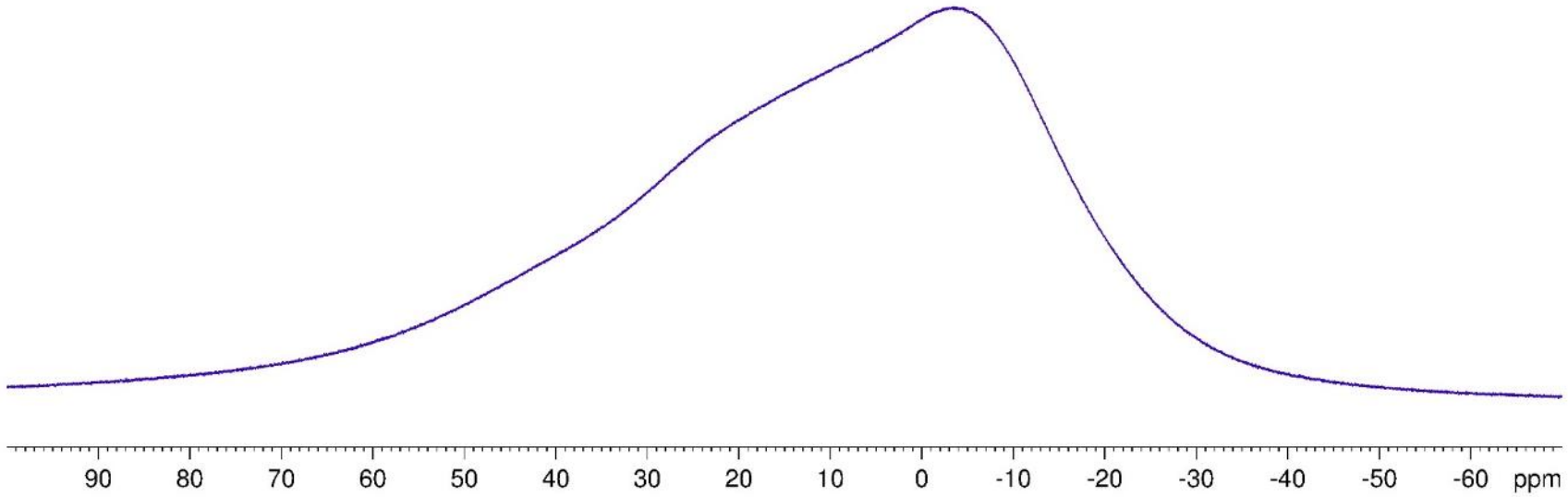

Figure S37. ^{11}B NMR spectrum of **2** in C_6D_5Br.

IR spectra

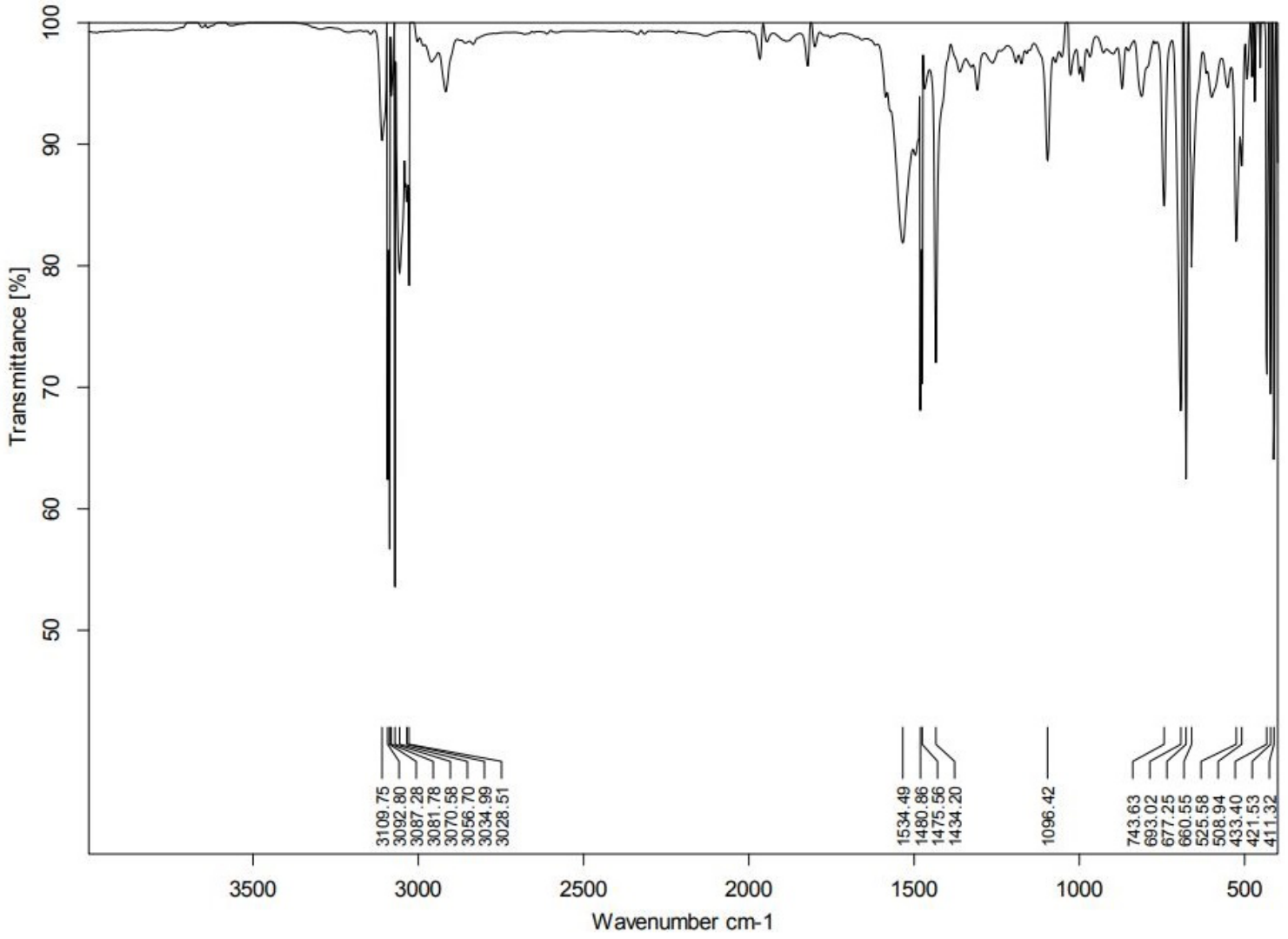

Figure S38. IR spectrum of **1-SMe$_2$** in benzene.

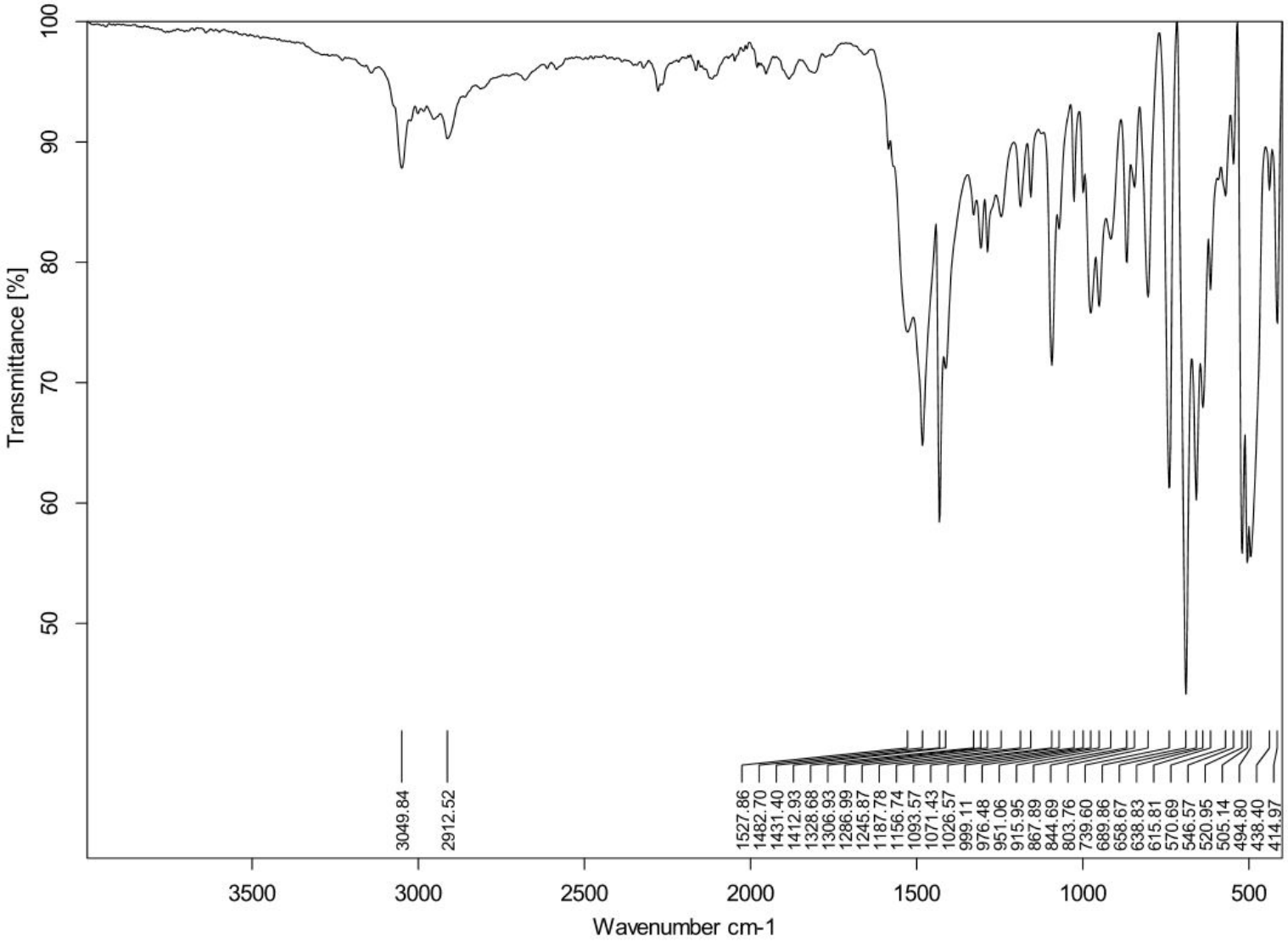

Figure S39. Solid-state IR spectrum of **1-PMe$_3$**.

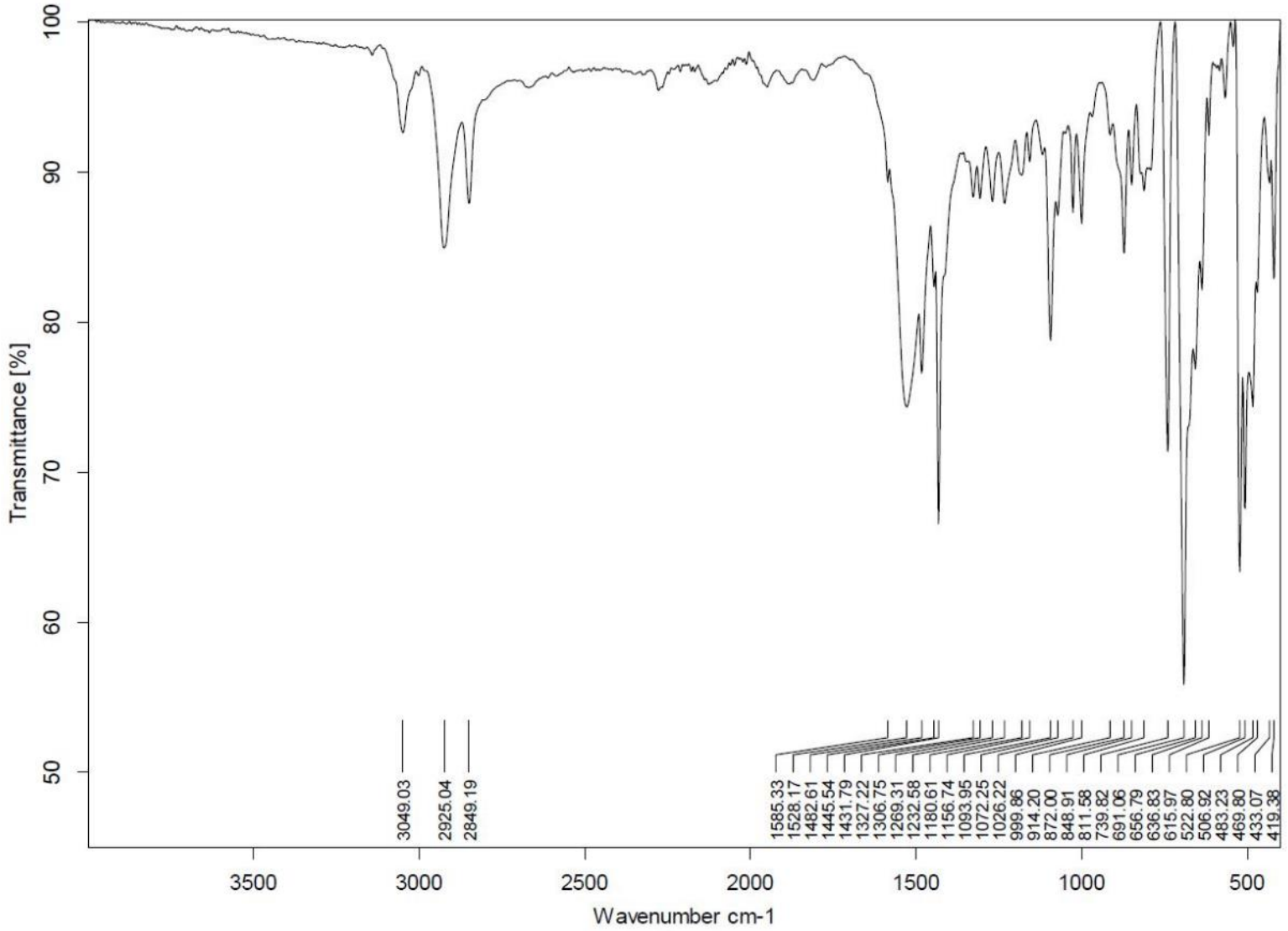

Figure S40. Solid-state IR spectrum of **1-PCy$_3$**.

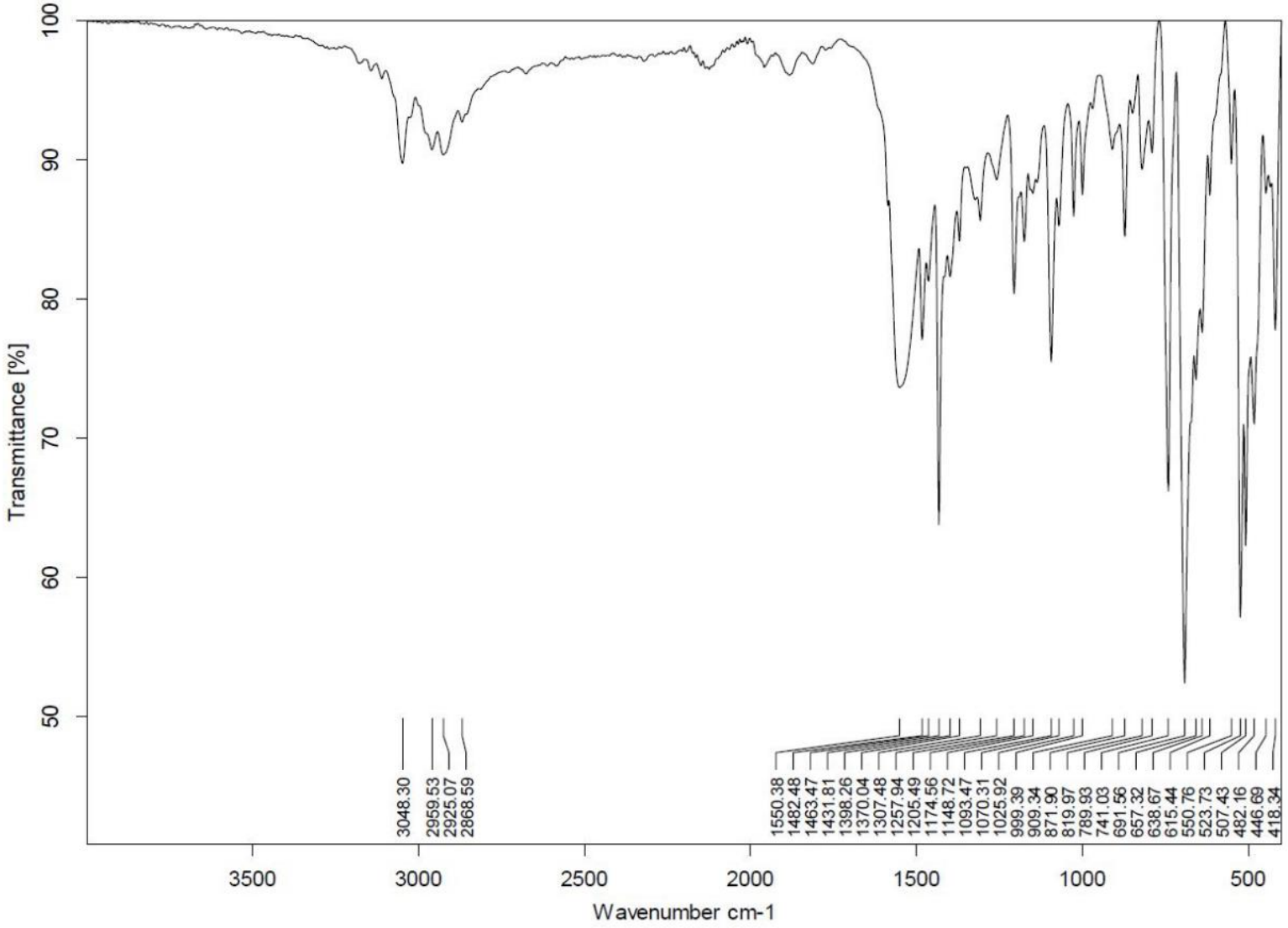

Figure S41. Solid-state IR spectrum of **1-IiPr**.

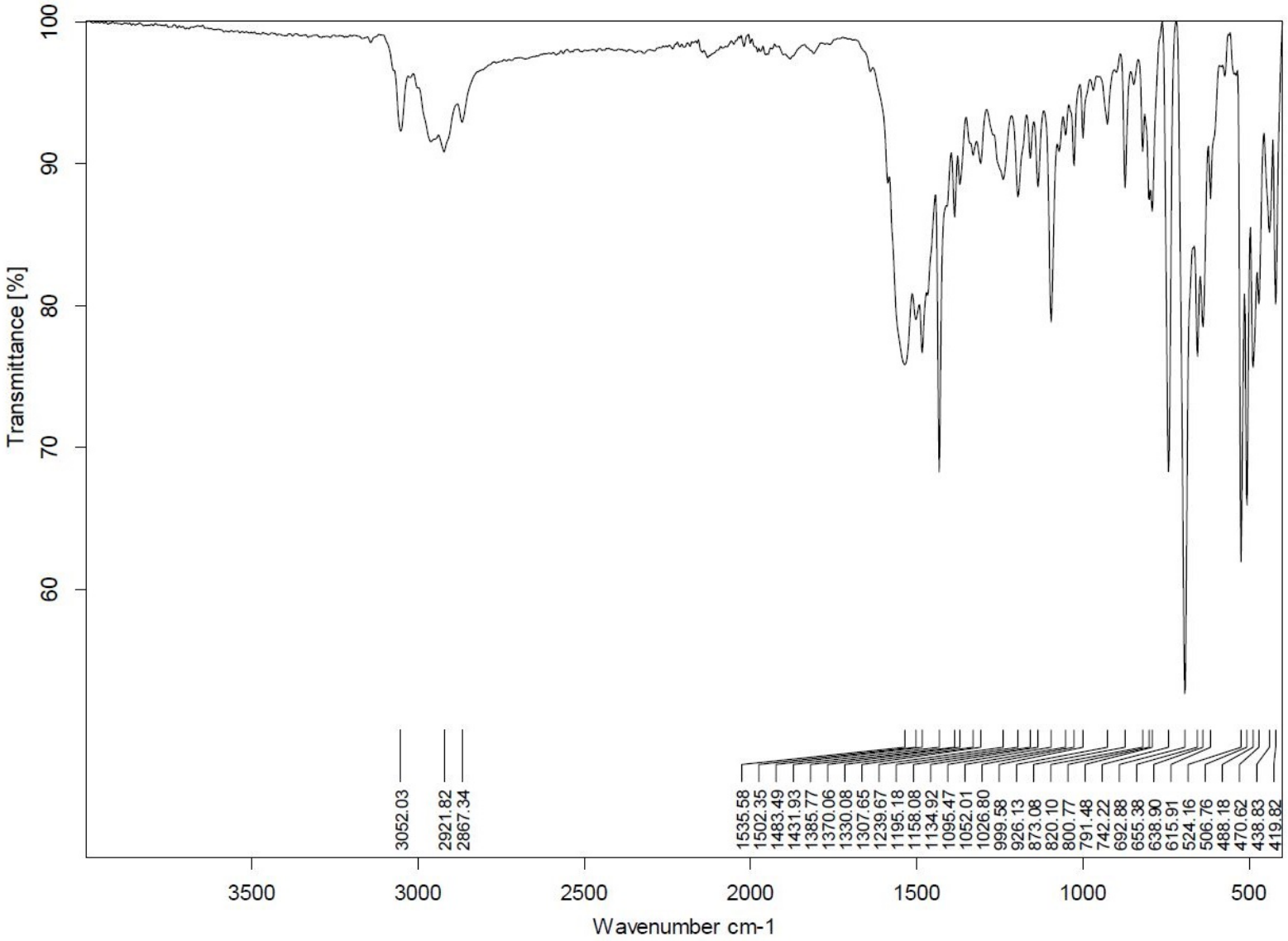

Figure S42. Solid-state IR spectrum of **1-CAAC**.

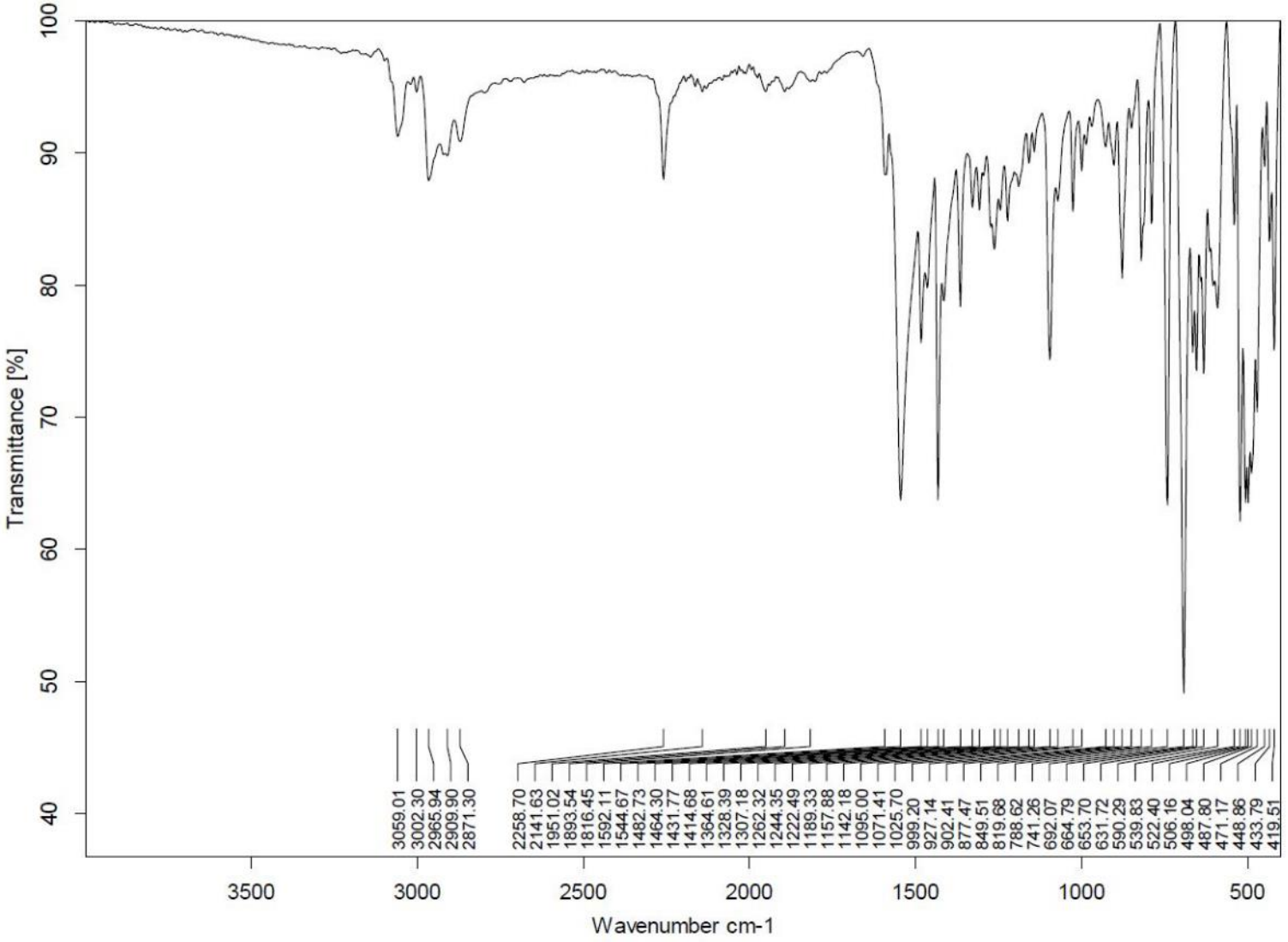

Figure S43. Solid-state IR spectrum of **1-CNMes***

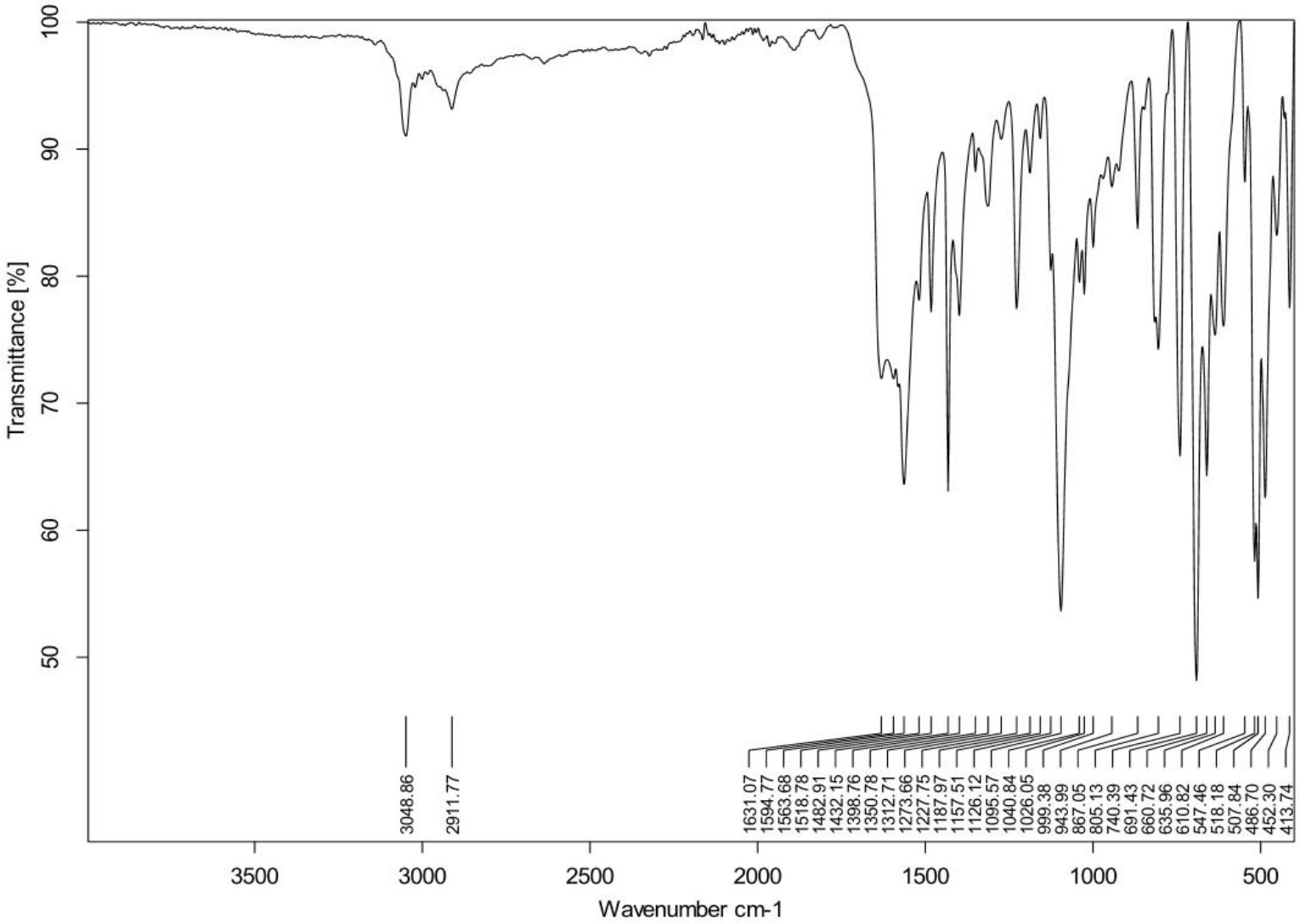

Figure S44. Solid-state IR spectrum of **3-DMAP**.

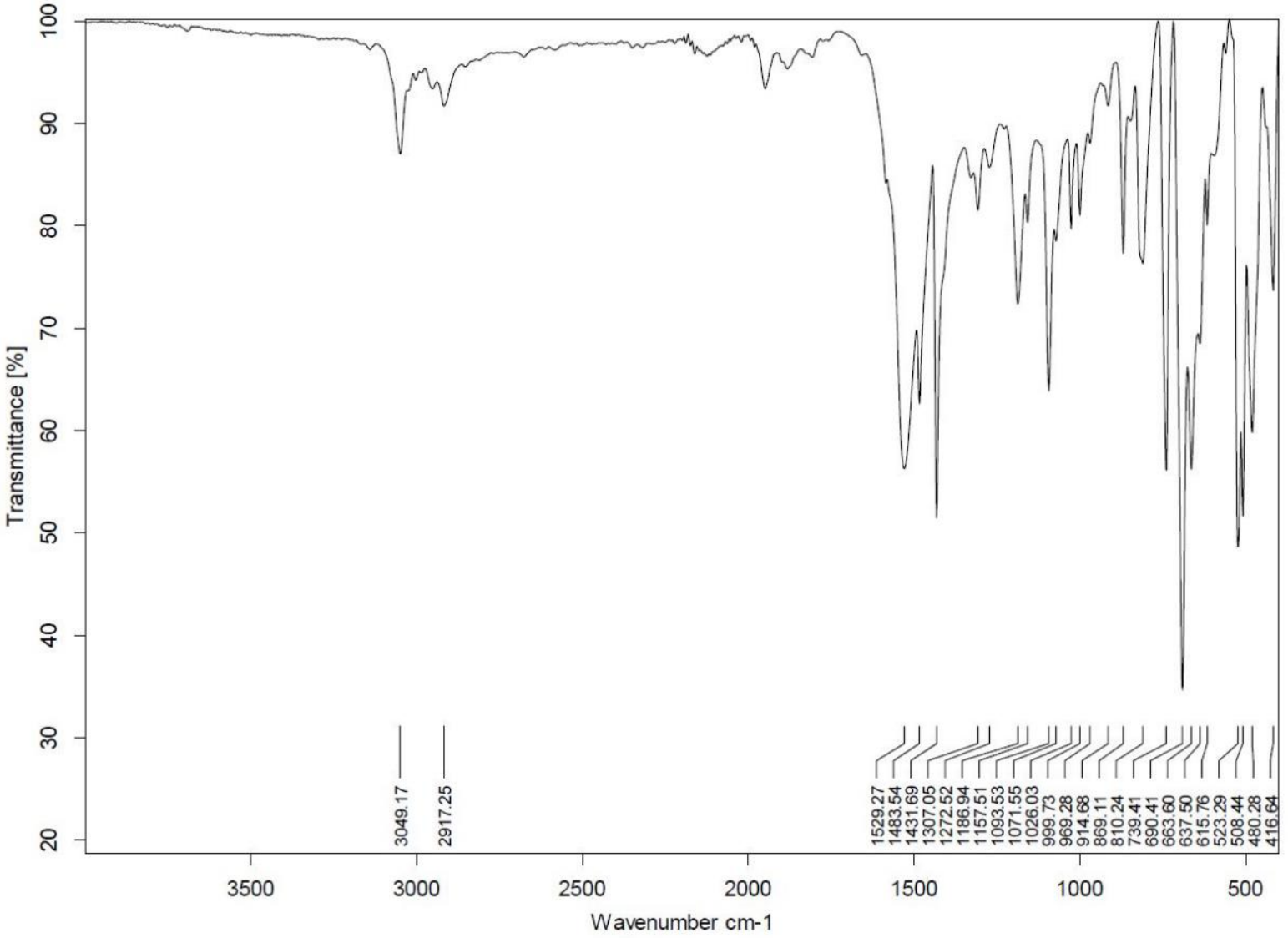

Figure S45. Solid-state IR spectrum of **2**.

UV-vis spectra

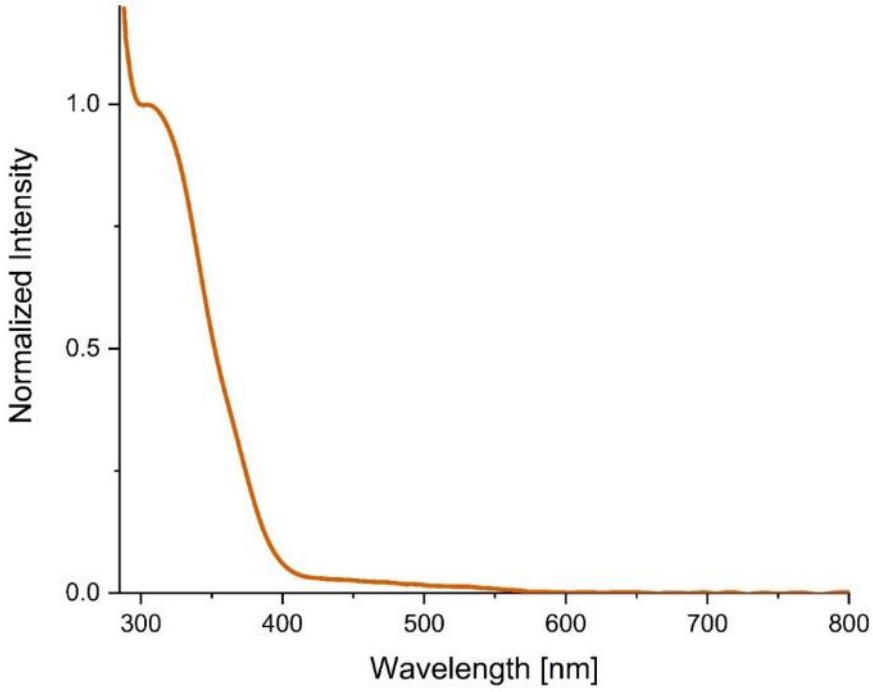

Figure S46. UV-vis absorption spectrum of **1-SMe$_2$** in benzene.

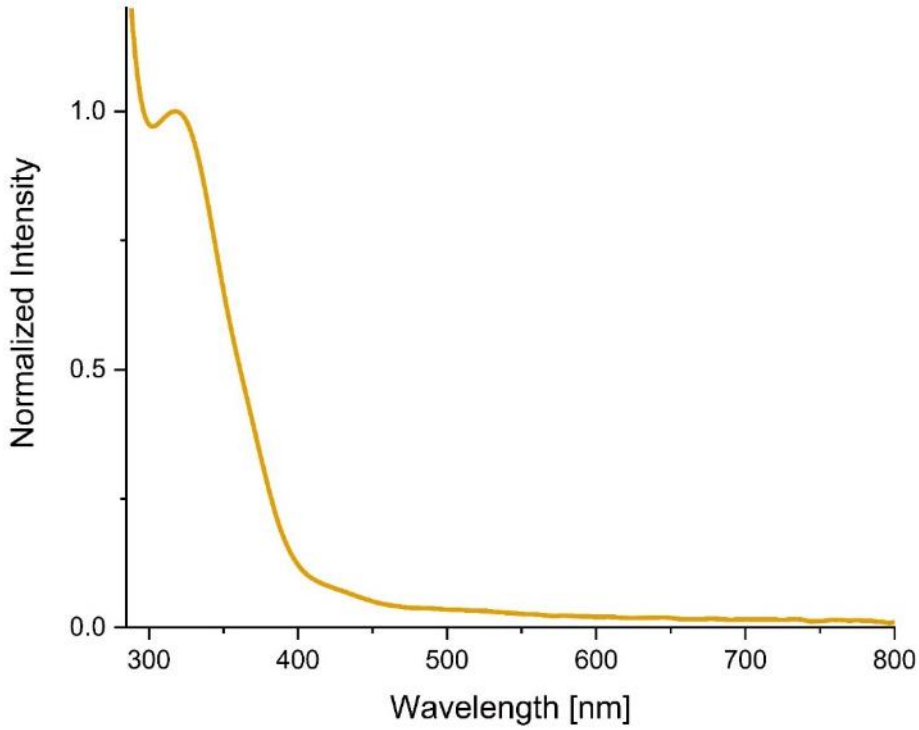

Figure S47. UV-vis absorption spectrum of **1-PMe$_3$** in benzene.

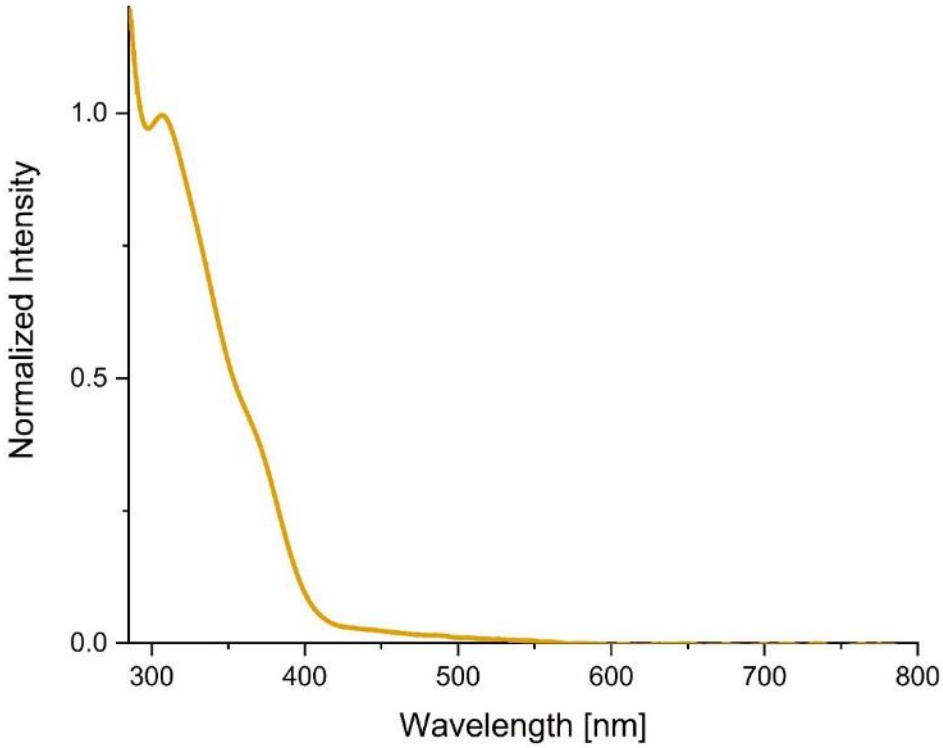

Figure S48. UV-vis absorption spectrum of **1-PCy$_3$** in benzene.

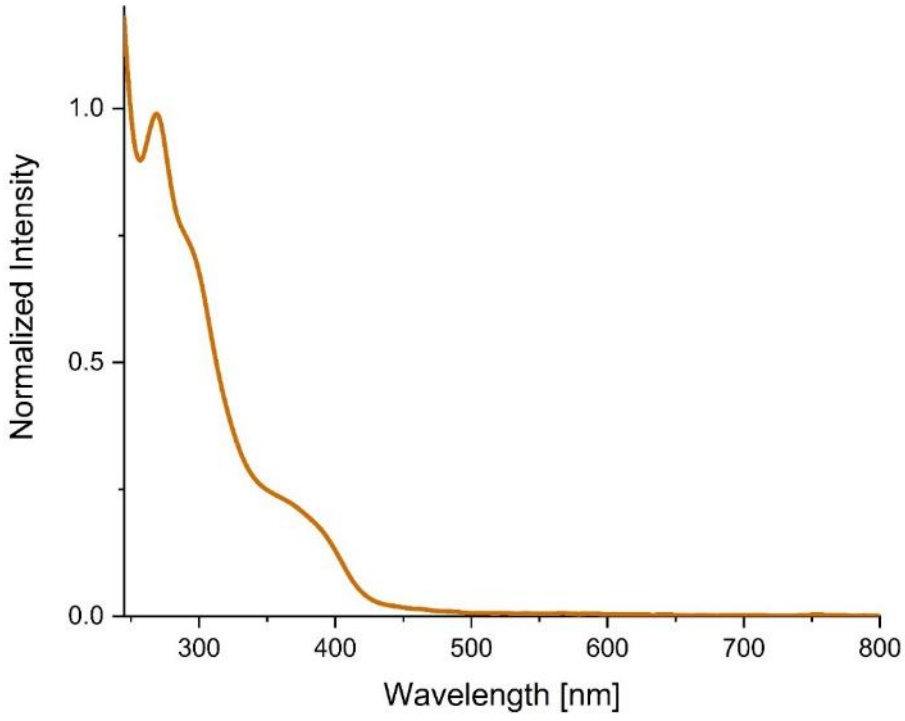

Figure S49. UV-vis absorption spectrum of **1-CNMes*** in dichloromethane.

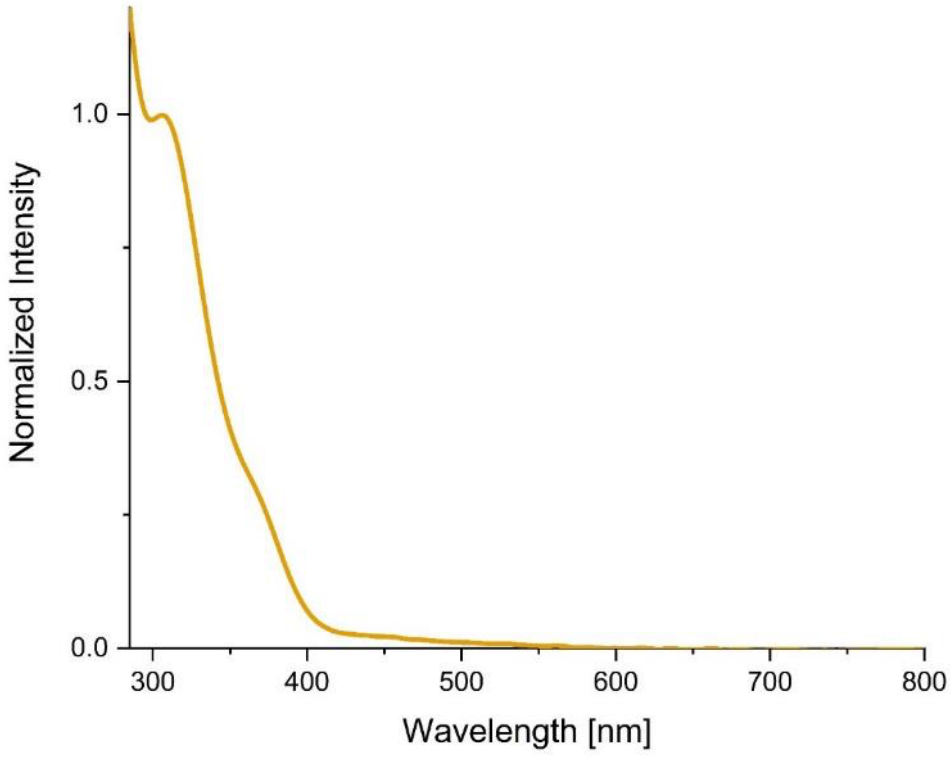

Figure S50. UV-vis absorption spectrum of **1-CAAC** in benzene.

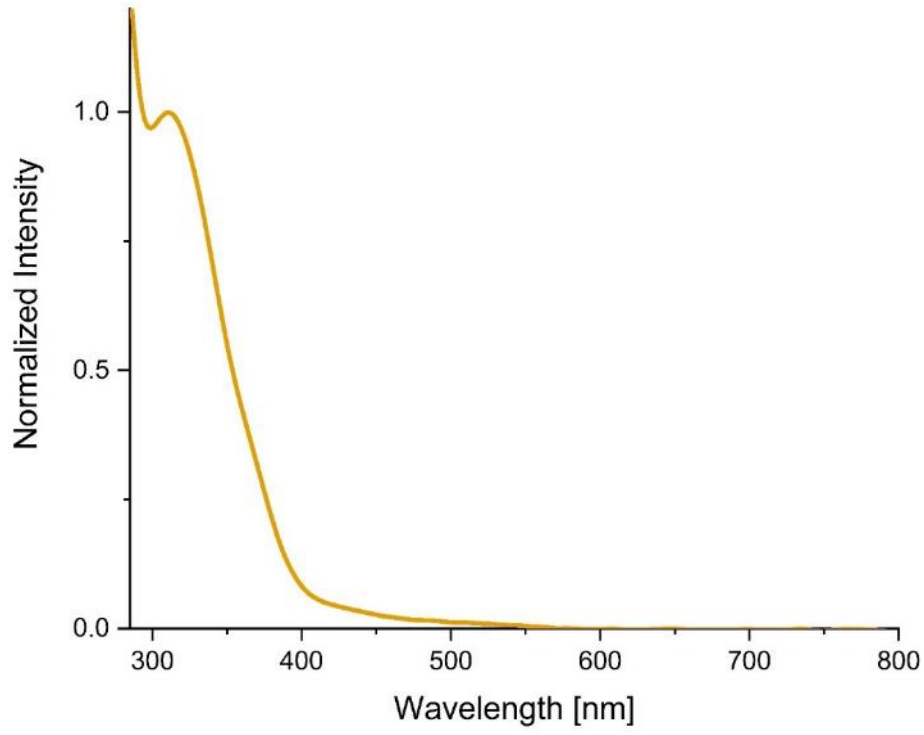

Figure S51. UV-vis absorption spectrum of **1-I*i*Pr** in benzene.

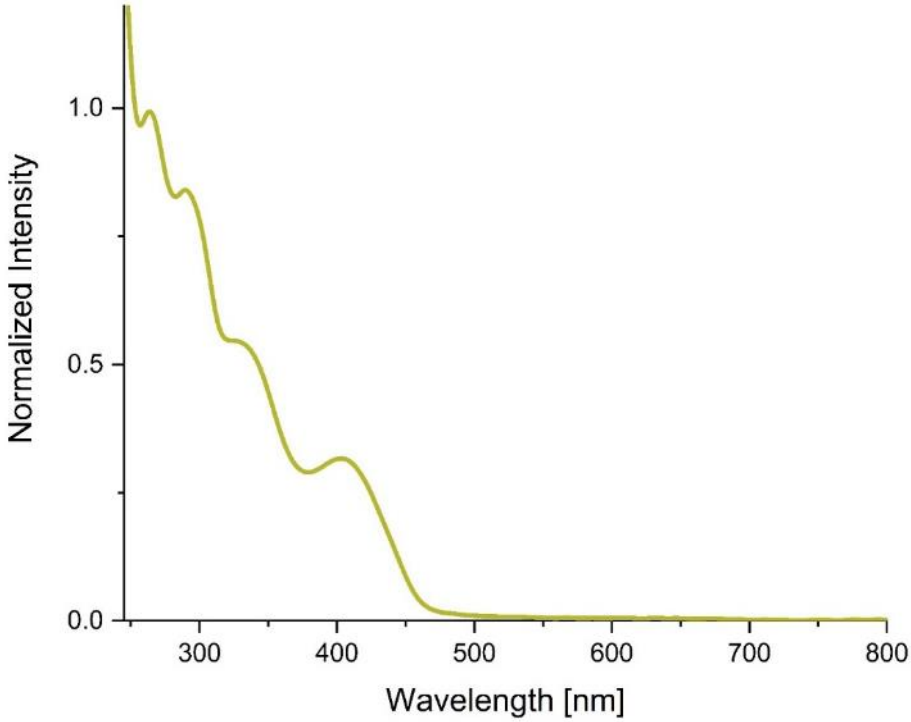

Figure S52. UV-vis absorption spectrum of **3-DMAP** in dichloromethane.

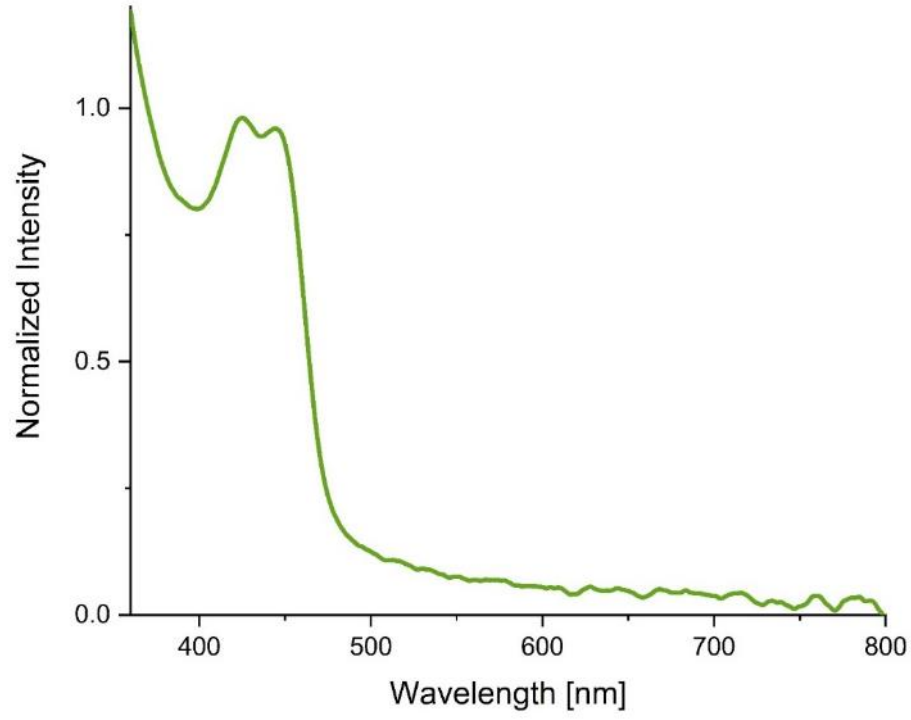

Figure S53. UV-vis absorption spectrum of **2** in bromobenzene.

X-ray crystallographic data

The crystal data of **1-PMe$_3$, 1-CNMes*** and **1-DMAP** were collected on a BRUKER D8 QUEST diffractometer with a CMOS area detector and multi-layer mirror monochromated Mo$_{K\alpha}$ radiation. The crystal data of **2** were collected on a RIGAKU OD XTALAB SYNERGY-S diffractometer with a HDAP area detector and multi-layer mirror monochromated Cu$_{K\alpha}$ radiation. The crystal data of **1-SMe$_2$** and **3-DMAP** were collected on a BRUKER X8-APEX II diffractometer with a CCD area detector and multi-layer mirror monochromated Mo$_{K\alpha}$ radiation. The structures were solved using the intrinsic phasing method,[9] refined with the ShelXL program and expanded using Fourier techniques.[10] All non-hydrogen atoms were refined anisotropically. Hydrogen atoms were included in structure factor calculations. All hydrogen atoms were assigned to idealised geometric positions.

Crystallographic data have been deposited with the Cambridge Crystallographic Data Center as supplementary publication nos. CCDC-2173522 (**1-PCy$_3$**), 2173523 (**1-SMe$_2$**), 2173524 (**1-CNMes***), 2173525 (**1-PMe$_3$**), 2173526 (**1-DMAP**), 2173527 (**2**) and 2173528 (**3-DMAP**). These data can be obtained free of charge from The Cambridge Crystallographic Data Centre *via* www.ccdc.cam.ac.uk/data_request/cif.

Refinement details for 1-SMe$_2$: The benzene molecule was modelled as twofold disordered in a 67:33 ratio. ADPs within the disorder were restrained with SIMU 0.01 and the hexagonal geometry with AFIX 6.

Crystal data for 1-SMe$_2$: $C_{54}H_{54}B_2Br_4N_2P_4SW \cdot C_6H_6$, $M_r = 1490.15$, orange block, 0.373×0.306×0.18 mm^3, triclinic space group $P\bar{1}$, $a = 10.399(5)$ Å, $b = 16.792(7)$ Å, $c = 17.471(8)$ Å, $\alpha = 90.149(13)°$, $\beta = 104.315(12)°$, $\gamma = 90.505(17)°$, $V = 2956(2)$ Å^3, $Z = 2$, $\rho_{calcd} = 1.674$ g·cm^{-3}, $\mu = 4.842$ mm^{-1}, $F(000) = 1468$, $T = 100(2)$ K, $R_1 = 0.0669$, $wR_2 = 0.0994$, 15915 independent reflections [$2\theta \leq 58.258°$] and 700 parameters.

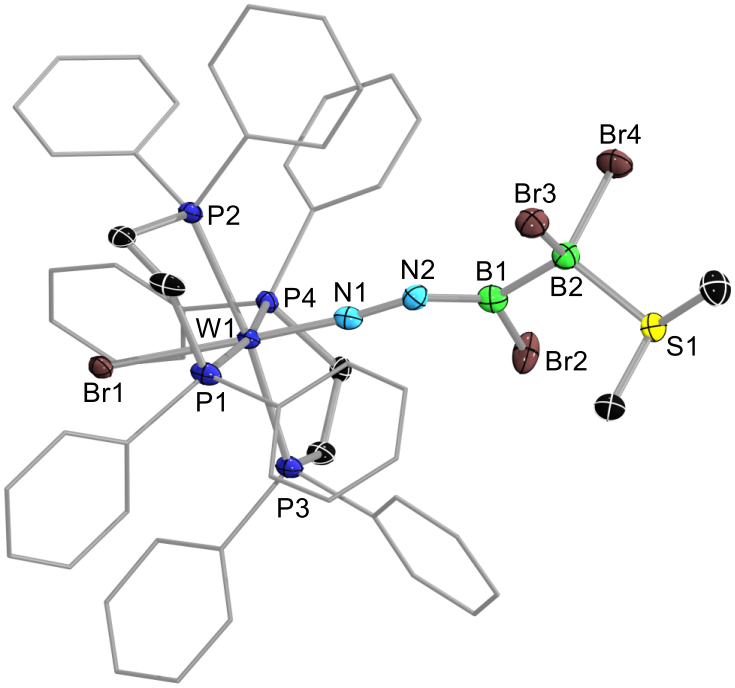

Figure S54. Solid-state structures of **1-SMe$_2$**. Thermal displacement ellipsoids at 50%. Ellipsoids of ligand periphery and hydrogen atoms omitted for clarity.

Refinement details for 1-PMe$_3$: The structure was refined as inversion twin and the BASF parameter was refined to 0.489. Xprep equally suggests either a C or I Lattice for the unit cell. Monoclinic I was chosen as suggested by IUCr. The asymmetric unit contains three crystallographically distinct molecules of **1-PMe$_3$**. Three of the six benzene molecules in the asymmetric unit showed twofold disorder. These were refined to a 32:68 (RESI 37 and 137), 60:40 (RESI 39 and 139) and 15:85 (RESI 42 and 142) ratio. ADPs within these disorders were restrained with SIMU 0.01 and the rings idealised with AFIX 66.

Crystal data for 1-PMe$_3$: $C_{55}H_{57}B_2Br_4N_2P_5W\cdot(C_6H_6)_2$, $M_r = 1582.20$, orange plate, 0.377×0.337×0.06 mm^3, monoclinic space group *Ia*, $a = 19.060(4)$ Å, $b = 38.289(8)$ Å, $c = 28.618(8)$ Å, $\beta = 112.100(6)°$, $V = 19351(8)$ Å^3, $Z = 12$, $\rho_{calcd} = 1.629$ g·cm^{-3}, $\mu = 4.435$ mm^{-1}, $F(000) = 9408$, $T = 100(2)$ K, $R_1 = 0.0382$, $wR_2 = 0.0596$, Flack parameter = 0.498(4), 34486 independent reflections [$2\theta \leq 50.698°$] and 2279 parameters.

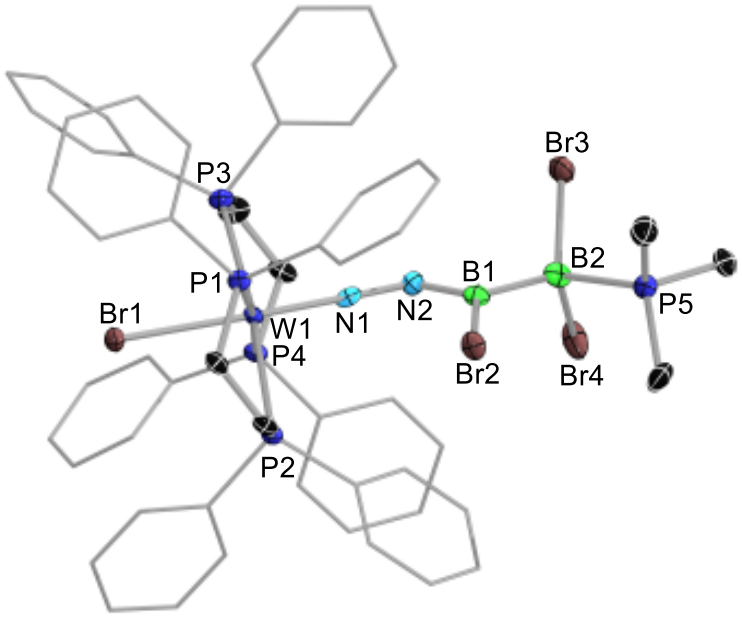

Figure S55. Solid-state structures of **1-PMe$_3$**. Thermal displacement ellipsoids at 50%. Ellipsoids of ligand periphery and hydrogen atoms omitted for clarity.

Refinement details for 1-PCy$_3$: The asymmetric unit contains one benzene molecule modelled as twofold disordered (RESI 15 and 115) in a 21:79 ratio. Furthermore the main complex itself is the overlap of two distinct complexes, one with PCy$_3$ ligand (71%, RESI 2), the other with an OPCy$_3$ ligand (29%, RESI 3). The ADPs of both residues were equalised using SIMU 0.01 and the Cy groups with SAME. One of the Cy groups of RESI 2 was modelled as twofold disordered (RESI 123 and 223) in a 1:1 ratio. H1_223 could not be afixed due to partitioning of the Cy groups in PART 1 and PART 3, with the corresponding P atom being PART 1. H1_223 was positioned with DFIX_223 1.0 C1 H1 and DFIX_223 2.06 C2 H1 C6 H1.

Crystal data for 1-PCy$_3$: $C_{76}H_{87}B_2Br_4N_2O_{0.29}P_5W{\cdot}C_6H_6$, $M_r = 1713.15$, yellow plate, 0.311×0.149×0.036 mm^3, monoclinic space group $P2_1/n$, $a = 13.687(4)$ Å, $b = 30.454(15)$ Å, $c = 17.661(7)$ Å, $\beta = 103.815(16)°$, $V = 7149(5)$ Å^3, $Z = 4$, $\rho_{calcd} = 1.592$ g·cm^{-3}, $\mu = 4.009$ mm^{-1}, $F(000) = 3433$, $T = 100(2)$ K, $R_1 = 0.0696$, $wR_2 = 0.1054$, 13255 independent reflections [$2\theta \leq 50.952°$] and 1080 parameters.

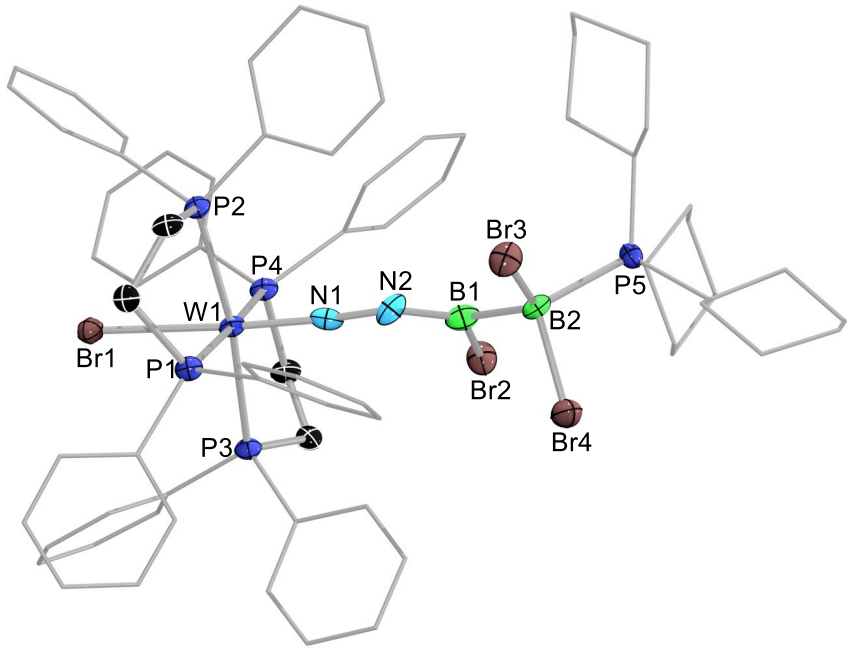

Figure S56. Solid-state structures of **1-PCy$_3$**. Thermal displacement ellipsoids at 50%. Ellipsoids of ligand periphery and hydrogen atoms omitted for clarity.

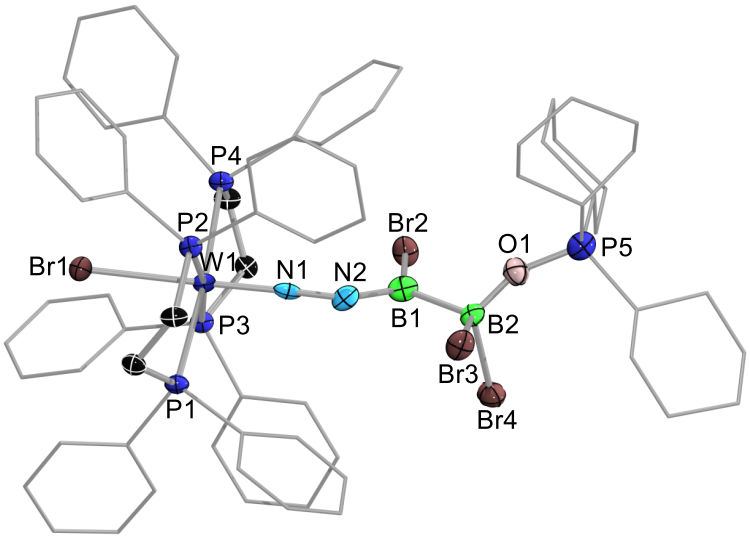

Figure S57. Solid-state structures of **1-OPCy$_3$**. Thermal displacement ellipsoids at 50%. Ellipsoids of ligand periphery and hydrogen atoms omitted for clarity.

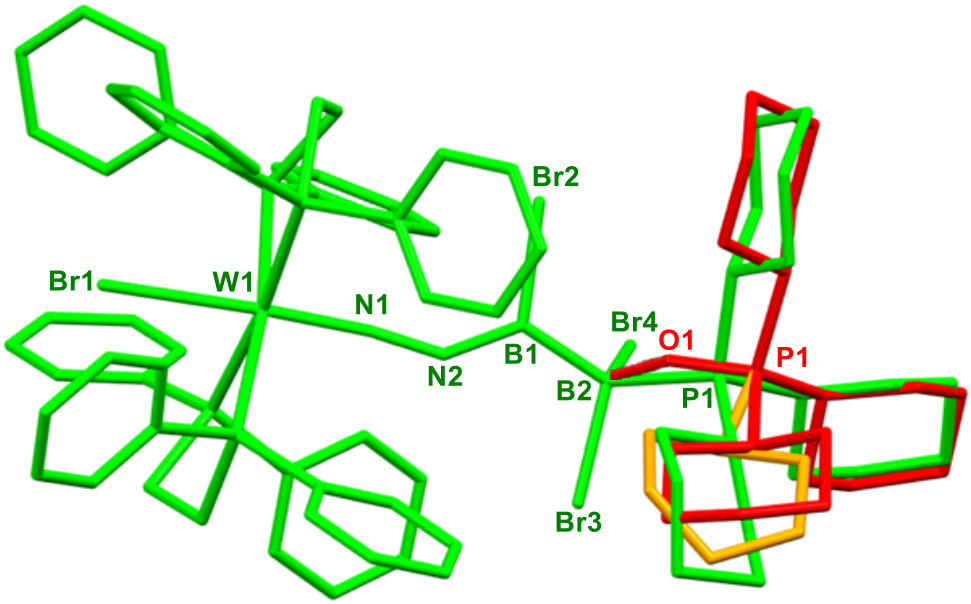

Figure S58. Overlay of **1-PCy$_3$** (green, 71%) and **1-OPCy$_3$** (red/orange, 29%) in the asymmetric unit in capped stick representation.

Refinement details for 1-CNMes*: The following most disagreeable reflection (-1 2 0) has been omitted during refinement. The asymmetric unit contains a twofold rotationally disordered benzene molecule (RESI 13 and 113) in a 16:84 ratio. ADPs within this disorder were restrained with SIMU 0.01 and the rings idealised with AFIX 66.

Crystal data for 1-CNMes*: $C_{68}H_{74}B_2Br_4N_3P_4W\cdot(C_6H_6)_{1.5}$, M_r = 1738.50, orange block, 0.348×0.314×0.144 mm^3, triclinic space group $P\bar{1}$, a = 14.517(3) Å, b = 16.761(4) Å, c = 16.951(4) Å, α = 91.443(19)°, β = 94.078(17)°, γ = 113.893(15)°, V = 3754.8(15) Å^3, Z = 2, ρ_{calcd} = 1.538 g·cm^{-3}, μ = 3.797 mm^{-1}, $F(000)$ = 1742, T = 100(2) K, R_1 = 0.0229, wR_2 = 0.0468, 14339 independent reflections [$2\theta \leq 51.506°$] and 887 parameters.

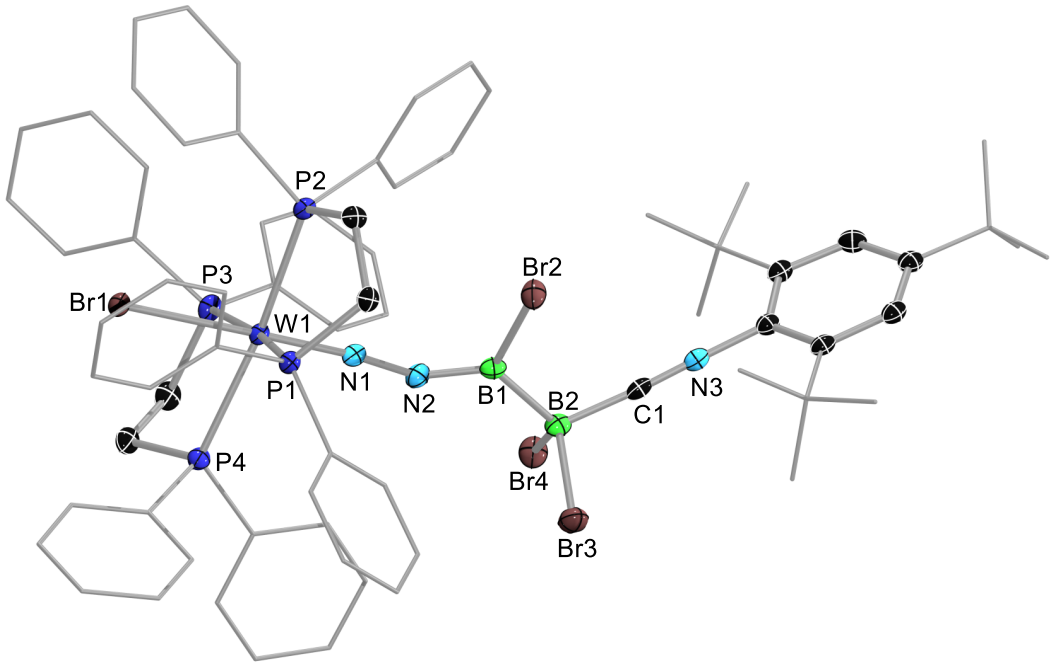

Figure S59. Solid-state structures of **1-CNMes***. Thermal displacement ellipsoids at 50%. Ellipsoids of ligand periphery and hydrogen atoms omitted for clarity.

Refinement details for 1-DMAP: The asymmetric unit contains 4.5 benzene molecules, one of which was modelled as twofold disordered (RESI 15 and 115) in a 61:39 ratio. ADPs within the disorder were restrained with SIMU and ISOR 0.01 and the rings idealised with AFIX 66.

Crystal data for 1-DMAP: $C_{59}H_{58}B_2Br_4N_4P_4W\cdot(C_6H_6)_{4.5}$, $M_r = 1823.56$, yellow plate, 0.24×0.199×0.112 mm^3, triclinic space group $P\,\bar{1}$, $a = 10.363(3)$ Å, $b = 18.694(4)$ Å, $c = 21.331(7)$ Å, $\alpha = 104.964(5)°$, $\beta = 93.977(8)°$, $\gamma = 96.840(7)°$, $V = 3942(2)$ Å^3, $Z = 2$, $\rho_{calcd} = 1.536$ g·cm^{-3}, $\mu = 3.621$ mm^{-1}, $F(000) = 1826$, $T = 100(2)$ K, $R_1 = 0.0450$, $wR_2 = 0.0848$, 22202 independent reflections [$2\theta \leq 59.302°$] and 943 parameters.

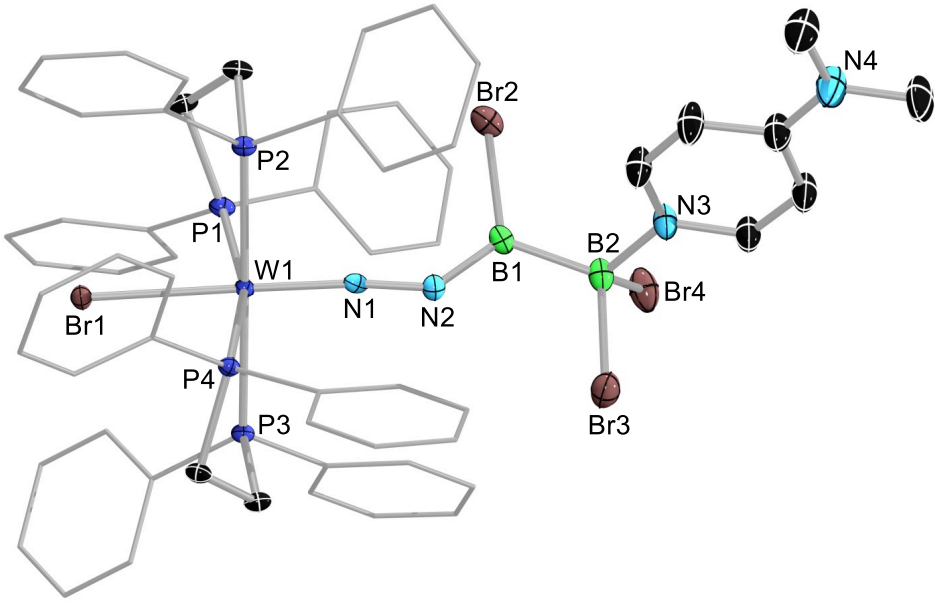

Figure S60. Solid-state structures of **1-DMAP**. Thermal displacement ellipsoids at 50%. Ellipsoids of ligand periphery and hydrogen atoms omitted for clarity.

Refinement details for 3-DMAP: The unit cell contains highly disordered benzene and hexane molecules which have been treated as a diffuse contribution to the overall scattering without specific atom positions by SQUEEZE/PLATON.[11] 781 electrons were thus squeezed from the unit cell, corresponding to ca. 12 hexane and 4 benzene molecules (768 electrons). After the application of SQUEEZE the absorption correction had to be recomputed. This was done using the Difabs absorption correction function of WinGX.[12] Three disagreeable reflections (4 1 5, 7 4 5, 10 5 6) were omitted. The large residual electron density is attributed to the presence of heavy atoms (W and Br). Two phenyl groups were modelled as twofold disordered (RESI 11/111 and 22/122), in a 40:60 and 63:37 ratio, respectively. ADPs within the disorders were restrained with SIMU 0.01 and the rings idealised with AFIX 66.

Crystal data for 3-DMAP: $C_{59}H_{58}B_2Br_4N_4P_4W$·(squeezed solvent), M_r = 1472.08, green plate, 0.199×0.129×0.108 mm^3, monoclinic space group $P2_1/c$, a = 18.893(9) Å, b = 28.420(13) Å, c = 25.635(16) Å, β = 90.67(3)°, V = 13764(13) Å^3, Z = 8, ρ_{calcd} = 1.421 g·cm^{-3}, μ = 4.130 mm^{-1}, $F(000)$ = 5792, T = 100(2) K, R_1 = 0.0663, wR_2 = 0.1559, 28152 independent reflections [$2\theta \leq 52.744°$] and 1357 parameters.

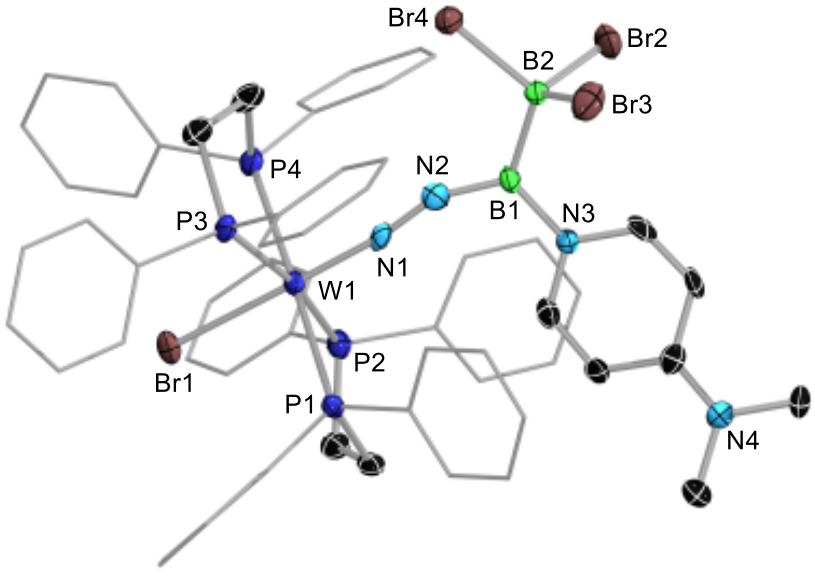

Figure S61. Solid-state structures of **3-DMAP**. Thermal displacement ellipsoids at 50%. Ellipsoids of ligand periphery and hydrogen atoms omitted for clarity.

Refinement details for 2: Two phenyl substituents of the phosphine ligands (RESI 4 and 14, 10 and 110) showed a twofold disorder (both 50:50). The displacement parameters of the carbon atoms (C1 to C6) were restrained with similarity restraint SIMU 0.01. Three of the 4.5 solvent molecules in the asymmetric unit (RESI 13 and 113, 15 and 115, 16 and 116) showed a twofold disorder (60:40, 63:37 and 55:45, respectively). The displacement parameters of the carbon atoms (C1 to C6) were restrained with similarity restraint SIMU 0.01 and the hexagonal geometry with AFIX 6.

Crystal data for 2: $C_{104}H_{96}B_2Br_4N_4P_8W_2\cdot(C_6H_6)_9$, $M_r = 3061.53$, yellow plate, 0.190×0.069×0.039 mm^3, triclinic space group $P\ \bar{1}$, $a = 14.76174(9)$ Å, $b = 16.09125(10)$ Å, $c = 16.44031(12)$ Å, $\alpha = 63.3289(7)°$, $\beta = 82.3742(6)°$, $\gamma = 80.1777(5)°$, $V = 3431.49(5)$ Å^3, $Z = 1$, $\rho_{calcd} = 1.482$ g·cm^{-3}, $\mu = 5.709$ mm^{-1}, $F(000) = 1544$, $T = 99.99(10)$ K, $R_1 = 0.0254$, $wR_2 = 0.0659$, 13521 independent reflections [$2\theta \leq 144.258°$] and 987 parameters.

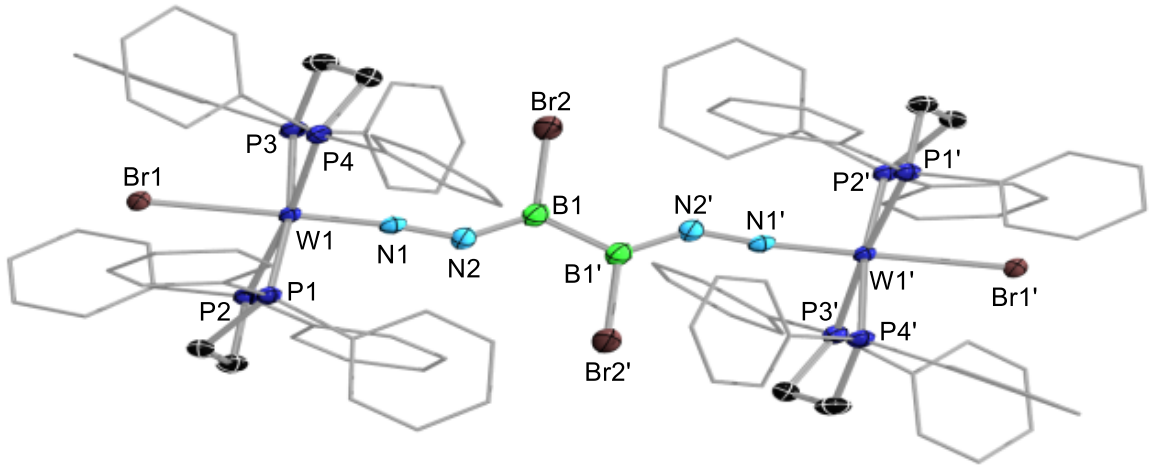

Figure S62. Solid-state structures of **2**. Thermal displacement ellipsoids at 50%. Ellipsoids of ligand periphery and hydrogen atoms omitted for clarity.

Table S1. ^{31}P NMR shifts (ppm, at 298 K unless stated otherwise), N=N IR stretching frequencies (cm^{-1}), selected bond lengths (Å), angles (°) and torsion angles (°) for **1-L**, **2** and **3-DMAP**. Bonding parameters for **2'** calculated at the B3LYP-D3(BJ)-Def2-SVP-ecp(Br,W) level of theory in square brackets.

Compound	^{31}P NMR	*ν*(N=N)	W1–N1	N1–N2	N2–B1	B1–B2	B–L	W1-N1-N2	N1-N2-B1	Br2-B1-B2-L
1-SMe$_2$	33.2	1535	1.788(4)	1.274(5)	1.359(6)	1.690(8)	1.945(5)	172.0(3)	140.8(4)	–47.0(4)
1-PMe$_3$	33.3	1528	1.798(7)	1.277(10)	1.447(12)	1.662(14)	2.049(11)	174.9(6)	135.4(7)	–24.3(9)
1-PCy$_3$[a]	37.6	1528	1.779(6)	1.255(7)	1.363(10)	1.702(11)	–	173.4(4)	141.1(6)	–
1-CNMes*[b]	34.2	1545	1.7910(19)	1.270(3)	1.356(3)	1.707(4)	1.575(4)	172.79(16)	141.3(2)	–27.7(3)
1-DMAP	–	–	1.798(3)	1.259(4)	1.372(4)	1.704(5)	1.570(5)	174.0(2)	140.6(3)	50.4(4)
1-CAAC	38.9, 38.4	1536	–	–	–	–	–	–	–	–
1-I*i*Pr	39.1	1550	–	–	–	–	–	–	–	–
3-DMAP[c]	33.5, 24.1[d]	1564	1.797(7)	1.250(10)	1.377(13)	1.701(15)	1.534(12)	172.1(6)	148.0(8)	–
2	34.9	1529	1.7959(19)	1.256(3)	1.370(4)	1.681(5)	–	173.71(17)	124.5(3)	–
			[1.813]	[1.241]	[1.375]	[1.690]		[171.6]	[142.4]	

[a] Although crystals of **1-PCy$_3$** were obtained these always showed partial oxidation to **1-OPCy$_3$** (up to 30%), the structures of the two fully overlapping in the asymmetric unit, with the exception of the PCy$_3$/OPCy$_3$ ligand, thus precluding discussion of B–L bonding parameters. [b] First of the three molecules of **1-CNMes*** present in the asymmetric unit. [c] First of the two molecules of **3-DMAP** present in the asymmetric unit. [d] At 223 K.

Computational details

Geometry optimisations were carried out at the B3LYP[13]-D3(BJ)[14]-def2-SVP[15] level of theory using the Turbomole[16] user interface TmoleX2021.[17] The def2-ecp[18] and defpp-ecp basis[19] sets were applied to the W and Br atoms, respectively, to account for relativistic effects. Due to the large size of the systems calculations were carried out on the simplified models **1-DMAP'**, **1-CAAC'**, **3-DMAP'** and **2'**, in which all P-bound phenyl rings were replaced by methyl groups. The optimised geometries were confirmed as true minima by frequency calculations, which provided no negative frequencies. Molecular orbital representations were generated in TmoleX2021. ^{11}B NMR shift calculations were carried out at the B3LYP-D3(BJ)-def2-SVP-ecp(W,Br) level of theory. When $B_2Br_2(NMe_2)_2$ (δ_{11B} = 38 ppm) was used as a reference, the calculated shifts for **1-CAAC'** were in good agreement with the experimental solid-state NMR shifts (Table S1).

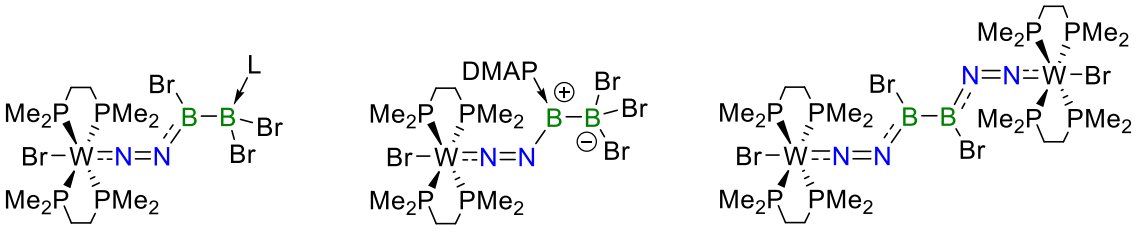

Figure S63. Simplified models of complexes **1-DMAP**, **1-CAAC**, **3-DMAP** and **2** for the DFT calculations.

Table S2. Calculated ^{11}B NMR shifts at the B3LYP-D3(BJ)-def2-SVP-ecp(W,Br) level of theory for **1-CAAC'** and $B_2Br_2(NMe_2)_2$ (δ_{11B} = 38 ppm) as a reference.

	$B_2Br_2(NMe_2)_2$	**1-CAAC'**	
calc. ^{11}B NMR shielding (ppm)	66.94092	84.69907	107.6867
calc. ^{11}B NMR shift (ppm)	38 (reference)	20.24186	-2.74573
exp. ^{11}B NMR shift (ppm)	38	23.7	–6.2

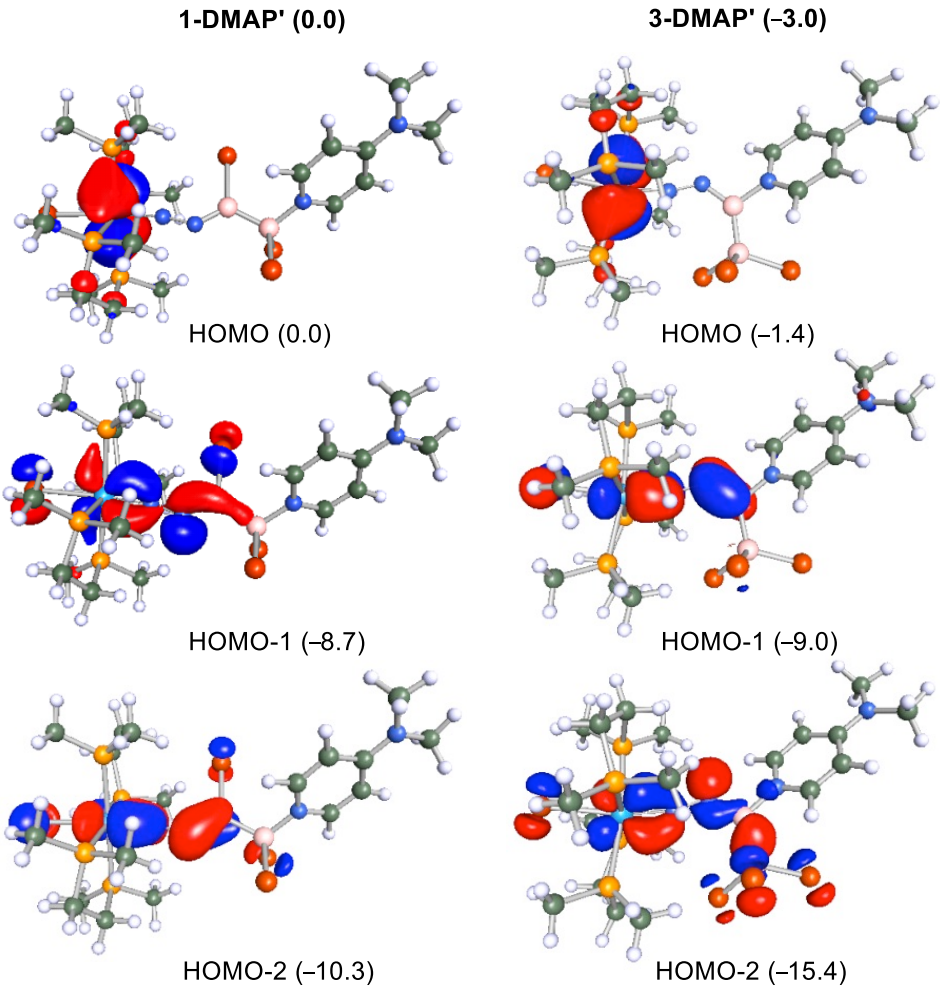

Figure S64. Representation of the frontier molecular orbitals (MOs) of **1-DMAP'** and **3-DMAP'**, calculated at the B3LYP-Def2-SVP-D3(BJ)-ecp(Br,W) level of theory. Isovalues 0.04. Relative energies in parentheses in kcal mol^{-1}.

Table S3. Optimised geometries of the studied complexes calculated at the B3LYP-D3(BJ)-Def2-SVP-ecp(Br,W) level of theory.

1-DMAP' E(scf) = –4104.02304937830 a.u.	**3-DMAP'** E(scf) = –4104.01823441821 a.u.
Br 2.137089 6.083449 2.250512	Br -1.984914 18.333828 8.773154
W 2.399370 4.070217 4.054520	W -0.261094 20.256378 7.883972
N 2.693289 2.732277 5.203605	N 0.644303 21.633877 7.183644
N 3.091493 1.803408 5.936357	N 0.969797 22.705803 6.594745
B 2.587305 1.064195 6.968994	B 2.090626 23.512869 6.697147
Br 0.602250 1.373572 7.500271	N 1.871420 24.848803 5.929682

B 3.494553 0.002708 7.930829	C 1.285647 24.864895 4.711732
Br 4.361791 1.233109 9.356670	H 0.959374 23.892483 4.342344
Br 4.934822 -0.972314 6.818215	C 1.115406 26.021729 3.983420
N 2.665964 -1.137103 8.647642	H 0.648646 25.951559 3.003484
C 2.860656 -1.532444 9.921894	C 1.555658 27.266968 4.514577
H 3.613625 -0.967604 10.472748	N 1.416989 28.431906 3.826295
C 2.151428 -2.565830 10.498139	C 0.806639 28.433176 2.507259
H 2.367726 -2.819858 11.533484	H 1.373068 27.808807 1.794365
C 1.166845 -3.262859 9.748289	H 0.787569 29.458174 2.118021
C 0.987647 -2.830311 8.405959	H -0.232342 28.061357 2.537340
H 0.260190 -3.297923 7.746463	C 1.893713 29.678904 4.403071
C 1.738314 -1.788926 7.910297	H 1.369931 29.920288 5.344511
H 1.623931 -1.445312 6.883489	H 1.713529 30.496964 3.695657
N 0.438324 -4.281017 10.279942	H 2.976207 29.641346 4.614326
C 0.662105 -4.695910 11.654841	C 2.146124 27.221693 5.805733
H 1.698278 -5.042201 11.813149	H 2.500396 28.121092 6.303886
H -0.013214 -5.525088 11.897562	C 2.296836 26.019197 6.462100
H 0.463861 -3.875266 12.366107	H 2.734349 25.957754 7.458481
C -0.563102 -4.959217 9.473322	B 3.559084 23.322916 7.526316
H -1.342856 -4.261787 9.121073	Br 3.083047 24.004826 9.470421
H -1.050139 -5.733855 10.077250	Br 5.105509 24.457190 6.767692
H -0.115173 -5.446604 8.589636	Br 4.173315 21.358448 7.579998
P 1.420667 5.598588 5.748581	P -2.081486 20.802832 6.298480
C -0.437744 5.644753 5.530861	C -3.121877 22.185623 7.032624
H -0.919393 6.043395 6.439584	H -2.592335 23.122709 6.788241
H -0.630598 6.358448 4.711664	H -4.107200 22.228689 6.539392
C -0.973178 4.254125 5.174170	C -3.255306 22.034206 8.551322
H -2.050719 4.282677 4.939885	H -3.838953 21.132524 8.801437
H -0.829557 3.555992 6.015857	H -3.763967 22.902952 9.002020
P -0.007489 3.517488 3.749461	P -1.569659 21.786572 9.323618
C 1.631177 5.059692 7.492618	P 0.882745 18.460875 6.605680
C 1.862874 7.383109 5.787185	C 1.916099 17.425386 7.771019
C -0.507635 1.749503 3.809257	H 1.216950 16.704733 8.228540
C -0.895925 4.153915 2.268245	H 2.660727 16.846830 7.199273

P 4.784279 4.700757 4.339160	C 2.581011 18.288744 8.846936
C 5.831312 3.584762 3.256255	H 3.339901 18.951620 8.405543
H 6.836837 4.015427 3.116366	H 3.079354 17.667458 9.609666
H 5.952466 2.644068 3.820144	P 1.332929 19.421425 9.654813
C 5.138159 3.318362 1.917245	C -1.553799 21.542120 4.699917
H 5.691063 2.579703 1.312699	C -3.348854 19.569450 5.791889
H 5.063166 4.247154 1.326682	C -0.879875 23.487032 9.392913
P 3.380606 2.745829 2.203400	C -1.975749 21.385105 11.069529
C 5.376318 6.384669 3.896327	C 2.089553 19.079296 5.367325
C 5.496764 4.401285 6.006814	C -0.067959 17.178331 5.690754
C 2.675427 2.744513 0.505795	C 2.345532 20.573788 10.656632
C 3.583572 0.961661 2.605632	C 0.633163 18.330156 10.966209
H -1.968055 3.904070 2.304508	H -1.103530 20.755449 4.075953
H -0.439748 3.716037 1.368110	H -0.781872 22.293264 4.927173
H -0.757305 5.242178 2.205264	H -2.393777 22.005253 4.158155
H 3.342047 2.253125 -0.220700	H 1.430631 18.014187 11.657071
H 2.496838 3.789240 0.211664	H -0.139906 18.881981 11.519224
H 1.708974 2.218449 0.526730	H 0.151245 17.455236 10.512332
H 5.180699 3.405414 6.355469	H 2.837323 21.308655 10.009436
H 5.098968 5.152697 6.705566	H 1.677826 21.112154 11.346097
H 6.596697 4.460610 6.000281	H 3.102538 20.023958 11.237857
H 4.868501 7.117568 4.540390	H -0.857274 16.795881 6.354615
H 5.085328 6.603797 2.859477	H -0.543053 17.648632 4.816448
H 6.467231 6.474842 4.017608	H 0.576141 16.351494 5.350971
H 1.209864 4.050929 7.610588	H -1.050333 21.424391 11.663210
H 1.143145 5.755103 8.193686	H -2.710017 22.087975 11.494121
H 2.704928 4.993934 7.721940	H -2.373539 20.359972 11.100057
H -1.602751 1.633436 3.768278	H 0.137928 23.456461 9.810340
H -0.050782 1.220253 2.959785	H -1.517092 24.166096 9.980735
H -0.128003 1.320817 4.748061	H -0.777994 23.862619 8.364024
H 1.818729 7.772550 4.759410	H -2.843723 18.720751 5.308466
H 2.896150 7.481442 6.153017	H -4.078395 20.015928 5.097961
H 1.191101 7.959168 6.443380	H -3.854904 19.184189 6.687076
H 4.025863 0.855487 3.608379	H 2.777323 19.779896 5.864456

H 4.205595 0.440726 1.860941	H 2.654751 18.256908 4.900846
H 2.587458 0.495222 2.640829	H 1.542026 19.637732 4.593205
1-CAAC'	**2'**
E(scf) = -4556.73036594553 a.u.	E(scf) = –5739.66644204069 a.u.
C 3.202627 5.058882 5.156901	W 12.364212 6.988431 6.620841
H 2.719740 4.136901 4.792946	Br 10.425627 8.849320 6.200416
H 3.893544 5.399648 4.367301	N 13.703048 5.814314 6.803434
C 3.970235 4.819559 6.460007	B 15.128420 3.960598 7.454568
H 4.797486 4.104175 6.316432	Br 13.889632 3.177889 8.900642
H 3.301357 4.412236 7.237028	N 14.716187 5.083498 6.777648
C 1.286794 11.059183 8.252254	P 13.899917 8.927460 6.741474
H 0.694973 11.972345 8.071702	C 14.116609 9.628184 5.023068
H 0.895431 10.588000 9.170069	H 13.198655 10.202937 4.814573
N 3.724709 8.872335 5.509418	H 14.968179 10.328988 4.995358
C 2.778533 11.376038 8.403654	P 12.949634 7.191491 4.214574
H 2.968898 12.018799 9.279388	C 14.287262 8.494215 4.008736
H 3.160711 11.898970 7.511526	H 15.246154 7.974290 4.174561
B 5.171284 10.280038 4.173915	H 14.297548 8.873130 2.973503
B 6.632218 10.186127 3.317294	P 10.574492 5.273714 6.446726
N 4.455822 9.175077 4.542765	C 9.633209 5.207475 8.062688
P 1.932175 6.428827 5.354929	H 8.905342 6.036221 8.025218
P 4.612573 6.440876 7.131026	H 9.061812 4.266739 8.131664
P 1.000878 9.820122 6.875578	P 11.676623 6.875772 9.013741
P 3.770249 9.796591 8.517222	C 10.585282 5.376262 9.251177
Br 1.576165 6.888659 8.927458	H 11.277442 4.520528 9.320109
Br 4.603177 12.089017 5.007011	H 10.034854 5.443806 10.204500
Br 6.770934 8.262112 2.438000	C 13.528304 10.423828 7.742254
Br 7.972798 10.259717 4.908540	C 15.612184 8.471849 7.236542
W 2.839542 8.157701 6.887399	C 11.692825 7.692952 2.968685
C 6.955258 11.027036 1.994067	C 13.747170 5.711231 3.472486
C 8.075997 11.977612 0.104438	C 11.163399 3.547208 6.227364
C 6.661412 11.550959 -0.322402	C 9.224267 5.429700 5.207680
H 6.715632 10.593713 -0.861927	C 10.663043 8.244205 9.713365
H 6.196366 12.287673 -0.993221	C 12.978669 6.634508 10.286956

C	5.854597	11.349756	0.972296	N	18.001711	1.297359	7.861108
C	8.324224	13.484045	-0.001512	H	15.377936	-2.183163	7.612084
H	9.310143	13.746348	0.405236	H	15.773911	-0.464392	8.000241
H	7.562596	14.081469	0.511252	H	16.090759	-1.088850	6.375934
H	8.312909	13.764269	-1.065103	H	13.587590	10.160948	8.809379
C	9.140669	11.256423	-0.718338	H	14.228201	11.247948	7.531348
H	10.154143	11.521158	-0.388615	H	12.498192	10.735924	7.514949
H	9.033219	11.564241	-1.769683	H	11.720057	3.479594	5.280812
H	9.019053	10.167798	-0.667184	H	10.325188	2.832373	6.215440
C	5.186966	12.672417	1.430976	H	11.858765	3.300189	7.042682
H	4.398253	12.932355	0.708367	H	12.140134	7.818274	1.970244
H	5.893921	13.510818	1.473221	H	11.222146	8.629529	3.299676
H	4.736012	12.571108	2.425931	H	10.906857	6.924428	2.928421
C	4.748640	10.303639	0.798029	H	8.854990	6.465563	5.226586
H	4.031324	10.672614	0.047277	H	8.400632	4.726730	5.410067
H	4.206128	10.132813	1.738914	H	9.636255	5.223783	4.208124
H	5.152367	9.339569	0.467251	H	21.384888	4.278006	8.429206
C	9.326985	11.668504	2.331668	H	19.992535	3.634878	9.370403
C	9.481470	12.866785	3.072983	H	19.848030	3.809464	7.608518
C	10.700656	13.080249	3.727658	H	22.854950	0.646318	9.423212
H	10.836177	13.994331	4.308572	H	23.310307	2.384137	9.232934
C	11.729411	12.146118	3.669148	H	22.078568	1.891874	10.440774
H	12.673688	12.334979	4.185909	H	17.182482	1.764982	10.508041
C	11.538023	10.957116	2.974651	H	17.536226	1.192506	12.181321
H	12.330269	10.206029	2.969943	H	18.722452	2.206270	11.292654
C	10.338348	10.679901	2.304684	H	20.810568	0.194973	11.730061
C	10.179168	9.290657	1.696248	H	20.491783	-1.510670	11.364591
H	9.184024	9.224559	1.237152	H	19.579416	-0.694606	12.694923
C	10.223464	8.216565	2.799232	H	21.326675	-0.929458	3.909314
H	9.959117	7.234365	2.377293	H	20.439516	-2.071657	4.982402
H	9.514755	8.444832	3.603236	H	21.916172	-1.298380	5.577141
H	11.233762	8.141618	3.234511	H	9.778152	8.399985	9.081151
C	11.247068	8.969784	0.636496	H	11.251771	9.172862	9.683929
H	12.248494	8.906970	1.091347	H	10.361638	8.026494	10.750130

H	11.297833	9.718258	-0.166207
H	11.036754	7.990903	0.176009
C	8.382646	13.906447	3.272168
H	7.529700	13.631536	2.642502
C	7.877160	13.909069	4.725476
H	7.046565	14.624186	4.835065
H	8.680500	14.207017	5.419059
H	7.514705	12.919470	5.025064
C	8.827690	15.324001	2.875292
H	7.970320	16.014732	2.920355
H	9.249697	15.368320	1.861266
H	9.591266	15.709914	3.569139
N	8.103623	11.498199	1.556980
C	1.700204	6.966816	3.611350
C	0.386218	5.514373	5.749609
C	6.111775	6.762601	6.118062
C	5.277611	5.962626	8.776774
C	3.708342	9.397211	10.312535
C	5.504653	10.355212	8.283585
C	-0.749337	9.325039	7.152288
C	0.922662	10.882421	5.376485
H	5.870996	6.799872	9.174368
H	5.913672	5.065139	8.718955
H	4.428183	5.781527	9.451807
H	0.147216	11.660021	5.466671

H	17.468910	-4.137549	7.150999

$B_2Br_2(NMe_2)_2$

E(scf) = -5466.06566052776 a.u.

B	0.307081	-0.173170	-0.125503
Br	-1.370885	-0.885391	-0.890323
N	0.569705	-0.331155	1.236327
B	1.339700	0.546479	-1.265220
Br	2.898486	-0.564614	-1.758531
N	1.148033	1.784207	-1.881491
C	1.984125	2.375432	-2.914045
C	0.006149	2.620229	-1.536545
C	1.799541	0.183384	1.823409
C	-0.271478	-1.014152	2.206204
H	0.339898	3.600612	-1.150694
H	-0.614861	2.134692	-0.773774
H	-0.624716	2.805312	-2.424369
H	1.400518	2.535446	-3.838556
H	2.367451	3.358640	-2.586679
H	2.834227	1.723291	-3.143445
H	-1.188207	-1.381709	1.731765
H	-0.545821	-0.331310	3.030345
H	0.267340	-1.871560	2.648198
H	2.389915	-0.634922	2.273233
H	2.420036	0.670645	1.061315
H	1.577245	0.915550	2.620912

H	0.710263	10.247293	4.503678
H	1.906899	11.348949	5.222835
H	6.178018	9.508080	8.481893
H	5.650848	10.677437	7.243865
H	5.756527	11.185344	8.962882
H	-1.105969	8.782051	6.263731
H	-1.402801	10.193200	7.334144
H	-0.779551	8.639256	8.011896
H	2.675138	9.155412	10.597250
H	4.088508	10.234758	10.918417
H	4.314945	8.498661	10.496236
H	5.829051	6.963121	5.073875
H	6.816365	5.917260	6.159114
H	6.610164	7.677255	6.472743
H	-0.448177	6.231169	5.779101
H	0.176273	4.727768	5.007923
H	0.481623	5.079759	6.754807
H	1.513413	6.116515	2.936229
H	0.852717	7.666544	3.560971
H	2.610564	7.500461	3.297093

References

1 J. Rohonczy, SOLA – Solid Lineshape Analysis Version 2.2.4, Bruker Biospin, Rheinstetten, Germany, 2013.

2 A. Rempel, S. K. Mellerup, F. Fantuzzi, A. Herzog, A. Deißenberger, R. Bertermann, B. Engels and H. Braunschweig, *Chem. Eur. J.*, 2020, **26**, 16019.

3 J. R. Dilworth and R. L. Richards, *Inorg. Synth.*, 1990, **28**, 33.

4 V. Lavallo, Y. Canac, C. Präsang, B. Donnadieu and G. Bertrand, *Angew. Chem. Int. Ed.*, 2005, **44**, 5705.

5 M. Niehues, G. Erker, G. Kehr, P. Schwab, R. Froehlich, O. Blacque and H. Berke, *Organometallics*, 2002, **21**, 2905.

6 W. Wolfsberger, H. Schmidbaur, *Synth. React. Inorg. Met.-Org. Chem*. 1974, **4**, 149.

7 K. Issleb, A. Brack, *Z. anorg. allg. Chem*., 1954, **277**, 258.

8 C. W. Tate, R. Shang, K. Radacki and H. Braunschweig, *Angew. Chem. Int. Ed.*, 2013, **52**, 729.

9 G. Sheldrick, *Acta Cryst.*, 2015, **A71**, 3.

10 G. Sheldrick, *Acta Cryst.*, 2008, **A64**, 112.

11 A. L. Spek, *Acta Cryst.*, 2015, **C71**, 9.

12 L. J. Farrugia, *J. Appl. Cryst*., 2012, **45**, 849.

13 a) A. D. Becke, *J. Chem. Phys*., 1993, **98**, 5648; b) C. Lee, W. Yang and R. G. Parr, *Phys. Rev. B*, 1988, **37**, 785; c) S. H. Vosko, L. Wilk and M. Nusair, *Can. J. Phys*., 1980, **58**, 1200; d) P. J. Stephens, F. J. Devlin, C. F. Chabalowski and M. J. Frisch, *J. Phys. Chem.*, 1994, **98**, 11623.

14 S. Grimme, S. Ehrlich and L. Goerigk, *J. Comput. Chem*., 2011, **32**, 1456.

15 F. Weigend and R. Ahlrichs, *Phys. Chem. Chem. Phys*., 2005, **7**, 3297.

16 TURBOMOLE V7.0, a development of University of Karlsruhe and Forschungszentrum Karlsruhe GmbH, 1989–2007; TURBOMOLE GmbH, since 2007; available from http://www.turbomole.com.TmoleX2021.

17 TmoleX2021, Dassault Systèmes, Versailles.

18 D. Andrae, U. Häußermann, M. Dolg, H. Stoll and H. Preuß, *Theor. Chim. Acta*, 1990, **77**, 123.

19 S. Grimme and M. Waletzke, *J. Chem. Phys*., 1999, **111**, 5645.

20 A. Moezzi, M. M. Olmstead and P. P. Power, *J. Chem. Soc.*, *Dalton Trans.*, 1992, 2429.